Faculty of Bioscience Engineering

Academic 2014-2015

'The Twittering Tree' — Real-time stress detection of forests by individual tree monitoring

Jonas von der Crone
Promotor and tutor: Prof. dr. ir. Kathy Steppe

Master thesis submitted in fulfillment of the requirements for the degree of Master in Bioscience Engineering: Forest and Nature Management

Faculteit Bio-Ingenieurswetenschappen

Academiejaar 2014-2015

‘The Twittering Tree’ — Real-time stress detectie van bossen op basis van het individueel monitoren van bomen

Jonas von der Crone
Promotor en tutor: Prof. dr. ir. Kathy Steppe

Masterproef voorgedragen tot het behalen van de graad van
Master in de Bio-Ingenieurswetenschappen: Bos- en Natuurbeheer

Declaration of Authorship

Ghent, June 2015

The promotor,

Prof. dr. ir. Kathy Steppe

The author,

Jonas von der Crone

Acknowledgements

Dit is het dan, de laatste lege pagina die kan gevuld worden. Het was een jaar vol enthousiasme, sensoren, ijver, dipjes, openbaringen, lange dagen, nog eens sensoren en toewijding. Dit alles mede mogelijk gemaakt door Professor Kathy Steppe. Reeds sinds het vak ecologie in het tweede bachelorjaar bleek dat zij met meer dan de nodige gedrevenheid achter het onderzoek van haar laboratorium van Plantecologie staat. Dit vermoeden werd bevestigd bij de cursus meteorologie, en tijdens het vak ecofysiologie was het hek van de dam.

Bij de voorstelling van de onderwerpen sprong 'The Twittering Tree' er uit. Een onderwerp waar ik mijzelf als echte 'bos- en natuurder' niet hoefde te onderdrukken en mijn eigen technologische interesses goed kon gebruiken. Van 's morgens tot 's avonds op mijn computerscherm kijken om te zien hoe de bomen groeiden, af en toe zelf naar het proefbos gaan en gestaag meer en meer vat krijgen op de hele resem aan sensoren. Had mij geen mooier laatste jaar kunnen inbeelden.

Professor Steppe, bedankt. Vanaf de eerste afspraak was uw ambitie voor dit project reeds naar mij overgesprongen. We hebben een goed aantal van de vele wegen die toen werden aangehaald reeds bewandelt. Ook kwam ik iedere keer weer vol motivatie uit uw bureau.

Geert en Phillip, bedankt om mij wegwijs te maken in de kelders, te helpen bij de installatie van sensoren en bij het plaatsen van een grote gasfles in het proefbos zodat ik zonder probleem een ganse dag waterpotentialen kon opmeten. Erik, waar zou het labo staan zonder jou technische expertise. Niemand vijst raspberries open zoals jij ze open vijst! Ook Dirk, bedankt voor de speed-PhytoSense-workshop waardoor ik er direct kon invliegen.

Lisa en Jeroen, twee top collega bos- en natuurders. Het is altijd lachen, zeker met jou, Jeroen. Je staat geen enkel mopje in de weg! Lisa, jij die altijd rechttoe rechtaan bent, het was super om met jou samen te kunnen lachen en werken.

Mama, dankzij jouw vele steun doorheen de afgelopen jaren en vertrouwen in mijn doorzettingsvermogen, sta ik waar ik vandaag sta. Het was niet altijd eenvoudig, zeker niet de eerste jaren, maar moeilijk gaat ook! Ook Pol, dankzij jou kon ik iedere zondag zonder zorgen vertrekken richting Gent waarbij ik wist dat je goed voor mama zou zorgen.

Als laatste maar niet minste, Lana, mijn vriendin. Al een geluk dat de blokjes je niet zo goed afgingen tijdens de practica van aardwetenschappen in het eerste jaar waardoor ik mijn subtiele openingszin, 'lukt het?', kon gebruiken. Nu zijn we beide gekomen tot ons laatste jaar, de laatste weekjes, en met elkaars steun ging de weg hiernaartoe toch net iets vlotter. Mede dankzij het vele discussiëren, het (al dan niet succesvol) proberen uitleggen aan elkaar als iemand iets minder begreep en elkaar blijven pushen. Je bent mijn *allerliefste* vriendin en je was een super collega bos- en natuurstudent!

Contents

Abbreviations

CHP	**C**ompensation **H**eat **P**ulse
DBH	**D**iameter at **B**reast **H**eight
EC	**E**ddy **C**ovariance
EFI	**E**uropean **F**orest **I**nstitute
EFISCEN	**E**uropean **F**orest **I**nformation **Scen**ario model
FAO	**F**ood and **A**gricultural **O**rganization
GPP	**G**ross **P**rimary **P**roduction
HFD	**H**eat **F**ield **D**eformation
HRM	**H**eat **R**atio **M**ethod
ICP	**I**nternational **C**o-operative **P**rogramme
ICOS	**I**ntegrated **C**arbon **O**bservation **S**ystem
iLEAPS	**I**ntegrated **L**and **E**cosystem - **A**tmosphere **P**rocesses **S**tudy
IPCC	**I**ntergovernmental **P**anel on **C**limate **C**hange
ITRDB	**I**nternational **T**ree-**R**ing **D**ata **B**ank
IUFRO	**I**nternational **U**nion of **F**orest **R**esearch **O**rganizations
LiDAR	**Li**ght **D**etection **A**nd **R**anging
MAB	**M**an **A**nd the **B**iosphere programme
NEP	**N**et **E**cosystem **P**roductivity
PAR	**P**hotosynthetically **A**ctive **R**adiation
REDD	**R**educing **E**missions from **D**eforestation and forest **D**egradation

RH	**R**elative **H**umidity
RMI	**R**oyal **M**eteorological **I**nstitute of Belgium
SF+	**S**ap **F**low **P**lus
SFM	**S**ustainable **F**orest **M**anagement
SIF	**S**olar **I**nduced **F**luorescence
SLA	**S**pecific **L**eaf **A**rea
TDP	**T**hermal **D**issipation **P**robe
TDP	**T**ime **D**omain **R**eflectometry
TER	**T**otal **E**cosystem **R**espiration
UN	**U**nited **N**ations
US	**U**nited **S**tates
UNESCO	**U**nited **N**ations **E**ducational, **S**cientific and **C**ultural **O**rganization
VWC	**V**olumetric **W**ater **C**ontent
WBD	**W**et **B**ulb **D**epression
WCR	**W**ater **C**ontent **R**eflectometer

Physical Constants

Speed of Light	c	=	299 792 458 $m.s^{-1}$
Planck's constant	h	=	$6.626\ 069\ 57 \times 10^{-34}$ $m^2.kg.s^{-1}$
Ideal gas constant	R	=	8.314 462 1 $J.mol^{-1}.K^{-1}$

Symbols

B	blue color channel value	—
C	hydraulic capacitance	$kg.m^{-3}.Pa^{-1}$
e_a	actual vapor pressure	Pa
e_s	saturated vapor pressure	Pa
F	vertical flux in turbulent flow	$kg.m^{-2}.s^{-1}$
F_{sapflow}	sap flow density	$L.s^{-1}$
F_{sapflux}	sap flux density	$m^3.m^{-2}.s^{-1}$
G	green color channel value	—
K	hydraulic conductance	$kg.s^{-1}.Pa^{-1}$
m	slope	—
PAR	photosynthetically active radiation	$mol.m^{-2}.s^{-1}$
r	correlation coefficient	—
R	red color channel value	—
R^2	determination coefficient	—
RH	relative humidity	%
RH_{ground}	relative humidity at ground level	%
RH_{P4}	relative humidity at platform 4	%
s	mixing ratio of substance ‘c’ in air	—
S_t	total incoming shortwave radiation	$W.m^{-2}$
SLA	specific leaf area	$m^2.kg^{-1}$

T	temperature	°C or K
T_{a}	air temperature or dry bulb temperature	°C
T_{d}	dew point temperature	°C
T_{ground}	temperature at ground level	°C
T_{P4}	temperature at platform 4	°C
T_{w}	wet bulb temperature	°C
V_w°	molar volume of pure water	$\mathrm{kg.mol^{-1}}$
VPD	vapor pressure deficit	Pa
VWC	volumetric water content	$\mathrm{m^3/m^3}$ or %
w	vertical wind speed	$\mathrm{m.s^{-1}}$
α	albedo	%
ΔD	diameter variation	m
ΔD_X	xylem diameter variation	m
ε_a	dielectric constant	—
Ψ_{atm}	atmospheric water potential	Pa
Ψ_{leaf}	leaf water potential	Pa
Ψ_{soil}	soil water potential	Pa
Ψ_{stem}	stem water potential	Pa
ρ_a	air density	$\mathrm{kg.m^{-3}}$

Summary

Trees have been with us for over 385 million years and since the beginning they have played a crucial role in the terrestrial ecosystem. They offer a multitude of ecosystem services (e.g. physical habitats, food and timber) which are unfortunately threatened to be reduced significantly due to global change, i.e. the combination of climate change and anthropogenic factors such as urbanization and air pollution. The knowledge regarding the integrated response of this change on forest ecosystems is limited and therefore, to further increase our understanding, it is necessary to monitor these forest ecosystems.

There are currently three main monitoring techniques: remote sensing, eddy covariance method and visual vitality assessment. (i) While remote sensing offers the ability to monitor over a very large spatial scale and does not require physical contact, it is a very costly technique and the temporal resolution is low. (ii) The eddy covariance method is well developed and offers continuous data, but it is costly, has its limitations and quite a few assumptions are made. (iii) Visual vitality checks are often used in current monitoring surveys, but it is very labor-intensive and can primarily be used for long-term trend analysis. 'The Twittering Tree' adopts the strong points and fixes the weak points of the previous techniques by only using a dendrometer to measure the diameter variation of an individual tree and a sap flow sensor to measure the sap flow rate in that tree. These sensors offer the possibility to collect continuous real-time data and through networking of several individually monitored trees, it is possible to monitor over larger spatial scales, very cost-efficiently. Furthermore, data is collected from the actual tree itself.

This study used several meteorological, pedological and physiological sensors in the experimental forest Aelmoeseneie and in a smaller set-up at the Faculty of Bioscience Engineering to collect as much information as possible from beech (*Fagus sylvatica* L.) and oak (*Quercus robur* L.). The response of both tree species to a changing microclimate was monitored for

over a year. Several interesting results were obtained during the timespan of this study. It appears that drought followed by extreme rain events are more harmful for oak than for beech. Also the bark hygroscopicity differs significantly for both species which needs to be taken into account when evaluating dendrometer measurements. It was possible to observe that oak had more trouble with its water flow during the growing season of 2014 when compared with beech. Beech however, was stressed a little bit during July and August due to the high amount of precipitation during this period.

It was observed that hysteresis occurs and that everything is interconnected, thus allowing to link variables with each other. For example the contribution of xylem shrinkage to total shrinkage (i.e. 24.6%), ratio between stem and leaf water potential (i.e. 0.52) and SLA along the tree crown were determined. Finally, it was concluded that one tree of each main species in a forest stand might already be sufficient to monitor the respective forest stand.

With the knowledge from this study, it was possible to already make a well-founded and prompt judgement on the status of beech and oak in the experimental forest Aelmoeseneie. Future research will offer the possibility to unlock the potential of this project and take it to the next level.

Samenvatting

Reeds 385 miljoen jaar staan er bomen op onze planeet en sinds het begin spelen ze een cruciale rol in het terrestrisch ecosysteem. Ze bieden een hele resem aan ecosysteemdiensten aan (e.g. fysieke habitats, voedsel en hout), maar deze dreigen helaas verloren te gaan of althans gedegradeerd te worden onder invloed van 'global change'. Dit is de combinatie van klimaatverandering en antropogene factoren zoals verstedelijking en luchtvervuiling. Kennis over de geïntegreerde respons van deze verandering op bosecosystemen is beperkt. Daarom is het monitoren van bosecosystemen een noodzaak daar het sterk kan bijdragen tot het doorgronden van deze respons.

Momenteel worden voornamelijk drie technieken gebruikt bij het monitoren van bossen: teledetectie, eddy covariantie methode en visuele vitaliteitscontrole. (i) Hoewel teledetectie de mogelijkheid biedt om over zeer grote oppervlaktes te monitoren en er geen fysiek contact nodig is, is het een zeer kostelijke techniek waarbij de temporele resolutie laag is. (ii) De eddy covariantie methode is goed ontwikkeld en biedt continue data aan, maar het is duur en een reeks veronderstellingen worden gemaakt. (iii) Visuele vitaliteitscontroles worden veelvuldig toegepast in huidige vitaliteitsinventarisaties. Het is echter zeer arbeidsintensief en de data is voornamelijk bruikbaar bij lange termijn trendanalyses. 'The Twittering Tree' tracht van deze drie technieken de positieve punten over te nemen en de negatieve op te lossen. Dit door middel van een dendrometer die de diameter variatie meet en een sapstroom sensor die de sap flux densiteit bepaalt. Deze sensoren maken het mogelijk om continue real-time data te verzamelen en het netwerken van verschillende individuele bomen maakt het mogelijk om grotere spatiale schalen te monitoren wat de kostenefficiëntie ten goede komt. Bijkomend wordt data verzameld van de bomen zelf.

Tijdens dit onderzoek werden meteorologische, bodemkundige en fysiologische sensoren gebruikt, in het experimentele proefbos Aelmoeseneie en in een kleinschaliger experiment

op de Faculteit Bio-Ingenieurswetenschappen, om zo veel mogelijk informatie te verzamelen van zowel beuk (*Fagus sylvatica* L.) en eik (*Quercus robur* L.). De respons van beide boomsoorten op een wijzigend microklimaat werd gemonitord gedurende meer dan een jaar. Er werden interessante resultaten bekomen tijdens deze studie. Zo blijkt droogte gevolgd door extreme regenval meer schadelijk te zijn voor eik dan voor beuk. Ook is de hygroscopiciteit van de schors sterk verschillend voor beide soorten wat aldus in rekening dient gebracht te worden bij het evalueren van dendrometer metingen. Verder werd bepaald dat eik meer moeite ondervond met zijn sapstroom tijdens het groeiseizoen van 2014 en dat beuk licht gestresseerd was in juli en augustus door de grote hoeveelheid neerslag.

Er werd bevestigd dat hysteresis plaatsvindt en dat alles is geïnterconnecteerd, wat toestaat om diverse variabelen met elkaar te linken. Bijvoorbeeld de contributie van xyleemkrimp ten opzichte van de totale krimp (24.6%), ratio tussen stam- en bladwaterpotentiaal (i.e. 0.52) en SLA op verschillende kroonhoogtes werd bepaald. Finaal werd geconcludeerd dat één boom van iedere hoofdsoort in een bosbestand reeds voldoende kan zijn om het gehele bestand te monitoren.

Met de kennis bekomen in deze studie was het mogelijk om reeds een goed onderbouwde en prompte beslissing te maken over de status van beuk en eik in het experimentele proefbos Aelmoeseneie. Toekomstig onderzoek zal toelaten het potentiaal van dit project ten volle te ontplooien.

Introduction

The importance of forests

The earliest tree-like organism is most likely *Wattieza*, which existed in the Middle Devonian about 385 million years ago [Stockmans, 1968, Berry, 2000]. Since the beginning these perennial plants play a crucial role in the terrestrial ecosystem [Lowman, 2009]. They dominate the area in forest ecosystems and drive aboveground biomass from tropical to moderate lowland forests [Satō and Madgwick, 1982, Slik et al., 2013].

Forests are the dominant terrestrial ecosystem on Earth. They cover 31% of the world's land area, i.e. 4.03 billion hectare [FAO, 2010], and while for example tropical forests cover only 7% of the Earth's land mass, they house more than 50% of the world's plant and animal species [Rainforest Foundation US, 2015]. Forests account for 75% of the terrestrial GPP (gross primary production) and 80% of the Earth's total plant biomass [Beer et al., 2010]. Consequently they hold more carbon in their biomass than is stored in the atmosphere [Prentice et al., 2001, Schaphoff et al., 2006, Pan et al., 2011].

Trees are fundamental for life on Earth and can truly be called ecosystem engineers [Jones et al., 1996] as they modulate the availability of resources and create habitats for other species via their own physical infrastructure. Trees harvest the energy of the sun by converting light energy to chemical energy and are an important step in the carbon, nutrient and water cycle [Taiz and Zeiger, 2010]. Forests have the greatest potential for carbon storage of all biome types [Canadell and Raupach, 2008] as photosynthetic uptake of carbon from the atmosphere provides fuel for biotic processes such as cell growth and metabolism where, in turn, CO_2 is respired [Taiz and Zeiger, 2010]. Decomposition of litter from the canopy provides organic matter to the soil and drives nutrient cycling. Trees provide a coupling between the water in the soil and the atmosphere through water uptake via the roots, transport of sap in the trunk and transpiration of water at leaf level, which makes them a very important modulator of the regional climate. Even more they provide a multitude of ecosystem services, e.g. food, timber, medicine, better air quality, shelter, aesthetic values, spiritual values and habitats [Mooney et al., 1996, Gamfeldt et al., 2013,

Pan et al., 2013], especially in tropical regions [Brandon, 2014]. It is clear that besides environmental benefits, trees also contribute several economic and sociocultural benefits.

All these important functions are being directly and indirectly affected by global change [Foley et al., 2007, Mooney et al., 2009, Seidl et al., 2011, IPCC, 2013]. Global change denotes climate change together with worldwide anthropogenic factors such as urbanization and air pollution [Pautasso et al., 2010]. Increasing CO_2 levels may enable trees to be more productive [Frank et al., 2015], but sufficient water and nutrients need to be available [Morison and Lawlor, 1999, Boisvenue and Running, 2006, Lindner et al., 2014]. Warming can increase the length of the growing season, but it can also shift the geographical ranges of species making their current habitats no longer suitable and cause extinction [Morison and Lawlor, 1999, Lindner et al., 2014]. Extreme drought (Figure 1) and flooding events can induce large amounts of stress and ultimately cause tree mortality due to a deteriorating water balance [Morales et al., 2007, Lindner et al., 2014]. All of this is acknowledged by Forest Europe in 1993, leader in pan-European forest policy, which used the numerous functions of trees to develop criteria and indicators for sustainable forest management (SFM) in conjunction with EFI (European Forest Institute) [Baycheva et al., 2014].

While scientists already know a fair amount about how these individual variables affect trees through small and medium scale experiments, e.g. increased CO_2 levels [Reddy et al., 2010], there is little knowledge on what the *in situ* effects are [Morison and Lawlor, 1999] and what the global status of forests is [Fagan and DeFries, 2009]. What is the integrated response of forest ecosystems to the accelerated climate change? How resilient and resistant are trees to a rapidly changing environment? Will trees be able to maintain their crucial role in the terrestrial ecosystem? A network of individually monitored trees that can visualize the status and response of a tree or forest to a changing climate, in real-time, could offer an answer to all these questions, but more data and knowledge is required.

FIGURE 1: Crown dieback due to severe 2010 drought in Central Indiana [Carter, 2011].

Chapter 1

Literature review

1.1 Scales and types of tree monitoring

Tree monitoring is an essential tool required in analyzing forest ecosystem health, vitality, productivity and responses to climate change [Lindner et al., 2014, Michalak, 2014]. Continuous and real-time data has the potential to provide useful information not only about the microclimate, but also about important (eco)physiological data such as tree water relations and tree growth [Meinzer et al., 2004]. Furthermore it can help us understanding the dynamics of forest functioning and the response of trees to a changing environment [Lindner et al., 2014]. The key to effective tree monitoring is having a long-term commitment [Tobin and Nieuwenhuis, 2012] and collect continuous data instead of point measurements. Data collection can be performed on different scales. What follows is an overview of several methods on different scales currently used in scientific research.

1.1.1 Large scale monitoring

1.1.1.1 Remote sensing

Monitoring on the largest spatial scale, i.e. thousands of hectares [Fagan and DeFries, 2009], is commonly carried out by using remote sensing. This is the acquisition of information using imagery of a particular ecosystem without making physical contact with the ecosystem, i.e. no *in situ* measurements. Aerial sensor technologies are being used, attached to aircrafts and satellites [Schott, 2007].

Remote sensing by satellites has made it possible to greatly improve our understanding of the climate system and its changes by quantifying processes and spatiotemporal states of the land, the oceans and the atmosphere [Yang et al., 2013] (Figure 1.1). Relevant applications include environmental assessment, ecosystem monitoring, global change detection

and forest mapping [Schowengerdt, 2007]. Holmgren [2008] discusses the possibilities of the use of remote sensing in UN-REDD (*vide infra*) where satellite imagery and scenario modeling is used to map deforested areas and analyze historical trends. Also Gibbs et al. [2007] and more recently Vicharnakorn et al. [2014] discuss the possibility to even monitor carbon stocks in the REDD programme using remote sensing. It is particularly useful in inaccessible tropical forests, e.g. the Amazon basin.

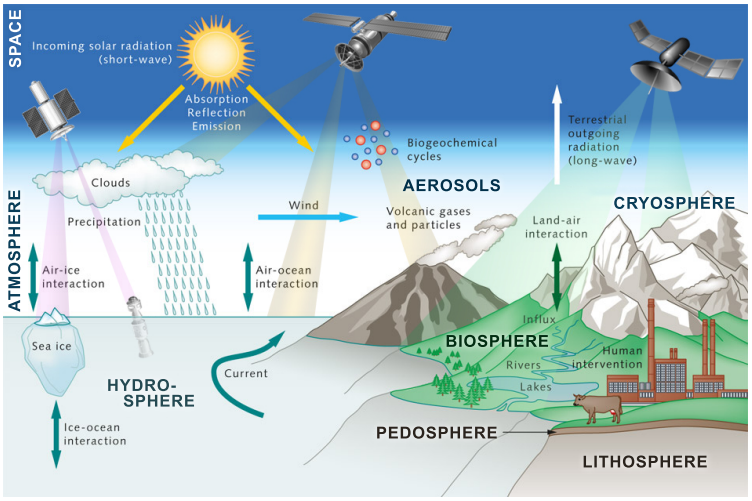

FIGURE 1.1: Gathering information from each part of the Earth system. The role of satellite remote sensing in climate change studies. [Modified image, originally by Bollmann et al. [2010]]

A pristine example of remote sensing is the Landsat program, started in 1972 (`http://landsat.gsfc.nasa.gov/`). It is one of the longest running enterprises to acquire satellite imagery of Earth. The images are used in numerous fields, from agriculture to forestry, surveillance and education. Landsat 7 has a moderate spatial resolution of 15-60 m and a temporal resolution of 16 days. Regarding forestry it is mainly used to monitor deforestation and land use changes. Another recent initiative, with a spatial resolution of 5 m, is the European Earth Observation Programme called Copernicus (`http://copernicus.eu`). It is fully operational since 2014 and it aims at achieving multi-level Earth observations. Copernicus provides access to geographical information on land cover, variables related to the vegetation state or the water cycle and climate indices. Another initiative, the GeoEye-2, is planned to be launched mid 2016 and will be a commercial Earth observation satellite with the highest resolution ever, namely 34 cm [EXELIS, 2012].

It is clear that a lot of advances have been made in the last two decades [Holmgren and Thuresson, 1998, Fagan and DeFries, 2009] and satellite images contain more and more useful information. Most recent advances in this field are hyperspectral remote sensing [Thenkabail et al., 2011, Ramoelo et al., 2015] and remote sensing of solar induced fluorescence (SIF) [Meroni et al., 2009, Tol et al., 2014]. Both are 'hot topics' in scientific research and have a great potential to directly detect stress in plants over large areas.

There are however limitations regarding remote sensing. The high cost, ranging from €0.10/km^2 (radar) to €300/km^2 (LiDAR, i.e. light detection and ranging), and the high complexity which makes it difficult to find a consistent index, are the major issues. Also the temporal resolution is often too low, mostly several days or weeks, to provide useful information regarding the dynamic processes in tree physiology. And while for example LiDAR instruments and stereo cameras offer very accurate estimates of variables and have a high pixel resolution, e.g. a narrow LiDAR beam can map physical features of up to 30 cm.px^{-1} [Carter et al., 2012], they are spatially too limited [Fagan and DeFries, 2009]. The GeoEye-2 however offers interesting perspectives for the future.

1.1.1.2 Eddy covariance

The eddy covariance (EC) technique is a well-developed and commonly used method for measuring the exchange of CO_2 between terrestrial ecosystems and the atmosphere, i.e. net ecosystem productivity (NEP) [Aubinet et al., 2012]. This technique uses several sensors, commonly installed on a tower and measures besides NEP, also water vapor and energy fluxes [Burba and Anderson, 2007]. This allows defining the condition of an ecosystem and determining the response of accelerated climate change [Baldocchi, 2003]. It is therefore used to validate and improve models, e.g. global climate models, ecological models and weather models [Fisher et al., 2008, Liu et al., 2014]. The measurements are continuous, semi-automatic and typically integrate an area of the order of 20 ha [Watson et al., 2000].

The basic principle of the EC method is considering an air flow as a horizontal flow consisting of numerous rotating eddies, i.e. turbulent fluxes of variable sizes (Figure 1.2). EC relies on direct and very fast measurements of actual gas transport by a 3D wind speed in this air flow. These measurements are subsequently used in calculations of turbulent fluxes within the atmospheric boundary layer [Burba and Anderson, 2007]. Series of calculations finally results in a general 'Eddy flux' equation (Equation 1.1):

$$F \approx \overline{\rho_a}\,\overline{w's'} \tag{1.1}$$

with F, vertical flux in turbulent flow (kg.m^{-2}.s^{-1}); $\overline{\rho_a}$, mean air density (kg.m^{-3}); $\overline{w's'}$, mean covariance between deviations in instantaneous vertical wind speed w (m.s^{-1}) and mixing ratio s of substance 'c' in air (—).

Vertical flux can thus be presented as a covariance of the vertical wind velocity and the density of either terrestrial carbon, water vapor or another entity of interest. Sensible heat flux and latent heat flux are computed in a similar manner. However, a few important assumptions are made in order to obtain these 'simple' equations. For example air density fluctuations are assumed negligible, as is mean vertical flow because a horizontal and homogenous terrain (i.e. no divergence/convergence) is presumed. Detailed and thorough calculations of these deviations can be found in Lee et al. [2006] and Baldocchi [2009].

FIGURE 1.2: Air flow as a horizontal flow of numerous rotation eddies [LI-COR, Inc., 2015].

While EC is a commonly used technique and has a large amount of scientific support, there are a few limitations. Measurements need to be obtained at a point representing an upwind area, inside the boundary layer of interest and inside the constant flux layer. The flux is assumed to be fully turbulent and the terrain should be flat with an uniform vegetation [Burba and Anderson, 2007]. Proper site selection and experimental setup are thus a high priority and the requirement for high precision measuring devices make it a rather costly technique of the order of €45000 [Watson et al., 2000]. Furthermore does a tower site not operate over a large enough area (i.e. 20 ha) to provide a sufficiently unbiased sample area [Watson et al., 2000]. For example Aelmoeseneiebos (28.5 ha), Kloosterbos (100 ha) and Meerdaalwoud (2050 ha) are a few important forests in Flanders which already exceed the operating area of an EC tower. Finally, the argument could be made that the EC technique does not provide a 'true' evaluation of the ecosystem as it does not measure on the vegetation itself to estimate the vitality and productivity of the study ecosystem.

1.1.2 Small scale monitoring

1.1.2.1 Diameter monitoring

Measurements of the diameter at breast height (DBH) (mm) of trees are included in many forest inventories and monitoring initiatives [Wouters et al., 2008]. Diameter monitoring allows a forest manager to analyse the radial growth and thus to calculate the volume increment of a stand [Jansen et al., 1996] which is useful in production forests. It has its applications in the field of dendrochronology [Drew and Downes, 2009] and the measurements are also very helpful in forest ecology and tree physiology as dendrometers provide easily interpretable information about the stem diameter change which can then be used as a proxy for several physiological processes [Zweifel et al., 2001, 2010, De Schepper and Steppe, 2010, De Swaef and Steppe, 2010, Steppe et al., 2015b].

Diameter change data can help to monitor either short and long-term growth patterns. It is thus important to carefully consider the required measurement accuracy [Keeland and Young, 2014]. Periodic inventories or long-term studies of forest growth response [King et al., 1998] which are carried out over long intervals, i.e. several years, do not require a high level of accuracy. A resolution of 1 mm is already sufficient. Studying the contribution of the several tissues (i.e. xylem cylinder, cambial zone, bark and phloem) to the diurnal shrinkage in stems [Zweifel et al., 2000, Daudet et al., 2005] requires a much higher accuracy, in the order of magnitude of micrometers.

Dendrometers can be segregated in either contact and non-contact instruments [Clark et al., 2000, Drew and Downes, 2009]. A traditional dendrometer band is a commonly used contact instrument in forestry to obtain repeated measurements of tree stem growth at a fixed height. Other contact methods to measure tree diameters include calipers, diameter tapes or point dendrometers. Non-contact instruments include optical calipers (e.g. mirror relascope by Bitterlich et al. [1984]), prisms and optical forks [Drew and Downes, 2009]. Dendrometer bands tend to underestimate first-year growth due to slack in the bands after installation and species differences related to bark and stem characteristics [Keeland and Sharitz, 1993], but generally offer good results. Diameter tapes are quick and easy to read, but the impossibility to position the tape in the exact same place during repeated measurements can result in potentially large errors [Bower and Blocker, 1966].

When monitoring is discontinuous, the amount of error introduced by analogue methods is acceptable. Continuous monitoring however requires a high accuracy. Point dendrometers fit the bill perfectly as they make it possible to detect changes in the stem radius with a resolution of less than 1 µm [Steppe and Lemeur, 2004, Zweifel, 2012]. Furthermore they are easy to install, are non-invasive and the temporal resolution can be set as desired. These attributes make the point dendrometer an ideal instrument for tree monitoring.

1.1.2.2 Measuring sap flow

Determining the sap flux density (F_{sapflux}) ($cm^3.cm^{-2}.s^{-1}$) and the amount of sap (F_{sapflow}) ($L.h^{-1}$ or $g.h^{-1}$) a tree transports has gained more and more interest in plant science and can roughly be separated in three main approaches [Atwell et al., 1999]. (i) Applying tracing dyes in the stem has already been used for centuries. Careful selection of the dye is crucial [Sano et al., 2005], preferably a dye with negatively charged ions to reduce association with the negatively charged vessel walls. Application of the dye is a precarious task as for example water-deficient tissues will tend to artificially suck in the dye after application. An alternative to dyes is (ii) the use of radioisotopes [Atwell et al., 1999]. These are useful tracers of water flow, but are confronted with the same issues as dyes. For example, cationic isotopes tend to bind to the xylem walls. Radioactive phosphorus (^{32}P) has the potential

to be a good tracer because it is anionic and is a strong emitter. Deuterated water (D_2O) is also frequently used in water transport research [Meinzer et al., 2006].

Since the application of dyes and radioisotopes, many other methods have been developed. Most of these are based on the (iii) application of heat in the sapwood, i.e. heat-flow and heat-pulse methods. They offer a non-invasive measurement of water flow in stems. There are several approaches to this two techniques, but they are all based on the same working principle [Vandegehuchte and Steppe, 2013]. A heating source surrounded by temperature detectors (e.g. thermocouples) applies heat to a part of the stem (Figure 1.3). If water flow is present, the thermal profile will be transported upwards providing a temperature shift. If there is virtually no sap flow, a 'zero-flow' profile will be observed.

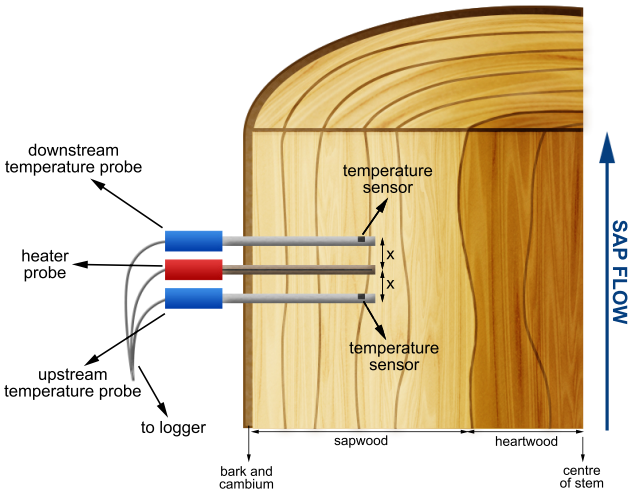

FIGURE 1.3: An HRM sap flow sensor configuration. [Redrawn from ICT International [2015]]

The heat-flow methods, heat field deformation (HFD) method [Nadezhdina et al., 2012] and thermal dissipation probe (TDP) [Granier, 1985], apply continuous heat to the sapwood. Because a measured temperature ratio is empirically linked to F_{sapflux}, a calibration for each species might be necessary. Furthermore it can lead to over- or underestimations depending on various factors inherent to the tree [Vandegehuchte and Steppe, 2012b, 2013].

Heat-pulse methods apply heat in a pulsating manner. It includes the compensation heat-pulse (CHP) method [Huber and Schmidt, 1937], Tmax method [Cohen et al., 1981], heat ratio method (HRM) [Burgess et al., 2001] (Figure 1.3) and SapFlow+ method [Vandegehuchte and Steppe, 2012c]. While CHP method does not require the determination of wood characteristics, it is incapable of measuring low, very high and reverse flows [Steppe et al., 2010]. The Tmax method determines the thermal diffusivity correctly, but needs 'zero-flow' in order to do this. Furthermore this technique is unable to correctly estimate low and reverse flows [Green et al., 2008]. HRM is a very accurate method, but has a nonlinear relation at higher flow rates [Burgess and Dawson, 2008] and applies an inaccurate protocol to determine the thermal diffusivity [Vandegehuchte and Steppe, 2012a].

The most recent and advanced method is referred to as SapFlow+ and is the only method leading to good results for negative, low and high sap velocities. It is furthermore capable of determining thermal wood properties (included in model calibrations) and water content of the sapwood (simultaneously estimated with heat velocity). The SapFlow+ method is however computationally intensive as the model is fit to each pulse every 10 to 15 minutes.

1.1.2.3 Visual vitality assessment

Visual assessment of the crown condition is a commonly used method to determine the vitality of a tree. ICP Forests (*vide infra*) developed a list of methods and criteria for harmonized sampling, assessment, monitoring and analysis [Eichhorn et al., 2010]. Defoliation and leaf discoloration are the two most important parameters regarding tree stress. The latest technical report from ICP Forests from 2014 recommends to assess these parameters in 5% steps [Michel et al., 2014]. Subsequently five defoliation and discoloration classes are differentiated (e.g. Sioen and Roskams [2014]). Vitality research offers a great insight in the amount of stress a tree is experiencing and helps monitoring it on a spatial scale. Especially this last factor can assist to demarcate risk zones to spatially limit tree diseases [Santos and Bond, 2014]. There are however disadvantages. In most cases it is too late to save a tree experiencing advanced defoliation or leaf discoloration as it does not allow early determination of stress. In addition, the monitoring is very labor-intensive as it requires one or even two persons to inspect each tree individually [Sioen and Roskams, 2014].

1.2 Current monitoring networks

While monitoring is done on several different spatial scales, it is also executed on different regional levels. There are some very large networks in place which try to monitor trees or (forest) ecosystems as a whole and while their primary idea is generally the same, i.e. collect data regarding ecosystem functions, there are very large differences in their goals, methodology, data processing and data usage. What follows is a brief listing and evaluation of several prominent monitoring networks and/or framework initiatives.

1.2.1 International networks

ICP Forests (`http://icp-forests.net/`) is launched in 1985 and collects data of more than 7500 plots in 42 countries. They distinguish between extensive Level I monitoring (since 1985) and intensive Level II monitoring (since 1995) plots. Level I monitoring aims at representative estimates on tree condition across Europe measuring crown (annually) and soil condition (two times since 1990). Level II monitoring focuses on ecological interactions

in forest ecosystems and measures flux, soil and meteorological variables. Only at Level II plots data is collected continuously over time. Their strong point is having a harmonized method across all plots to take measurements to ensure high quality data. This makes ICP Forests unique in global forest monitoring efforts. Tree growth is measured only once every five years and the phenology is evaluated several times per year. While they collect a very large amount of data, it is primarily used for trend reporting and developing policies The annual crown assessments and five-yearly diameter measurements are not sufficient to monitor and predict the dynamic effects of climate change on forests.

FLUXNET (`http://fluxnet.ornl.gov/`) combines EuroFlux (1996) and AmeriFlux (1997) since 1998 but also coordinates CarboEuroFlux, Fluxnet-Canada, ChinaFlux, Asiaflux, OzFlux and an assortment of smaller regional networks. It is thus a worldwide network of regional networks of micrometeorological tower sites and provides an infrastructure to compile and distribute data with a uniform terminology to the scientific community [Chapin III et al., 2002]. They use the EC method to measure the fluxes of terrestrial carbon, water vapor and energy between the biosphere and the atmosphere and there are almost 700 tower sites operated on a long-term and continuous basis. Their main goals are quantifying spatial differences, temporal dynamics and fluxes due to changes in temperature, soil moisture, CO_2 and water vapor. Some sites collect data regarding vegetation, soil, hydrology and meteorological characteristics, but data related to the actual trees (e.g. tree diameter and sap flow) is not collected or not used to its full potential.

The United Nations Programme on Reducing Emissions from Deforestation and Forest Degradation (**UN-REDD** Programme, `http://un-redd.org/`), established in 2008, provides technical and financial support to developing countries to help them develop the capacities necessary to implement **REDD+**. REDD+ is an international mechanism to reward developing countries for reducing emissions from deforestation and forest degradation with not only environmental but also social and economical benefits. To achieve this it is necessary to monitor deforestation, forest degradation and more importantly carbon stocks. Deforestation can easily be monitored with remote sensing technology, but forest degradation and carbon stocks require ground measurements, although advances are being made [Vicharnakorn et al., 2014]. A trade-off has to be made between cost and accuracy of the meansurements. Official guidelines are yet to be established, though IPCC has developed the important first steps [Angelsen et al., 2008]. Because few developing countries have comprehensive national inventories the data is often uncertain. New cost-effective techniques could greatly increase the reliability of the REDD+ program.

iLEAPS (Integrated Land Ecosystem - Atmosphere Processes Study, `http://ileaps.org/`) focusses on the basic biogeochemical processes that link land-atmosphere exchange, climate, the water cycle and tropospheric chemistry. They recognize the need for an integrated way of doing environmental earth science. iLEAPS assists in planning and implementation of research, database management and data syntheses. Also communicating

research results to the broader scientific community as well as the policy community and general public is on their activities list. According to the iLEAPS Science Plan 2010, the biggest priority is a ground-based ecosystem observation system and observational network. iLEAPS acknowledges the fact that models are advanced to the point where they can fully simulate the coupling between the physical, chemical and biological processes in the climate system, but lack suitable data for calibration, evaluation and realistic simulations.

In a recent article **IUFRO** (International Union of Forest Research Organizations) discusses the possibilities for a network of supersites [Matyssek et al., 2015]. Their goal is very ambitious as they want to create a global network, focussing on the tropics, where sophisticated state-of-the-art instruments are used and a multitude of factors in the ecosystem are measured to obtain baseline data. They will share the information and knowledge gained from the Supersite network to help people understand how forests affect the climate and vice versa. Once in place, this network will have a great potential to offer a significant understanding of our ecosystems. The cost and labour however that will go into setting up this network are most likely very high, making it (currently) unrealistic.

The Man and the Biosphere Programme (**MAB**) launched in 1971 by **UNESCO** (`http://unesco.org/`) aims at improving the relation between people and their environment on the basis of scientific research. One of their main goals is to assess changes in the biosphere caused by human and natural activities and its effects, particularly in the context of climate change. MAB is active in 119 countries and currently counts 631 biosphere reserves ('sites of excellence'). It is clear that this programme is active on a very large scale and is more leaning towards the socio-economic side of ecosystems instead of the ecological side. Monitoring and research are mainly executed in function of sustainable development and policies. While their World Network of Biosphere Reserves (WNBR) is very important as it allows people to work together and share ideas, it focuses on economic and social sustainability rather than the actual collection of physiological and ecological parameters. As they say in one of their promotion videos [UNESCO, 2014]: "Biosphere reserves are not about nature conservation, they are about people".

ITRDB (International Tree-Ring Data Bank, `http://ncdc.noaa.gov/`) is the world's largest archive of tree ring data. It includes raw data on tree ring width, wood density, isotope measurements and site growth index chronologies. Over 3000 sites on six continents are included. The data is quality checked, has an annual resolution and spans many decades of forest growth. Gea-Izquierdo et al. [2014] puts forward the idea that these tree-ring records could be used as an input in traditional empirical models or process-based models [Misson, 2004, Drew et al., 2010] to for example estimate ecosystem productivity. While this data has the great potential to gain large scale information regarding several ecosystem parameters, it can not be used to determine dynamic (stress) responses of trees to changes in the climate. This requires continuous measurements or at least measurements with a much higher temporal resolution than an annual resolution.

1.2.2 European networks

The European monitoring network **ICOS** (Integrated Carbon Observation System, `http://icos-infrastructure.eu/`), founded in 2001, is a research infrastructure dedicated to high precision observations of greenhouse gas concentrations and fluxes. Currently there are 17 participating countries with in total 70 observation stations. Through its European network it tries to fully understand the global carbon cycle, the evolution of greenhouse gasses and the impact of climate change on regional greenhouse gas balances. Besides understanding the present state, it provides the ability to predict future behavior and assess the effectiveness of carbon sequestration and/or greenhouse gases emission reduction activities. They focus on long-term, continuous and near real-time measurements of atmospheric greenhouse gas concentrations, local terrestrial exchange of carbon, water vapor and energy and oceanographic air-sea fluxes using flux towers. ICOS sites also measures other variables such as precipitation, soil water content, litterfal and tree diameter but this data is not available on every site nor is continuous.

FOREST EUROPE (`http://foresteurope.org/`), previously known as the **MCPFE** (Ministerial Conference on the Protection of Forests in Europe), helps developing the policy on sustainable management for forests in a pan-European context. FOREST EUROPE offers common strategies to its 46 member countries and the European Union. They developed six criteria for sustainable forest management (SMF) with as (i) first criteria the maintenance of forest resources and their contribution to global carbon cycle and as (ii) second criteria the maintenance of forest ecosystems' health and vitality. At the most recent conference, Oslo 2011, the 'European 2020 targets for forest' were assembled. FOREST EUROPE does not monitor forests as such, but they do use and analyse data from several sources, e.g. ICP Forests (cf. section 1.2.1), to develop their policies and strategies.

TreeNet Switzerland (`http://treenet.info/`) is a monitoring and research network which is part of the Swiss Federal Institute for Forest, Snow and Landscape Research (**WSL**). TreeNet continuously measures tree stem diameter fluctuations with point dendrometers in 26 different locations. It is currently constructing new sites in Finland, Sweden and Poland. The data is processed and analyzed to evaluate the response of forest ecosystems to climate change. Also microclimatic variables of air and soil, carbon and water exchange between forest and atmosphere, and site-specific ecophysiological variables are recorded. The project is initiated by Roman Zweifel (WSL) and Werner Eugster (ETHZ) in 2009. TreeNet tries to use tree diameter variation as a biological drought indicator, indicator for forest growth and thus to predict expected annual carbon sink of forest ecosystems. They do this by linking the tree diameter fluctuations to the tree water relations. TreeNet is however not using sap flow measurements to complement their tree diameter measurements. Sap flow measurements can greatly increase the understanding of stress responses of trees to a changing climate and unravel the dynamic hydraulic functioning of trees.

1.3 Eddy covariance versus tree monitoring

As explained earlier, the EC technique allows the gathering of very useful data regarding carbon, water and energy fluxes between the biosphere and the atmosphere. There are however quite a few limitations and assumptions regarding this method. It is costly to operate which causes limited spatial coverage of the ecosystem, data is complex to collect, requires high-precision instruments and the EC method only measures external variables in comparison to variables linked with the actual trees, e.g. diameter variation and sap flow. Another disadvantage is the fact that the NEP measured by EC also includes carbon fluxes from the soil and vegetation on the forest floor and thus only represents a net carbon flux. Direct quantification of flux components (i.e. contributions from wood, fruits, leaves, soil) is not possible [Buchmann and Schulze, 1999, Baldocchi, 2003]. This is where individual tree monitoring is obviously superior on many levels and has the potential to become a key tool to extend carbon balances or ecosystem productivity on larger time scales and areas.

Standalone data regarding diameter variation is already a very good proxy for several physiological processes [Zweifel et al., 2001, 2010, Gea-Izquierdo et al., 2014]. Including sap flow data offers great possibilities to retrieve information about carbon sequestration and plant-water relations when monitored with a high temporal resolution. Consequently it enables the possibility to better understand the dynamic (stress) response of trees to changes in the regional climate. The added benefit from using data retrieved from the actual vegetation results in the possibility to offer a true analyses of the studied forest stand or ecosystem without the many limitations and assumptions made by the EC technique.

Another important aspect is the cost efficiency. A point dendrometer from Natkon (ZN11-T-WP) costs CHF 680 ($\approx$ €655) and a SFM1 Sap Flow Meter from ICT International €1500. This is a fraction of the cost of an EC tower, which is approximately €45000 [Watson et al., 2000]. Not only the reduced cost, but also the reduced complexity of individual tree monitoring, regarding installation and data collection, provides the possibility to monitor a broader area (Section 4.7) and collect a larger amount of data when comparing one flux tower, with a spatial resolution of 20 ha [Watson et al., 2000], for the same cost.

A final reason why to consider individual tree monitoring is regarding biodiversity studies. This is explained in a recent paper by Nadrowski et al. [2010]. It suggests that exploiting information at the scale of individual trees when studying biodiversity in forest ecosystems may offer greater benefits because diversity effects in forest communities can be traced down to interactions at the individual neighborhood scale. This as a result of trees storing their growing history in their woody tissue.

1.4 Tree diameter variation as key variable

1.4.1 Link with ecosystem productivity

NEP is the difference between GPP, i.e. CO_2 sinks (terrestrial plants), and total ecosystem respiration (TER), i.e. CO_2 sources (respiration, leaching and disturbance) [Chapin III et al., 2011]. It represents the total amount of organic carbon in an ecosystem available for storage, export or nonbiological oxidation (e.g. fire) [Chapin III et al., 2011]. Trees form the dominant carbon sinks of the ecosystem, as they use carbon for wood and phloem growth [Barford et al., 2001, Stoy et al., 2009]. Continuous measurement of diameter variation can offer great insight about this sink [Rocha et al., 2006]. Even more so, these measurements can be used to determine stem water content and thus help explaining tree-water relations [Steppe et al., 2006]. This approach offers the possibility to link ecophysiological plant responses to large scale processes such as climate change.

Already several forest growth measurements and models assume a close connection between the stem growth of a tree and its carbon balance [Zweifel et al., 2010, Steppe et al., 2015a]. Zweifel et al. [2010] addresses the relationship between continuously changing stem radii and corresponding ecosystem productivity. It was concluded that NEP, of the subalpine coniferous forest Seehornwald Davos in the Swiss Alps, is highly predictable from diameter variation at various integration times (30 min to years). Furthermore, they found that tree water relations and stem growth are representative for the productivity of this forest ecosystem. Recently, also Gea-Izquierdo et al. [2014] related tree-ring growth to ecosystem productivity for two tree species, *Pinus banksiana* Lamb. and *Picea mariana* Mill., using a model calibrated with EC data. The results agree with those of Berninger et al. [2004] and Zweifel et al. [2010], but the relationships were different for the two species, probably reflecting differences in phenology and species-specific carbon allocation strategies.

The hypothesis that tree growth can be used as a proxy for ecosystem productivity is currently accepted and confirmed [Berninger et al., 2004, Zweifel et al., 2010, Gea-Izquierdo et al., 2014] in the literature. It is, however, still unclear what the biotic drivers are and through what mechanisms diameter variation and NEP are linked. A deeper understanding of the possible interfering factors, in particular internal variations in carbohydrate allocation [Gea-Izquierdo et al., 2014], is required.

1.4.2 Link with water flow

Stem water storage capacity and diurnal patterns of water use have already been studied widely for several decades [Schulze et al., 1985, Goldstein et al., 1998, Meinzer et al., 2004, Steppe et al., 2006]. The variables sap flow F_{sapflow} (L.h^{-1}), leaf water potential Ψ_{leaf} (MPa), diameter variation ΔD (mm) and photosynthetically active radiation or PAR

(μmol.m^{-2}.s^{-1}) all show a clear diurnal pattern (Figure 1.4) and are closely linked [Tyree and Ewers, 1991, Meinzer et al., 2004]. As PAR rises at dawn, the stomatal diffusion resistance will decrease resulting in a decreasing, i.e. more negative, Ψ_{leaf} which is here used as a proxy for transpiration [Uddin et al., 2014]. Also F_{sapflow} will increase, although there is a small time lag (*vide infra*). After peaking at midday, F_{sapflow} will decrease and Ψ_{leaf} will increase, i.e. less negative, again in the evening due to an increasing stomatal diffusion resistance which, in turn, is the result of the lowering PAR level.

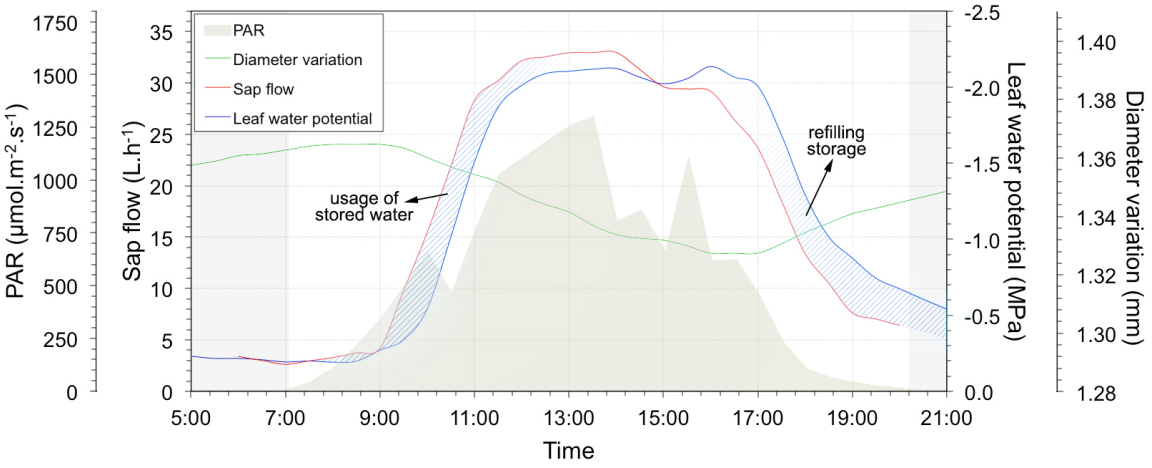

FIGURE 1.4: Diurnal pattern of F_{sapflow}, Ψ_{leaf}, diameter variation and PAR on a semi-clear day (4 September 2014) in the experimental forest Aelmoeseneie.

In the morning the uptake of water (F_{sapflow}) is less than the loss of water through transpiration (Ψ_{leaf}) because water stored in the stem is being used [Meinzer et al., 2001, 2004, Steppe and Lemeur, 2004]. This will cause the stem to shrink. During the day water uptake and loss stabilize and the stationary van den Honert concept can be used [van den Honert, 1948]. In the evening uptake of water is higher than the loss of water and the water reservoir in the stem is being refilled, resulting in swelling of the stem.

The observed time lag between F_{sapflow} and Ψ_{leaf} can be explained by mechanisms such as elasticity of the plant tissue, capillary storage and cavitation release [Zimmermann, 1983, Tyree and Ewers, 1991, Vergeynst et al., 2015]. The ability of a tree to store water in its stem is defined as water storage capacity of the plant tissue [Tyree and Ewers, 1991, Vergeynst et al., 2015]. Stored water is estimated to contribute 5-22% of total water use [Steppe et al., 2015a]. On cloudy or rainy days this dynamic reservoir may well contribute an even larger fraction of up to 65% [Zweifel et al., 2001, McLaughlin et al., 2003]. Stored water provides a very good buffer against drought stress and plays an important role in whole-tree water relations [Hao et al., 2013, Vergeynst et al., 2015]. All these processes and responses can help evaluating the storage and retrieval of water from and to the stem, thus resulting in respectively swelling and shrinking of the stem.

1.5 Modeling opportunities

Mathematical models are generally used to describe natural systems with its relevant system variables [Imboden and Pfenninger, 2012]. In the context of this master thesis an individual tree can be considered as the 'system' with different inputs (e.g. water uptake) and outputs (e.g. transpiration). While mathematical models are already being developed for several decades [Aris, 1978], it is only more recently that models are being used in the field of plant physiology, for example: estimation of root pressure [De Swaef et al., 2013], revealing a phloem-generated turgor signal [Mencuccini et al., 2013], studying hydraulic redistribution [David et al., 2013] and understanding plant hydraulic functioning [Steppe et al., 2015b]. Modeling the diameter variation and sap flow of plants can help gaining insight in the underlying physiological processes. Furthermore through calculation of hydraulic parameters (e.g. conductance K and capacitance C), as a result from diameter and sap flow data, it might be possible to detect and even predict stress.

Currently, the mathematical model to link these variables originally developed by Steppe et al. [2006], is one of the most advanced models using a comprehensive flow and storage model including whole-tree leaf transpiration as the only input variable. Steppe et al. [2006] concluded that existing models were incomplete and that inclusion of a stem growth component in the stem diameter variation is essential to obtain accurate simulations.

Individual tree monitoring offers continuous, real-time data and because of the reduced cost and complexity it is possible to create a large network of these individual trees (Section 4.7) to collect data over a large spatiotemporal scale. These accurate and precise data of sap flow dynamics and daily stem diameter variations can be used to develop and improve models to link both variables [Zweifel et al., 2001, Steppe et al., 2006] and explain radial stem growth using the underlying principles [Steppe et al., 2015b]. Besides modeling the responses, the developed model also allows accurate assessment of physiological characteristics that are difficult to measure such as hydraulic resistance and hydraulic capacitance [Steppe et al., 2006, 2008]. Using models like this, improving them through implementation of data retrieved from stress events and greater understanding of the underlying processes, offers great possibilities in evaluating the dynamic response of trees and offers the opportunity to detect stress in the early stages.

1.6 Upscaling the data

While individual tree monitoring may offer a greater understanding in the dynamic responses of trees to changes in the regional climate due to the large temporal scale, it is necessary to upscale this information to a larger spatial scale, e.g. a forest stand. A suitable method needs to be selected or developed to upscale the results retrieved from diameter

variation and sap flow. There are generally two main methods to achieve this: the forest inventory approach and the remote sensing approach [Ceulemans, 1999].

A forest inventory allows easy determination of a particular tree's share regarding diameter of the total forest stand through calculation of the basal area. The result of the individual tree can subsequently be scaled to the total stand by simply using ratios or as input in the European Forest Information Scenario Model (EFISCEN) [Schelhaas et al., 2007]. Also sap flow data can be scaled up using a forest inventory where ratios between the biometric parameters of the monitored trees are used [Čermák et al., 2004]. Typical forest inventory parameters such as DBH or basal area can be used for this purpose. Unfortunately a decent forest inventory is not always available, e.g. due to a lack of resources. It is, however, possible to upscale data by only measuring the large diameter trees (i.e. DBH $>$ 100 cm) in the forest stand [Miller et al., 2007, Slik et al., 2013]. Already a little over 1% of the stems can account for more than 30% of the basal area, 36% of woody debris and almost 50% of biomass [Lutz et al., 2012, 2013]. It is also found in many studies that dominant trees account for about 65% of the total stand water loss, medium trees about 25% of water loss and suppressed trees only about 10% [Čermák and Kučera, 1990]. This was confirmed recently by Miller et al. [2007] who reported that although large diameter trees account for less than 10% of the population, they contribute to almost 40% of total stand flux. Furthermore, large diameter trees have a large ecological importance [Lutz et al., 2012] and are essential for a forests structural heterogeneity [Lutz et al., 2013].

Reyes-Acosta and Lubczynski [2013] recently proposed a new upscaling method using remote sensing. This method has already been demonstrated more than two decades ago by Čermák and Kučera [1990] and Ceulemans [1999]. Reyes-Acosta and Lubczynski [2013] consider such a scaling up procedure a good alternative for estimating tree transpiration at high spatial scales. They concluded, after comparing remote sensing with stand scale scaling up [Lubczynski, 2009], that it is a good tool for understanding the hydrological dynamics of the plant-soil-water interactions but also for quantitative estimates. While it is a good method and has its advantages, it is (currently) a complex and costly method.

Sap flow data can however also be scaled up by a third approach, namely using hydrological models. It is being proposed as a good perspective for the future by Čermák et al. [2004]. These models can adequately describe hourly transpiration under (non-)limiting soil water conditions [Meiresonne et al., 2003], but the complexity of the more sophisticated models can however cause some issues as is the requirement for a number of parameters. Simple models need fewer parameters but lack the temporal scale.

As soon as the diameter variation and sap flow data are accurately upscaled to the forest stand it will be possible to analyze the vitality of the stand and monitor the dynamic (stress) responses of the complete forest to a changing climate.

1.7 Objectives

The main goal of this research is to monitor beech (*Fagus sylvatica* L.) and oak (*Quercus robur* L.) during the timespan of more than one year in order to gain as much information as possible of their response to a changing microclimate. This information is gathered using a multitude of different meteorological, pedological and physiological sensors (Figure 1.5, step 1). Through analyzing the extensive dataset with data from the air, soil and tree, it should be possible to characterize the response of the tree to the microclimate (step 2).

After characterization of these responses and evaluating the differences and similarities between beech and oak, the established relationships can be reversed to allow a well-founded determination of the status of a particular tree by evaluating the gathered plant sensor data (step 3). It is furthermore the intention to reduce the set of sensors to one dendrometer and one sap flow sensor. With these two sensors it should be possible to make an accurate and precise judgement on the (dynamic) status of a particular tree.

Finally, the data from one tree will be upscaled and it will be determined what area an individually monitored tree can integrate. This enables the potential to not only evaluate the individual tree that is being monitored, but monitoring the status of the complete forest stand. Furthermore because the data is collected in real-time, it will be possible to make a prompt judgement on the status of a tree and subsequently the forest. This way the trees and forests will truly act as 'climate predictors'.

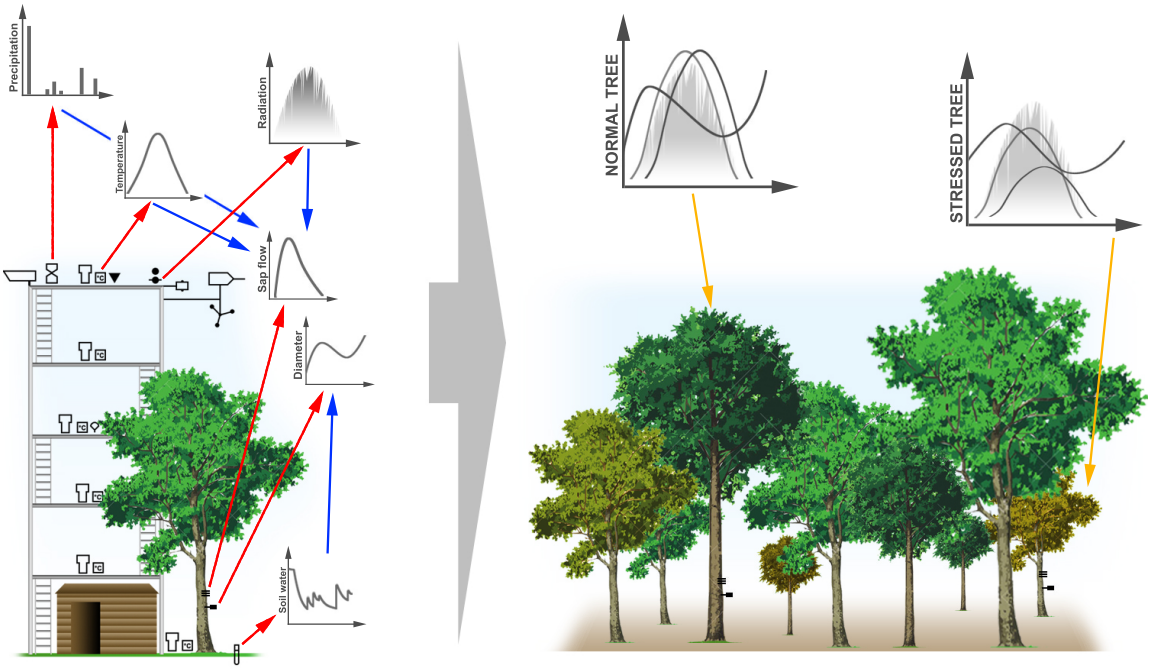

FIGURE 1.5: Schematic overview of the objectives. Step 1: Gather as much data as possible from the tree and the microclimate (red arrows). Step 2: Evaluate how the tree responds to a changing microclimate (blue arrows). Step 3: Analyze the data to make a well-founded judgement on the status of a tree and forest (orange arrows).

Chapter 2

Methodology

2.1 Study area

This study takes place in Flanders (Belgium) with a temperate/mesothermal climate, more specifically a 'Cfb' climate [Peel et al., 2007], i.e. relatively moist climate with distinct seasons but no extreme differences in average temperatures between summer and winter. Data was collected in the experimental forest Aelmoeseneie of Ghent University during the complete timespan of the dissertation but continuous data was already available since May 2014. An additional set-up was carried out at the Faculty of Bioscience engineering (UGent) in fall of 2014 for four consecutive weeks to gather supplementary data.

2.1.1 Experimental forest 'Aelmoeseneie'

The Aelmoeseneie forest, total area of 28 ha, is situated near Ghent (Belgium) in Gontrode ($50°58'35'', 3°49'30''$) with a surface elevation between 11 and 21 m above sea level [Samson et al., 1997]. A specific area of 1.83 ha is fenced and designated for scientific research. This zone (designated '5n' in the forest management plan by ForNaLab [2007]) contains a deciduous forest which was planted in 1920 [ForNaLab, 2007]. The forest is owned by Ghent University and managed by the Forest & Nature Lab (ForNaLab). It has an Ldc soil, i.e. a sandy loam soil which is moderately wet. It currently consists of an oak-beech (*Quercus robur* L. - *Fagus sylvatica* L.) stand in the Eastern direction and an ash-maple (*Fraxinus excelsior* L. - *Acer pseudoplatanus* L.) stand in the Western direction along the brook 'Bloedbeek'. A measuring tower is installed in this scientific zone right on the transition between the two forest types. The tower holds five protected horizontal platforms at 7.5, 14.6, 21.6, 28.8 and 36.0 m, respectively, and is equipped with several sensors which are discussed in detail in section 2.2.1. A log cabin at the base of the tower holds a Campbell datalogger, desktop computer and networking hardware.

In total there are nine trees being monitored in this scientific zone with several sensors (section 2.2.2). More specifically, five beech trees and four oak trees are continuously monitored since May 2014. The location of these trees is shown in Figure 2.1 as is the location of the measuring tower, the path through the forest and the brook 'Bloedbeek'. Two groups can be distinguished, one group along the path with three beeches and two oaks and another group along the fence in the Northern direction with two beeches and two oaks.

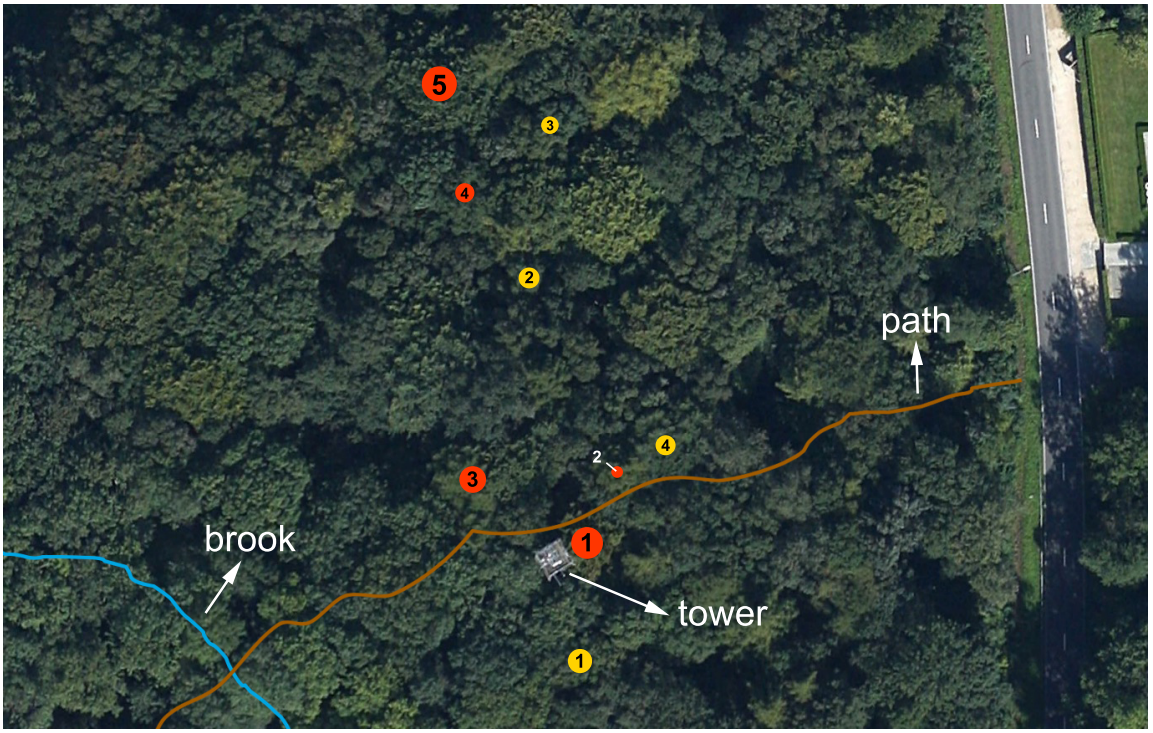

FIGURE 2.1: Location of the nine trees being monitored in the experimental forest Aelmoeseneie. Red and yellow circles represent beech and oak, respectively. The size of each circle is representative for the diameter of each tree. [Satellite image, by Google Earth, 2012]

2.1.2 Faculty of Bioscience engineering

An additional set-up was established on 18 September 2014 and ran till 16 October 2014 at the Faculty of Bioscience engineering (UGent). This will be referred to as the 'small scale set-up'. One beech and one oak tree were being monitored with the same sensors as used in the experimental forest Aelmoeseneie but also with several additional sensors measuring supplementary variables of the trees (section 2.2.2).

Both trees are growing in large pots with a diameter of 1 m and height of 1 m. The soil in the pots has a loamy-clay texture. There are several holes in the base of the pot to allow contact with the soil and drainage to the soil. Both trees were each selected from a set of three on the basis of visual vitality criteria, i.e. amount of leaves, leaf defoliation and leaf discoloration. Besides data from the two trees also microclimatic data was collected.

2.2 Gathered data

2.2.1 Atmospheric data

The atmosphere is a very important part of the Earth system as it represents the amount of water that is demanded from the tree. Measured variables include temperature (T) (°C), relative humidity (RH) (%), PAR (µmol.m^{-2}.s^{-1}), net radiation (W.m^{-2}), incoming (S_t) and reflected (αS_t) shortwave radiation (to calculate albedo) (W.m^{-2}), wind speed (km.h^{-1}), wind direction (°), 24 hour cumulated precipitation (mm) and air pressure (hPa). As these are measured using commercial measuring devices, they are not further discussed. A detailed overview of the meteorological sensors, i.e. type, brand and technical information, can be found in Appendix A.

In the experimental forest Aelmoeseneie all sensors are placed at the top level (P5) of the measuring tower (Figure 2.2). T and RH are however also measured on the lower four platforms, the ground level and in the vicinity of oak 2 (Figures 2.1, 2.2). Gathering meteorological information in the small scale set-up was achieved by mounting a reduced set of meteorological sensors to a large fixed pole extending above the crown of the trees. Measured variables included T, RH and PAR. T and RH were also measured below the crown for each of the two trees separately.

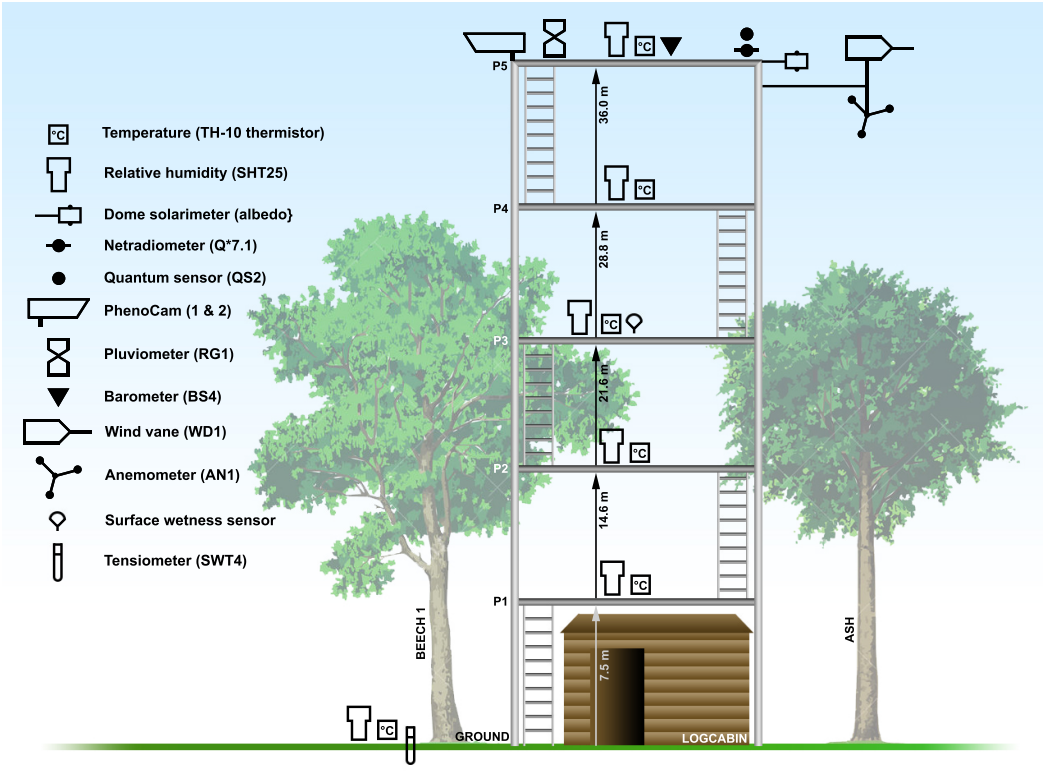

FIGURE 2.2: Schematic overview of the measuring tower with the present apparatus and log cabin in the experimental forest Aelmoeseneie. [Actualization of original image by Samson et al. [1997]]

2.2.2 Tree data

Technological advances have made it possible to gather data from the actual trees itself. The two most important sensors are the point dendrometer, monitoring changes in diameter (ΔD), and the sap flow sensor measuring sap flux density (F_{sapflux}).

The used point dendrometer is a commercial sensor produced by Natkon (`http://natkon.ch`), i.e. the ZN11-T-WP dendrometer (Figure 2.3A). It is mounted on the tree using a frame made out of one piece of carbon fibre (CFK), combined with stainless steel elements (rods and nuts) to fix on the stem of the tree. The sensing rod (Figure 2.3B) is pressed slightly against the tree stem by a spring and results in a voltage signal. The dendrometer is in fact an electronic displacement-sensor (linear motion potentiometer) and has a resolution of less than 1 µm. More information can be found in the datasheet [Zweifel, 2012].

(A) (B)

FIGURE 2.3: (A) Natkon ZN11-T-WP point dendrometer on oak in the experimental forest Aelmoeseneie. (B) Detailed picture of the sensing rod of a point dendrometer on beech.

One point dendrometer is installed on the bark of all nine trees in the experimental forest Aelmoeseneie. On three beeches (1, 2 and 3) a point dendrometer is also installed on the xylem of the stem after removing bark and cambium layers. This offers the possibility to gain interesting information about for example water storage and growth. In the small scale set-up a point dendrometer was also installed on the bark and xylem for both trees.

Another important characteristic is the sap flow within the tree. Sap flux density is measured using a sap flow sensor constructed at the Laboratory of Plant Ecology of the UGent Faculty of Bioscience engineering. It is based on the SapFlow+ method developed by Vandegehuchte and Steppe [2012c], but run in the HRM mode. Each tree in the experimental forest Aelmoeseneie and both trees in the small scale set-up are equipped with a SapFlow+ sensor. Figure 2.4 shows this sensor *in situ*, installed on an oak tree in the experimental forest Aelmoeseneie.

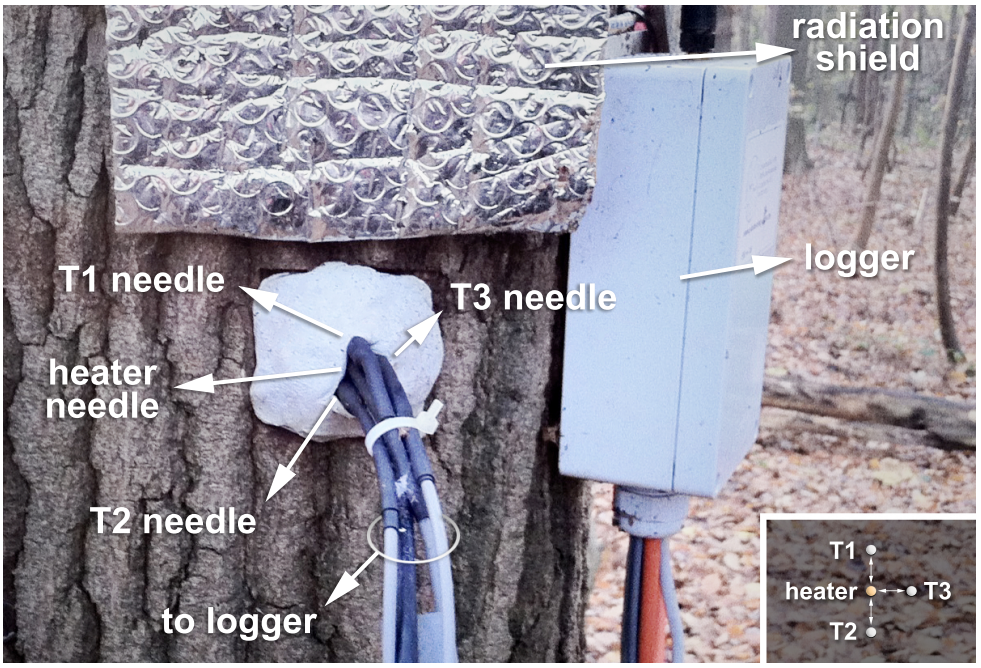

FIGURE 2.4: SapFlow+ sensor on oak in the experimental forest Aelmoeseneie. Bottom right corner shows a schematic overview of the position of the heater and the three temperature needles.

Three stainless steel temperature needles with a length of 35 mm and diameter of 1.1 mm are carefully positioned at 7.5 mm from a heater needle (Figure 2.4). This is done by using an accessory piece made out of solid steel to drill the four holes in the tree. After inserting the needles, they are covered with terostat-IX (Henkel Technologies) which is a kneadable synthetic rubber to seal gaps between wood, metal and plastic. This ensures a waterproof installation. An aluminum reflective insulation bubble foil is placed on top of the sensors to serve as a radiation shield. A wireless logger, also developed at the Laboratory of Plant Ecology, is positioned next to the sap flow sensor.

Besides 'SapFlow+ mode' [Vandegehuchte and Steppe, 2012c], it is possible to use the sap flow sensor in 'HRM-mode' [Burgess et al., 2001] by only using the output from the T1 and T2 needles. This offers the possibility to compare the two methods. In some cases it is more practical to use the HRM-mode because SapFlow+ requires model fitting for every heat pulse which can be computationally intensive and time consuming. The SapFlow+ method is however the most advanced and best method for measuring sap flow.

Beech 2 is also equipped with an additional stem flow monitor. More specifically an automatic stem drain measuring kit (Umwelt Geräte Technik UGT) using the tipping bucket mechanism with an electronic counter and datalogger. The volume of the bucket is 100 mL, which will result in 1 click when tipped. 1% of this volume (i.e. 1 mL) is stored for sampling. The remaining volume is diverted to a 35 L barrel which is used to check the registered volume by the automatic logger.

Additional variables are collected in the small scale set-up to subsequently link diameter variation and sap flow data. Figure 2.5 shows the beech in the small scale set-up, fully equipped with all sensors. The oak tree has a similar set-up.

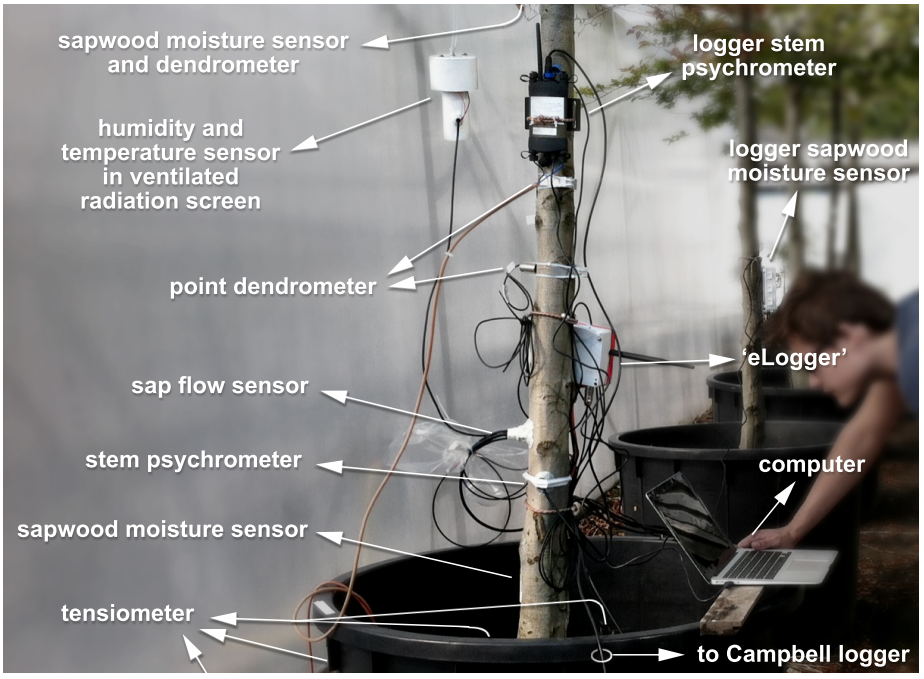

FIGURE 2.5: Beech in the small scale set-up, fully equipped with three point dendrometers, sap flow sensor, stem psychrometer, two sapwood moisture sensors, four tensiometers (*vide infra*) and humidity and temperature sensors in a ventilated radiation screen (*vide supra*).

Added sensors include the PSY1 stem psychrometer (ICT International) and GS3 sapwood moisture sensor (Decagon Devices), which are both commercially available. The stem psychrometer is used to measure the stem water potential (Ψ_{stem}) based on thermocouple psychrometry [Boyer, 1995]. This is a very useful method for 'measuring' the water status of the tree. It works over the entire range of water contents because it measures conditions in the gas phase and does not require a continuous liquid phase for measurement. The water does need to be able to evaporate from the sample to the air. Resolution is 0.01 MPa. Figure 2.6A shows a typical PSY1 stem psychrometer.

The measurement chamber is constructed with two thermocouples (Figure 2.6A). The *chamber* thermocouple, thermocouple-C, uses the Peltier effect, i.e. conversion of an electrical current to a temperature difference, to create a condensed water droplet on the thermocouple through cooling of the thermocouple from the air temperature or dry bulb temperature (T_a) to below the dew point temperature (T_d) (step 1 on the psychrometric chart in Figure 2.6B). After the Peltier effect is switched of the droplet will evaporate. First the temperature will increase rapidly until the wet bulb temperature, T_w, is reached (step 2). T_w will remain constant until the water droplet has completely evaporated (step 3). The difference between T_a and T_w is called the web bulb depression (WBD) (step 4).

After complete evaporation the temperature will increase rapidly to reach T_a again (step 5). Thermocouple-S, or *sample* thermocouple, measures the temperature gradient between the sample and measuring junction. Measuring this gradient allows for correction of the measurements as the data collection takes place in the field instead of an isotherm environment.

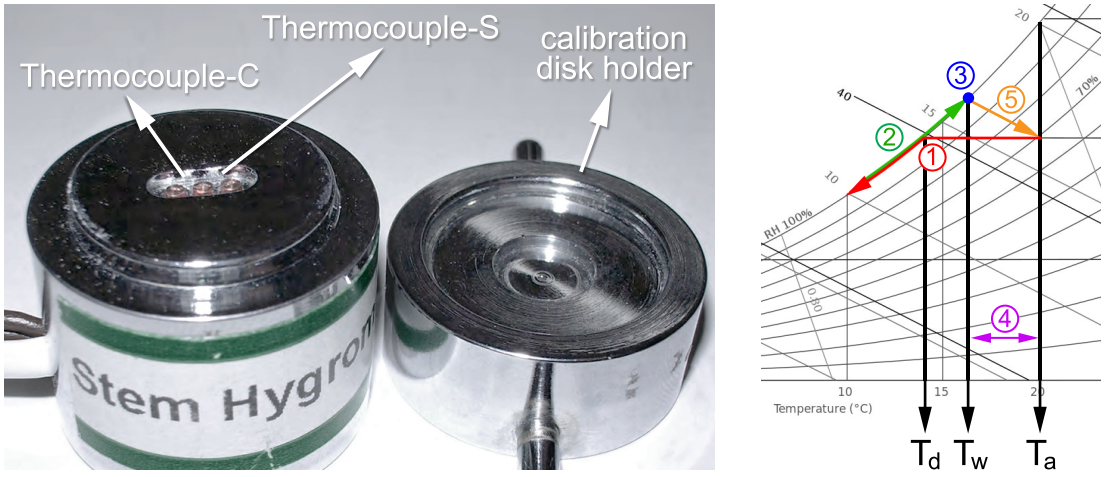

(A) (B)

FIGURE 2.6: (A) Image of a typical PSY1 stem psychrometer chamber. [Dixon and Downey, 2013] (B) Theoretical steps in the determination of the wet bulb depression (WBD) on a psychometric chart (or 'Mollier diagram') at sea level (barometric pressure 101.325 kPa) [Based on data from Carrier Corporation Cat. No. 794-001, dated 1975]

To install the sensor, a Frostner drill bit (Figure 2.7A) with a diameter equal to that of the sensor (i.e. 25 mm) was used to create a superficial hole in the bark until the xylem was visible (Figure 2.7B). Because it is from utmost importance that the chamber of the sensor is airtight and free from any external moisture, terostat-IX (*vide supra*) was applied around the sensor. Tie-wraps and white insulation tape were used to further secure the sensor to the bark (Figure 2.7C).

(A) (B) (C)

FIGURE 2.7: (A) Frostner drill bit. (B) Example of a hole in the bark of beech, after removal of the stem psychrometer. (C) Installed stem psychrometer on beech in the small scale experiment.

The second additional sensor in the small scale set-up is a sapwood moisture sensor (Decagon Devices) (Figure 2.8). It contains three needles which are carefully inserted in the stem after an accessory piece has been used to drill the holes at fixed distances. This sensor determines the volumetric content (VWC) by measuring the dielectric constant (ε_a) of the medium using capacitance / frequency-domain reflectometry [Hao et al., 2013]. An onboard thermistor measures the temperature. Electrical conductivity is measured using a stainless steel electrode array. A frequency of 70 MHz is used to minimize noise. The resolution is 0.2% VWC from 0%-40% VWC and 0.1% VWC from 40%-100% VWC.

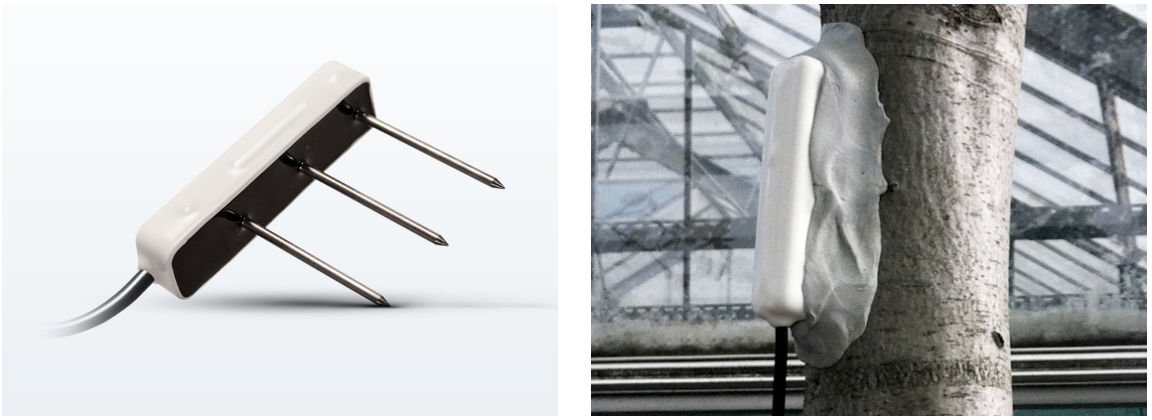

(A) (B)

FIGURE 2.8: (A) Image of the GS3 sapwood moisture sensor. [Decagon Devices, 2015] (B) Installed GS3 sapwood moisture sensor from Decagon Devices on beech in the small scale set-up.

Whereas the trees in the experimental forest Aelmoeseneie are equipped with a point dendrometer and sap flow sensor, the phenology of the forest is also monitored using two cameras. More specific with two IR-113E (Edimax) true day and night cameras, named 'PhenoCam' (Figure 2.9). They take an image every 15 minutes from where red, green and blue (RGB) signals are extracted. These signals can subsequently be used to calculate different indices which allow an evaluation of the phenology, e.g. start of the growing season.

FIGURE 2.9: Edimax IR-113E true day and night network camera mounted at the top platform (P5) of the tower in the experimental forest Aelmoeseneie (Figure 2.2).

Besides gathering data through continuously logging sensors, the leaf water potential (Ψ_{leaf}) was measured on three occasions using a pressure chamber (PMS Instrument Company model 1000) (Figure 2.10): 8 August 2014 (9:45-16:45) and 4 September 2014 (6:00-20:00) in the experimental forest Aelmoeseneie and 23 September 2014 (11:00-16:00) at the small scale set-up. For beech 1 the specific leaf area was determined on 5 September 2014 and the dry weight on 8 September 2014.

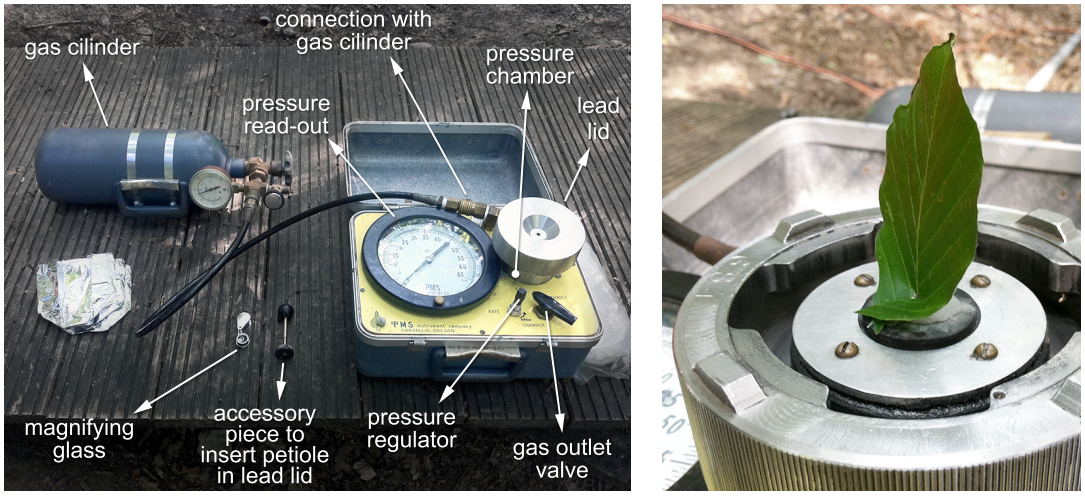

(A) (B)

FIGURE 2.10: (A) *In situ* setup of the pressure chamber. Aluminum foil bags (left) are used to measure the stem water potential. (B) Inserted leaf in lead lid.

The pressure chamber has a maximum operating pressure of 70 bar and was used with a portable (nitrogen) gas cilinder (Figure 2.10A), filled in advance till ca. 83 bar. On 8 August 2014, the sampled tree was beech 1 with a height of approximately 29 m. Samples were taken from platforms 2, 3 and 4 with a height of 14.6, 21.6 and 28.8 m, respectively, with a half hour between each platform, starting with platform 2. This rotation was repeated throughout the day. Besides measuring Ψ_{leaf}, also Ψ_{stem} was measured every half hour. This was achieved by using the pressure chamber to measure the water potential of a leaf that has been wrapped in an aluminum foil bag for one and a half hour. On 4 September 2014 three leaves were sampled from platforms 2, 3 and 4 every hour, i.e. nine leaves per hour, resulting in 135 measurements that day. A headlamp with red light was used before sunrise in order not to disturb the 'predawn'-values. On 23 September 2014 three leaves were sampled every hour from both the beech and oak tree.

After cutting the leaves from the tree, two incisions were made along the short petiole to allow a more easy insertion of the petiole in the lead lid of the pressure chamber (Figure 2.10B). With the help of an accessory piece (rubber cap) the petiole is inserted in the lead lid and terostat-IX is used to further seal the opening. The lid is properly placed on the pressure chamber and gas is released to the chamber using the pressure regulator

and by setting the gas outlet valve to 'chamber'. The cut is studied carefully with a magnifying glass. Whenever a droplet is visible, the pressure regulator is immediately turned to zero. Pressure (bar) can be noted down by looking at the read-out. Time between first sampling and last reading was approximately 5 min on 8 august 2014 and 10 min on 4 September 2014. It was less than 4 min on 23 September 2014 in the small scale set-up.

The sampled leaves of beech 1 on 4 September 2014 were collected in labeled pouches to determine the surface area of each leaf on 5 September 2014 using a LI-3000 leaf area meter (LI-COR). Afterwards the leaves were dried for more than 48 hours at 60°C in a drying oven. On 8 September 2014 the dry weight was measured (M-Power precision balance by Sartorius) allowing to calculate the specific leaf area (SLA) ($cm^2.mg^{-1}$).

2.2.3 Soil data

Where the atmosphere is the 'demanding side' for water from the tree, the soil is responsible for the supply of water to the tree as the tree will take up water through its roots. All water movement in soil is directly dependent on the soil water tension as water will always move from a point of higher to lower potential. Tensiometers and water content reflectometers can be used for determining how much water the soil can 'supply' to the tree, or in some cases 'demand' from the tree. For a description of soil characteristics and edaphic factors please refer to section 2.1.

Tensiometers were used to determine the soil water potential, i.e. a measure of the soil matrix potential Ψ_{soil}. It defines how strong the tree should 'work' in order to extract water from a unit volume of the soil. One EQ2x equitensiometer by Delta-t Devices is used in the experimental forest Aelmoeseneie in the vicinity of beech 1 and eight Tensio-Technik tensiometers in the small scale set-up, two inside and two outside the pot for both the beech and the oak tree. Tensiometers have contact with the soil through a ceramic cup which is porous and permeable to water. A pressure transducer conducts the soil water tension via a continuous signal.

In the experimental forest Aelmoeseneie also water content reflectometers (WCR) are used (CS616 by Campbell Scientific). These are used to determine the VWC ($m^3.m^{-3}$) of the soil. They are installed according to the schematic overview in Figure 2.11. Three locations hold four WCRs each at the following depths: 0-5 cm, 5-20 cm, 20-40 cm and 40-80 cm. One location also has temperature sensors at parallel depths. The WCRs locations are at a distance of approximately 6-9 m each from a central datalogger. These sensors use time domain reflectometry (TDR) to measure dielectric permittivity. Since water has a dielectric permittivity significantly larger than other soil constituents it is possible to determine the average water content of the medium. These sensors have a resolution of 0.1% VWC and accuracy of $\pm 2.5\%$ VWC.

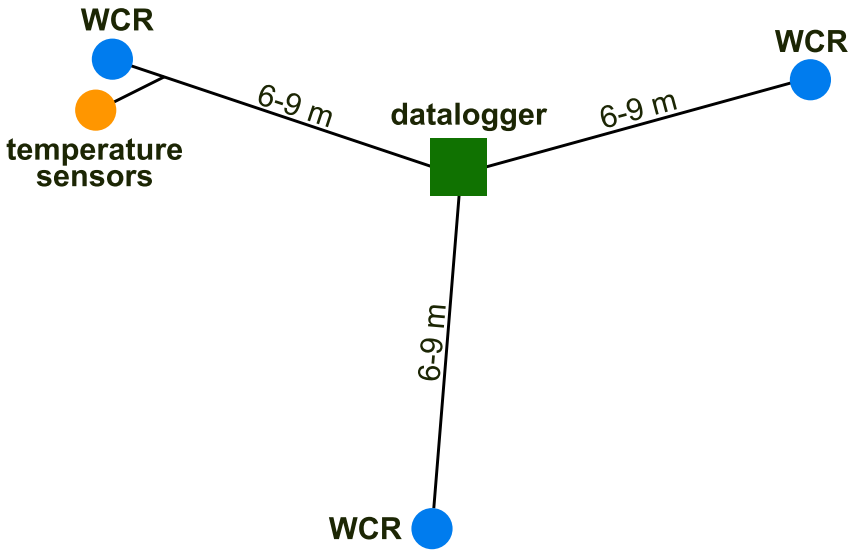

FIGURE 2.11: Schematic drawing of the location of the water content reflectometers (WCR).

2.3 Logging and processing the data

In the experimental forest Aelmoeseneie measurements are logged using 'eLoggers' developed at the Laboratory of Plant Ecology. Every tree, platforms 1, 2, 3 and platforms 4, 5 have their own eLogger and wirelessly transmit data, in mV, to a server. This data is used by the software PhytoSense (Phyto-IT) to visualize the data. Raw data is visible in PhytoSense as is calibrated data. Data can easily be exported as a space delimited `txt` file which can then be used in analyzing software such as Microsoft Excel, SigmaPlot or R+.

The small scale set-up also uses eLoggers, but only for two sap flow sensors, two relative humidity sensors, two temperature sensor, four of the six point dendrometers and two of the four sapwood moisture sensors. An EM50 datalogger (Decagon Devices) is used to log the other two sapwood moisture sensors. A Campbell CR1000 datalogger (Campbell Scientific) logs two point dendrometers, eight tensiometers, one PAR, one relative humidity and one temperature sensor. The two stem psychrometers each have their own dedicated logger (ICT International). While data from the experimental forest Aelmoeseneie is already calibrated by the Laboratory of Plant Ecology, the data in the small scale set-up required calibration. This was achieved using the calibration procedures explained in the manual of each respective sensor.

After exporting and when necessary calibrating the data, it was imported in either Microsoft Excel, SigmaPlot or R to analyze it. Data is checked for gaps and inconsistent data. Small gaps (i.e. 1-2 data points missing) are interpolated, while larger gaps ($>$ 2 data points missing) are left as is. Inconsistent data or unrealistic values (e.g. due to sensor errors), are removed from the dataset. Final result is a dataset which can easily be used to perform calculations, perform statistical tests, search for relations and more.

Chapter 3

Results

3.1 Meteorological data

3.1.1 Experimental forest Aelmoeseneie

Daily averages are used to visualize the following meteorological variables: 24 hour cumulated precipitation (mm), wind speed (km.h^{-1}), T (°C) and RH (%) at ground level and platform 4 during the timespan of a little over one year (1 April 2014 - 10 May 2015) (Figure 3.1). For PAR (mol.m^{-2}.day^{-1}) was the daily sum calculated (Figure 3.1). Measurements for incoming (S_t) and reflected (αS_t) shortwave radiation (W.m^{-2}) are shown from 15 May 2014 till 10 May 2015 (Figure 3.2). Several radiation variables are visualized in detail for one clear summer day (31 August 2014) and one clear winter day (28 December 2014) (Figure 3.3). The following variables were derived from these measurements:

- VPD (kPa), i.e. the difference between the saturated vapor pressure, e_s (kPa), and the actual vapor pressure, e_a (kPa) [Allen et al., 1998].

$$e_s = 0.6108 \times e^{\frac{17.27 \times T}{T+237.3}} \tag{3.1}$$

$$e_a = e_s \times \frac{RH}{100} \tag{3.2}$$

  with T, temperature (°C) and RH, relative humidity (%).

- Water potential of the atmosphere, Ψ_{atm} (MPa), using the Spanner equation.

$$\Psi_{\text{atm}} = -\frac{R \times T}{V_w^\circ} \times \ln\left(\frac{e_a}{e_s}\right) \tag{3.3}$$

  with R, ideal gas constant (J.mol^{-1}.K^{-1}); V_w°, molar volume of pure water (g.mol^{-1}); e_a, actual vapor pressure (kPa) and e_s, saturated vapor pressure (kPa).

- Albedo, α (%), as the ratio between reflected (αS_t) and incoming (S_t) solar radiation.
- Percentage PAR of the total incoming shortwave radiation. In order to calculate this ratio, PAR in $\mu mol.m^{-2}.s^{-1}$ must be converted to $W.m^{-2}$. The detailed steps for calculating the conversion factor are explained in Appendix B.

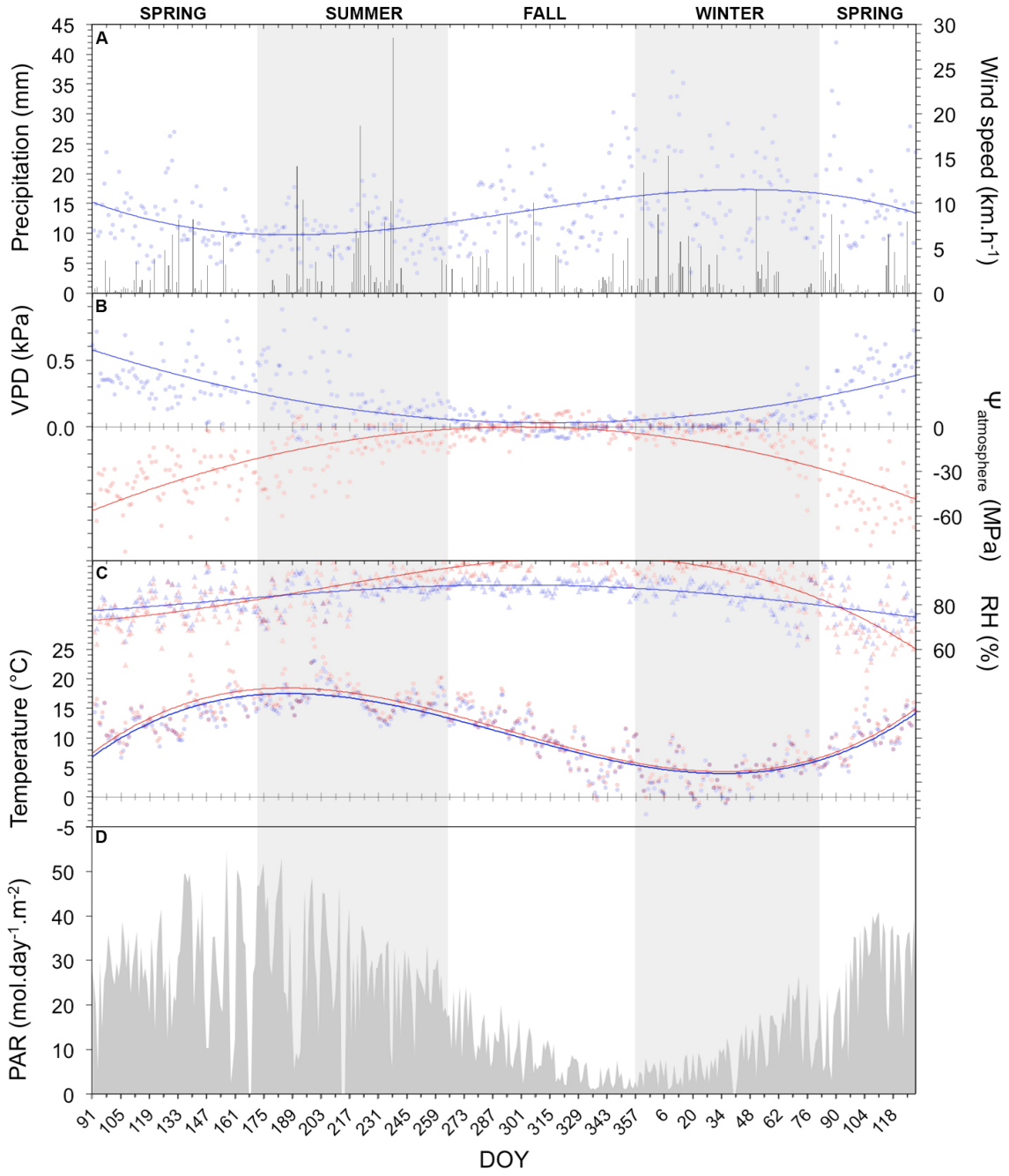

FIGURE 3.1: 24 hour cumulative precipitation (grey bars) and daily average wind speed (blue) (A), daily average VPD (blue) and Ψ_{atm} (red) (B), daily average T and RH on platform 4 (red) and ground level (blue) (C) and finally daily sum of PAR (D). Polynomial curves (solid lines) were fitted for wind speed (R^2 0.18), VPD (R^2 0.43), Ψ_{atm} (R^2 0.58), T on the ground level (blue, R^2 0.75) and platform 4 (red, R^2 0.75) and RH on the ground level (blue, R^2 0.32) and platform 4 (red, R^2 0.67). Data from 1 April 2014 till 10 May 2015 in the experimental forest Aelmoeseneie.

An annual pattern can be observed in the meteorological data. The highest wind speeds were measured during the winter and the highest amount of precipitation during the summer. More specifically, DOY 238 (26 August 2014) was a day with a very high amount of precipitation, 42.8 mm (Figure 3.1A). VPD and Ψ_{atm} are inversely proportional, both reaching their absolute maximum during the winter and absolute minimum during the fall where values of 0 kPa and 0 MPa were measured, respectively (Figure 3.1B). While the highest measurements for T were collected during the summer, the highest measurements of RH were collected during the fall where values of 100% were reached (Figure 3.1C). PAR peaks during the end of spring and the start of summer (Figure 3.1D).

S_t and αS_t show a very similar pattern to that of PAR, reaching their maximum during the spring and the summer. Dividing αS_t with S_t results in the albedo, α (Figure 3.2A), which was more or less constant during the year, approximately 12.1%. Determining the ratio PAR/S_t results in a practically constant value (slope $m = 0.0002$), 42.9% (Figure 3.2B).

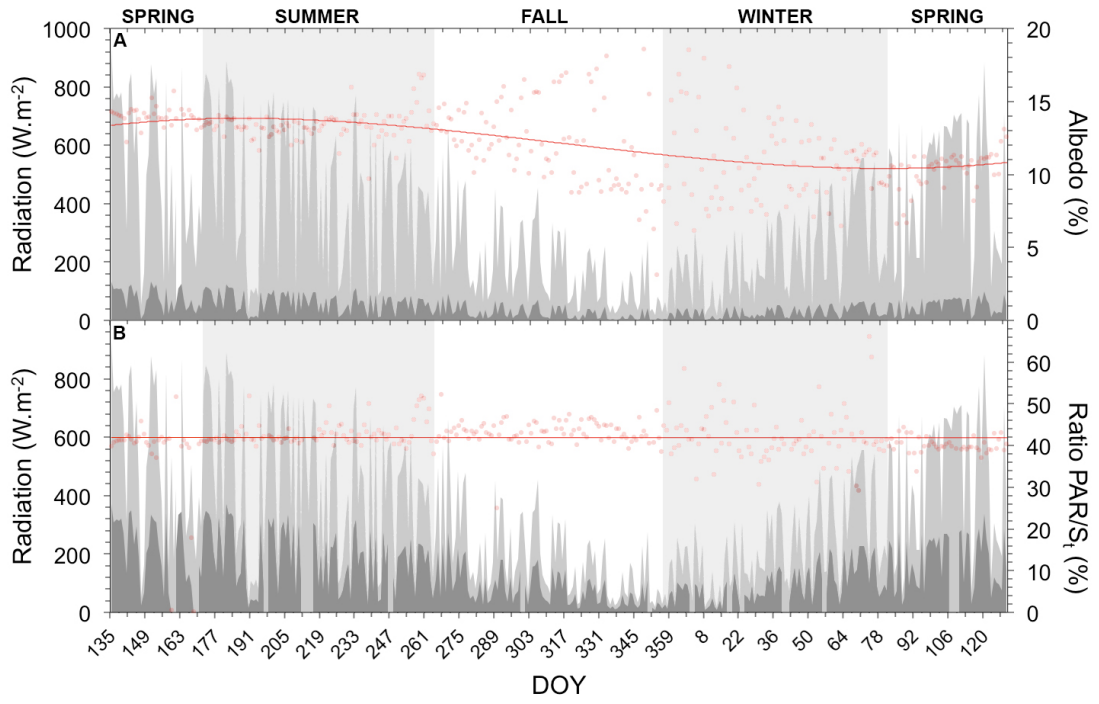

FIGURE 3.2: Measurements of S_t (light grey) and αS_t (dark grey) along with the derived albedo, α (red, R^2 0.28) (A). Percentage PAR (dark grey) of the total incoming shortwave radiation (light grey) is displayed in (B) (R^2 0.07). Data from 15 May 2014 till 28 April 2015 in the experimental forest Aelmoeseneie.

S_t, αS_t and PAR are visualized in Figure 3.3 for one clear summer day (DOY 243, 31 August 2014) and one clear winter day (DOY 362, 28 December 2014) day along with the derived α and PAR/S_t ratio for both days. It is clear that both α and the PAR/S_t ratio were more or less the same for both days although there is a visible difference between the amount of radiation on both days.

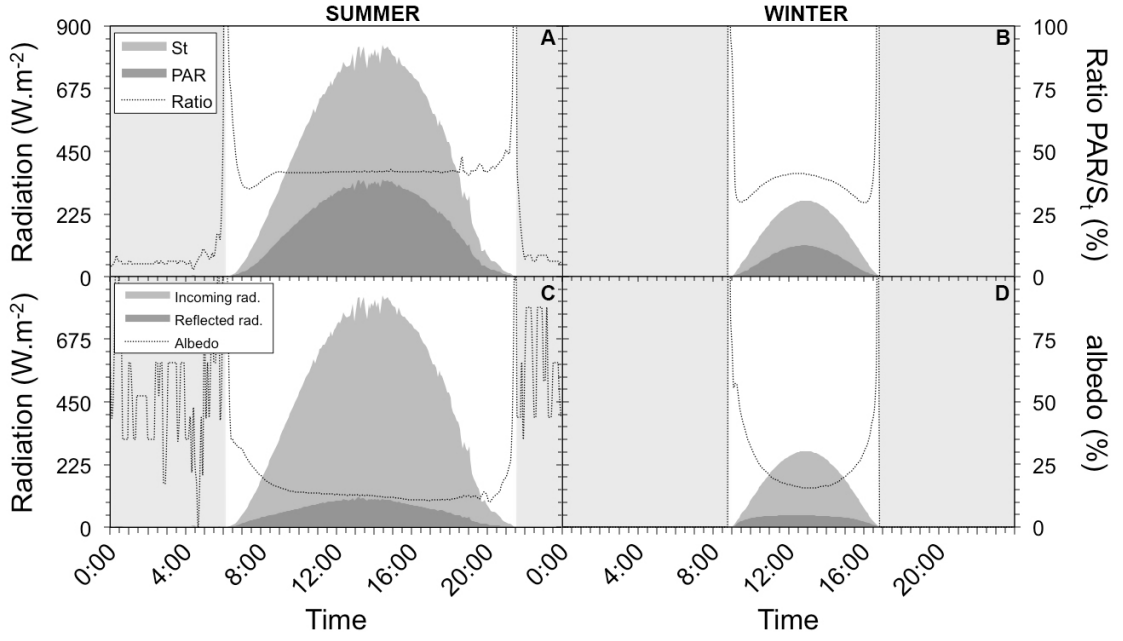

FIGURE 3.3: Measurements of S_t, αS_t and PAR along with derived α and ratio PAR/S_t for a clear summer day (DOY 243, 31 August 2014) (A,C) and a clear winter day (DOY 362, 28 December 2014) (B,D) in the experimental forest of Aelmoeseneie. Shaded areas represent nighttime.

While it is already visually noticeable that there is a correlation between some of the meteorological variables, a correlation table is used to make an objective judgement of this correlation. Table 3.1 presents the correlation coefficients (r) between PAR, T and RH at ground level and platform 4, precipitation, wind speed, VPD and Ψ_{atm}.

TABLE 3.1: Correlation (r) between PAR, T and RH at ground level (GR) and platform 4 (P4), precipitation ('Prec.'), wind speed ('Wind'), VPD and Ψ_{atm}. Color code represents the power of the correlation with white no correlation at all ($r = 0$) and bright green fully correlated ($r = 1$).

	RH_{GR}	RH_{P4}	T_{GR}	T_{P4}	VPD	PAR	Prec.	Wind	Ψ_{atm}
RH_{GR}	1.00	0.83	-0.09	-0.11	-0.74	-0.59	0.31	-0.11	0.76
RH_{P4}	0.83	1.00	-0.30	-0.33	-0.93	-0.76	0.21	0.03	0.37
T_{GR}	-0.09	-0.30	1.00	0.99	0.47	0.60	0.01	-0.27	0.41
T_{P4}	-0.11	-0.33	0.99	1.00	0.51	0.63	0.01	-0.30	0.80
VPD	-0.74	-0.93	0.47	0.51	1.00	0.82	-0.20	-0.13	0.99
PAR	-0.59	-0.76	0.60	0.63	0.82	1.00	-0.19	-0.32	0.22
Prec.	0.31	0.21	0.01	0.01	-0.20	-0.19	1.00	0.22	0.11
Wind	-0.11	0.03	-0.27	-0.30	-0.13	-0.32	0.22	1.00	0.93
Ψ_{atm}	0.76	0.37	0.41	0.80	0.99	0.22	0.11	0.93	1.00

Precipitation has the weakest correlation with the other variables. This is not the case for VPD and PAR which have a strong correlation with RH and T at both levels and with each other. T and RH have a weak correlation with each other. Ψ_{atm} has a very strong correlation with VPD and wind speed, but is also strongly correlated with RH_{GR} and T_{P4}.

3.1.2 Small scale set-up

T and RH measurements in the vicinity of both the beech tree and the oak tree are available (Figure 3.4). T and RH have a stronger correlation with each other when compared to the date of the experimental forest Aelmoeseneie, r = -0.56 and r = -0.53 for beech and oak respectively. A clear diurnal pattern can be observed. T decreases during the night and increases during the day. The opposite is true for RH. T measurements are more or less the same for both trees, but RH differs during the night with RH measurements around the oak tree being slightly higher than RH measurements around the beech tree.

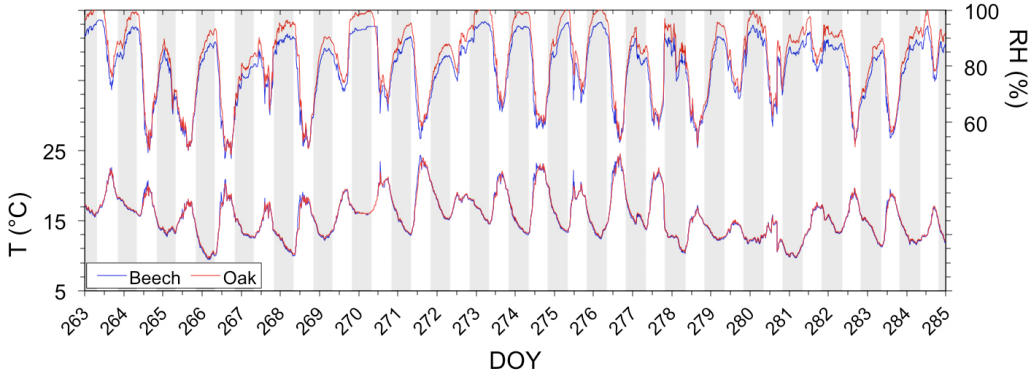

FIGURE 3.4: T and RH measurements in the vicinity of both the beech tree and the oak tree in the small scale set-up. Shaded areas represent nighttime.

3.2 Water status of the soil

3.2.1 Experimental forest Aelmoeseneie

The soil water potential, Ψ_{soil} (kPa), is measured in the vicinity of beech 1, approximately 1-2 m from the base of the tree (Figure 3.5). Ψ_{soil} increased when precipitation occurs. There is no further trend observable.

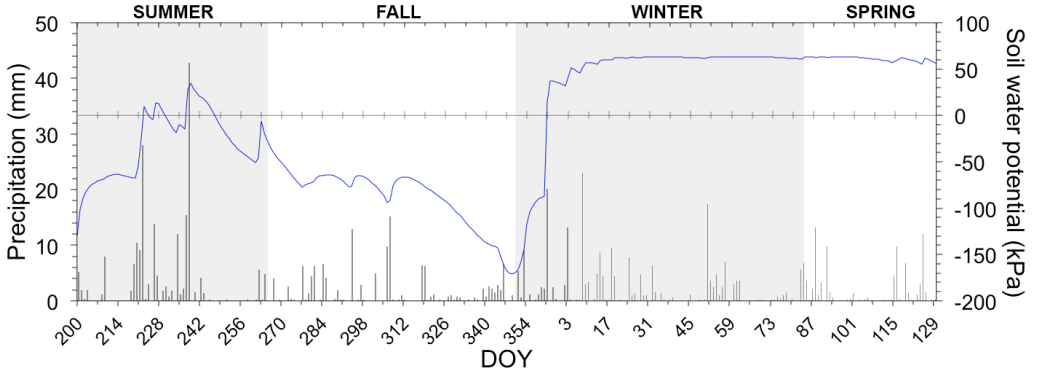

FIGURE 3.5: Ψ_{soil} measured in the vicinity of beech 1 in the experimental forest Aelmoeseneie. Precipitation is visualized as grey bars. Data from 1 August 2014 till 30 April 2015.

Volumetric water content, VWC (%), is gathered at three locations (A, B and C) at four different depths (Figure 3.6). It is not possible to deduce an annual or diurnal trend. An increase in VWC can be observed after a rain event. This effect more or less diminished at the deeper ranges, e.g. fourth depth range at locations B and C. This is less the case when a more extreme rain event, e.g. 42.8 mm on 26 August 2014 (DOY 238), occurs. At all three locations the highest VWC is measured by the deepest WCR. At location A VWC decreased from top to bottom. This is not the case for location B and C where the third deepest WRC measured the second highest VWC.

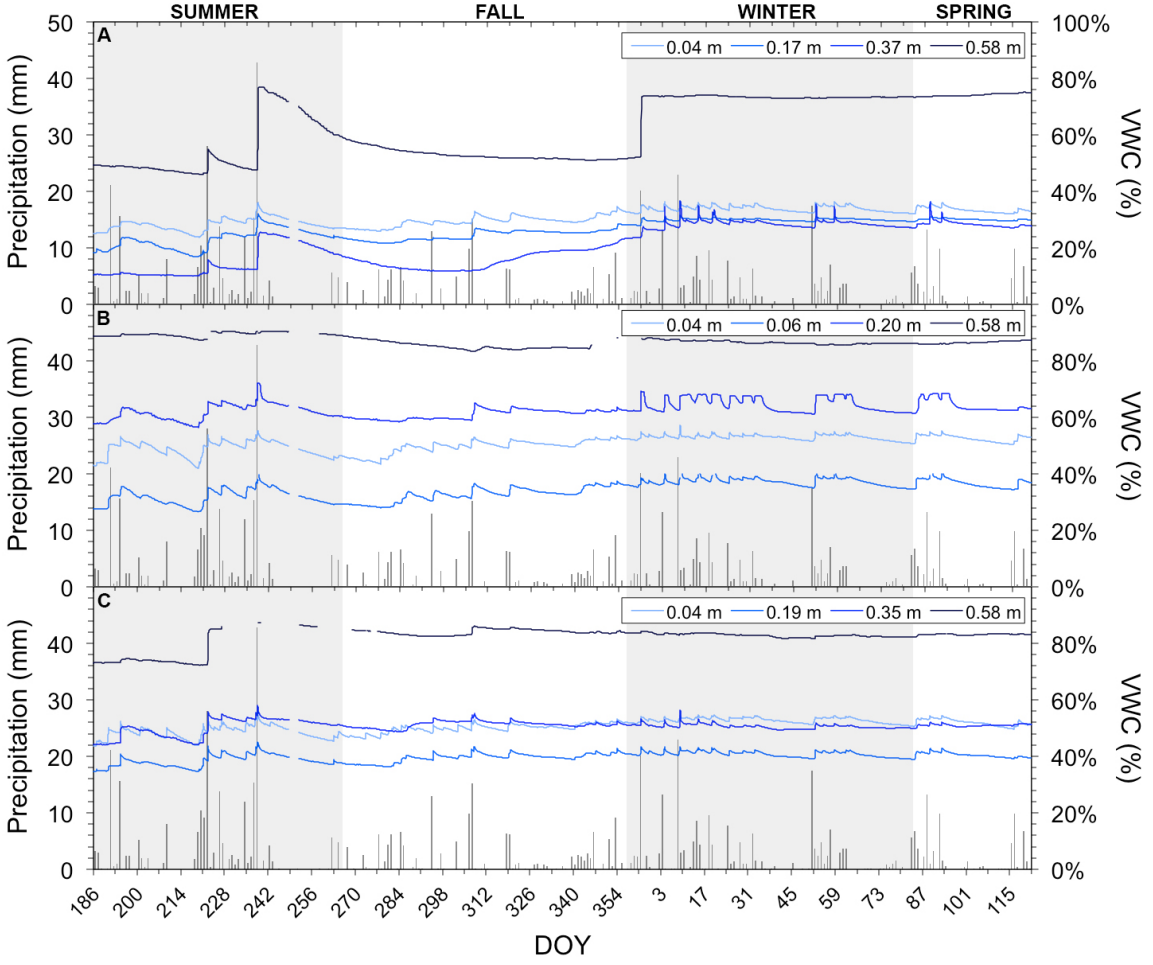

FIGURE 3.6: VWC, gathered from WCRs, at three locations (A, B and C) and four depths in the experimental forest Aelmoeseneie. Precipitation is visualized on the figures as shaded bars. Data from 5 July 2014 till 30 April 2015

3.2.2 Small scale set-up

For the small scale set-up information is also available about Ψ_{soil}. Each tree was surrounded with four tensiometers, two in the soil outside the pot ($\Psi_{soil,soil}$) and two in the soil in the pot ($\Psi_{soil,pot}$). Averages of the two tensiometers are used (Figure 3.7).

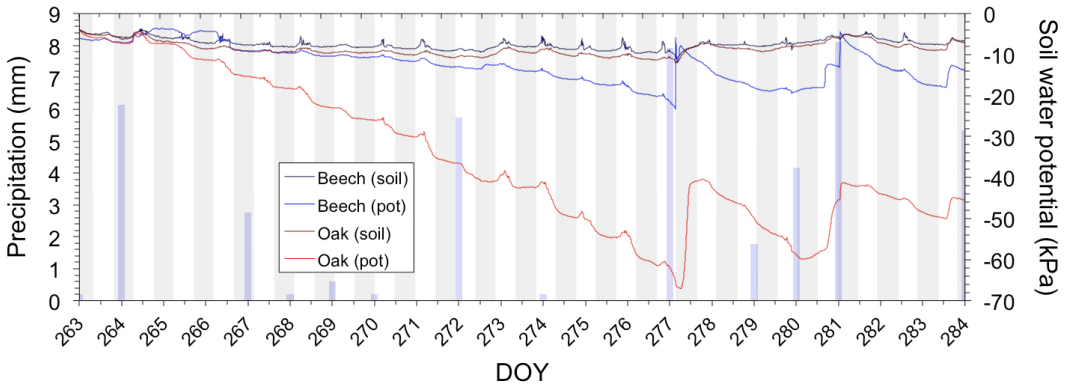

FIGURE 3.7: Ψ_{soil} for beech and oak, from soil and pot in the small scale set-up. Daily total precipitation is visualized as blue bars, data from weather station installed on the faculty of Bioscience Engineering, UGent. Shaded areas represent nighttime.

$\Psi_{soil,soil}$ remained more or less stable during the timespan of the experiment for both beech and oak. $\Psi_{soil,pot}$ had more fluctuations and a stronger decreasing trend indicating that the soil in the pot was more subjected to drought. At daytime there was a steeper decrease in $\Psi_{soil,pot}$ than at nighttime. After a rain event $\Psi_{soil,pot}$ increased sharply. Both $\Psi_{soil,soil}$ and $\Psi_{soil,pot}$ were more negative for oak in comparison with beech.

3.3 Monitoring tree parameters

3.3.1 Diameter variation

3.3.1.1 Experimental forest Aelmoeseneie

Figure 3.8A shows diameter variations on bark ΔD (mm), and Figure 3.8B diameter variations on xylem ΔD_X (mm). A clear increase in the diameter of the trunk, i.e. growing season, can be observed for both beech and oak, although beech has a more stable growing curve. The growth of the oak trees already started stagnating around 10 July 2014 (DOY 191). Beech 1 and 5 stopped growing on 1 September 2014 (DOY 244) and 19 September 2014 (DOY 262), respectively. Beech 2, 3 and 4 had the longest growing season lasting till 3 October 2014 (DOY 276).

The radius of beech 3 has increased the most with 5.3 mm over the total growing season of 2014. This is approximately twice that of the other four beeches, i.e. 2.5 mm, 2.8 mm, 3.0 mm and 2.9 mm for beech 1, 2, 4 and 5, respectively. The radius of the oaks has increased more or less equally, ranging from 1.4 to 1.9 mm. When looking closely at the most recent dendrometer on bark measurements, a subtle decrease in diameter can be observed around DOY 98 (2015), followed by an increase starting at DOY 112 (2015). This is most obvious for beech 2, 4, 5 and the oak trees.

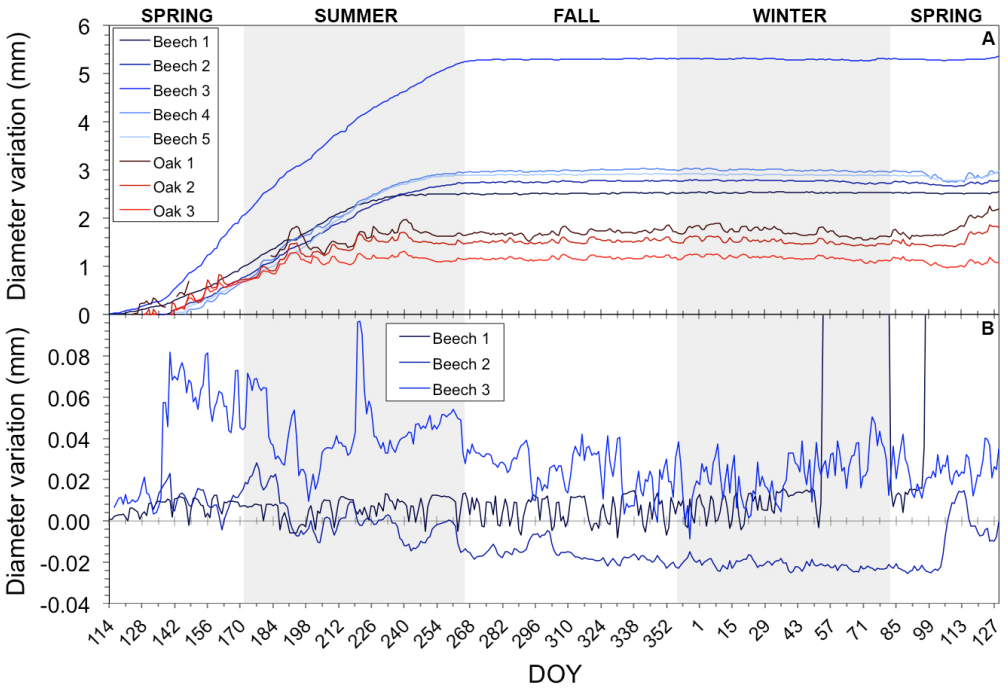

FIGURE 3.8: Diameter variation for five beech and three oak trees in the experimental forest Aelmoeseneie. Dendrometer on bark measurements for beech 1 and 3 started on 24 April 2014 (DOY 114), beech 2 on 14 May 2014 (DOY 134) and beech 4 and 5 on 23 May 2014 (DOY 143) (A). Dendrometer on xylem measurements started on 24 April 2014 (DOY 114) for beech 1, 26 April 2014 (DOY 116) for beech 3 and 14 May 2014 (DOY 134) for beech 2 (B). On bark measurements for oak 1 started on 4 May 2014 (DOY 124), oak 2 and 3 on 9 May 2014 (DOY 129) (A).

Analyzing the measurements from the dendrometers installed on the xylem of beech 1, 2 and 3 (Figure 3.8B) reveals no apparent growing trend when compared with the measurements from the dendrometers installed on the bark. There is however a diurnal pattern pattern in the diameter variation of all dendrometer measurements (Figure 3.9).

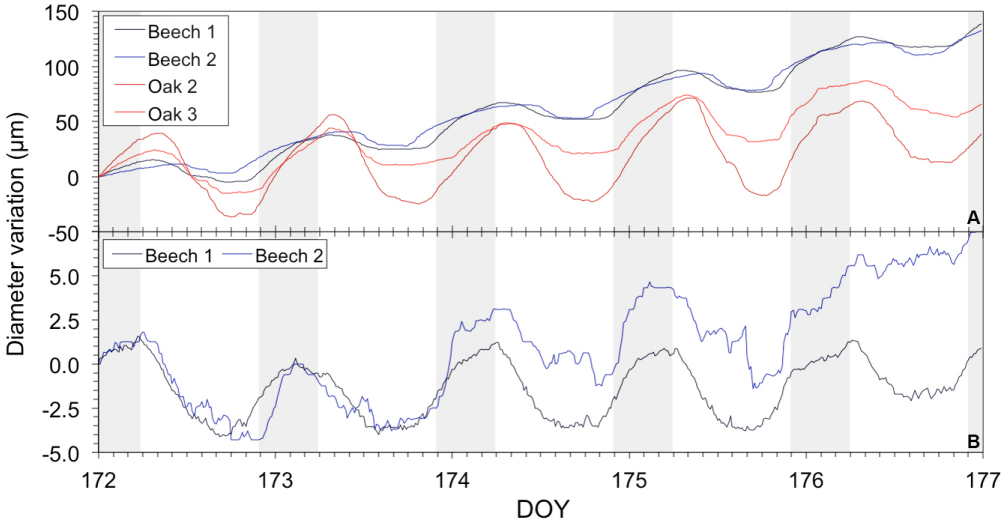

FIGURE 3.9: Diameter variation (µm) measured by dendrometers on bark (µm) for two beech trees and two oak trees (A) and on xylem of two beech trees (B) in the experimental forest Aelmoeseneie for five consecutive (semi-)clear days (21-25 July 2014). Shaded areas represent nighttime.

Diameter over bark increased during the night, followed by a decrease during the daytime (Figure 3.9A). A similar pattern was observed for the diameter over xylem but without the growing trend (Figure 3.9B). When fitting a lineair regression curve through the data (not displayed), a rising trend can be identified for on bark measurements, i.e. $m = 27$ for beech and $m = 11$ for oak. This is not the case for xylem measurements with $m = 0.87$.

Box 3.1 Hygroscopicity of the bark

From Figure 3.8A it can be noticed that the daily fluctuation range is larger for oak than for beech. This is especially the case during rain events. To expand the understanding behind this process, an experiment was set-up in the experimental forest Aelmoeseneie where water was poured on the trunk of three beeches and three oaks with a flow of 1 L.min^{-1} for 20 minutes on five different occasions (11 March, 18 March, 24 March, 5 April and 10 April 2015) before leaf development to exclude noise from sap flow. Water was poured around the dendrometer installed on the bark within a radius of approximately 10 cm. After excluding outliers, there were 11 repeats for both beech and oak available (Figure 3.10).

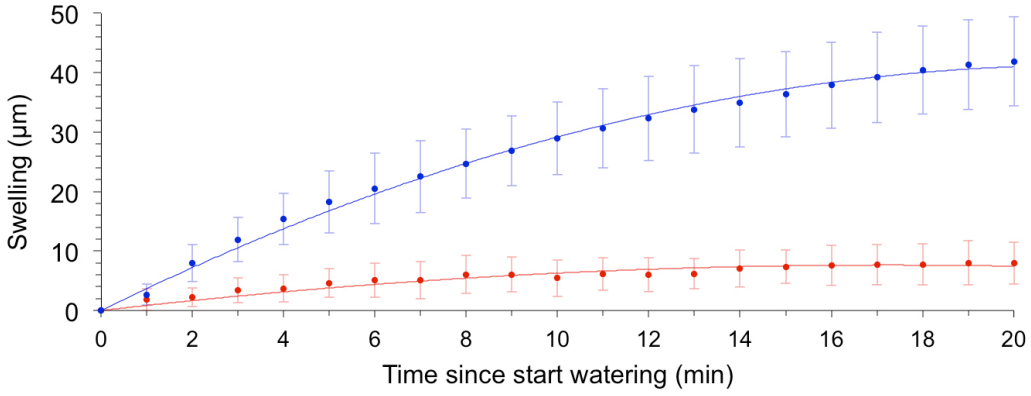

FIGURE 3.10: Diameter increase (µm) after pouring water on the trunk with a flow of 20 L.min^{-1}. Circles represent minute averages of all data. Solid lines show a polynomial fit through the data (R^2 0.924 for beech and R^2 0.995 for oak). Standard deviation is visualized with error bars.

The results clearly show a larger diameter increase for oak than for beech upon pouring the same amount of water, i.e. 20 L, during the same time period, i.e. 20 minutes. After 10 minutes the ratio between the swelling measurements of oak and beech remain more or less constant with a factor of approximately 5.2. The swelling is finite and starts stagnating between 10 to 20 minutes. A few hours after the pouring of water has stopped the tree shrunk to practically the same diameter as before the experiment.

Correlation between several microclimatic variables and ΔD of all trees is shown in Table 3.2. There is some correlation with all meteorological variables, but the correlation strength is the weakest with RH measured at the fourth platform. There is a moderately strong correlation with T at either the ground level and at platform four.

TABLE 3.2: Correlation (r) between bark diameter variation (ΔD) of all nine trees in the experimental forest Aelmoeseneie (beech = B; oak = O), including xylem diameter variation (ΔD_X) of beech 1, 2 and 3, with RH_{GR}, RH_{P4}, T_{GR}, T_{P4}, VPD, PAR, precipitation ('Prec.'), wind speed ('wind') and Ψ_{soil}.

	RH_{GR}	RH_{P4}	T_{GR}	T_{P4}	VPD	PAR	Prec.	Wind	Ψ_{soil}
ΔD_{B1}	-0.13	-0.38	0.39	0.39	0.44	0.49	-0.04	-0.22	-0.29
$\Delta D_{B1,X}$	0.54	0.43	0.14	0.14	-0.27	-0.14	0.11	-0.09	-0.49
ΔD_{B2}	-0.13	-0.36	0.51	0.53	0.48	0.57	-0.06	-0.31	-0.21
$\Delta D_{B2,X}$	-0.18	-0.41	0.62	0.63	0.53	0.66	-0.04	-0.38	-0.17
ΔD_{B3}	-0.12	-0.38	0.45	0.45	0.45	0.52	-0.03	-0.25	-0.22
$\Delta D_{B3,X}$	-0.02	0.11	-0.58	-0.57	-0.19	-0.34	-0.10	0.20	0.05
ΔD_{B4}	-0.10	-0.33	0.52	0.53	0.45	0.54	-0.06	-0.32	-0.17
ΔD_{B5}	-0.08	-0.31	0.52	0.53	0.44	0.53	-0.06	-0.31	-0.20
ΔD_{O1}	-0.16	-0.25	0.22	0.23	0.28	0.35	-0.06	-0.09	-0.26
ΔD_{O2}	-0.21	-0.37	0.32	0.34	0.44	0.48	-0.10	-0.19	-0.12
ΔD_{O3}	-0.27	-0.45	0.29	0.31	0.48	0.49	-0.10	-0.15	0.15
ΔD_{O4}	-0.07	-0.19	0.58	0.60	0.37	0.53	0.00	-0.31	-0.25

3.3.1.2 Small scale set-up

The diurnal pattern of ΔD in the small scale set-up (Figure 3.11) is not as obvious as the measurements from the experimental forest Aelmoeseneie (Figure 3.9), except for ΔD_X of oak (Figure 3.11B). An overall growing trend can be noticed (Figure 3.11A), i.e. 0.38-0.58 mm. Also the diameter of the xylem increased.

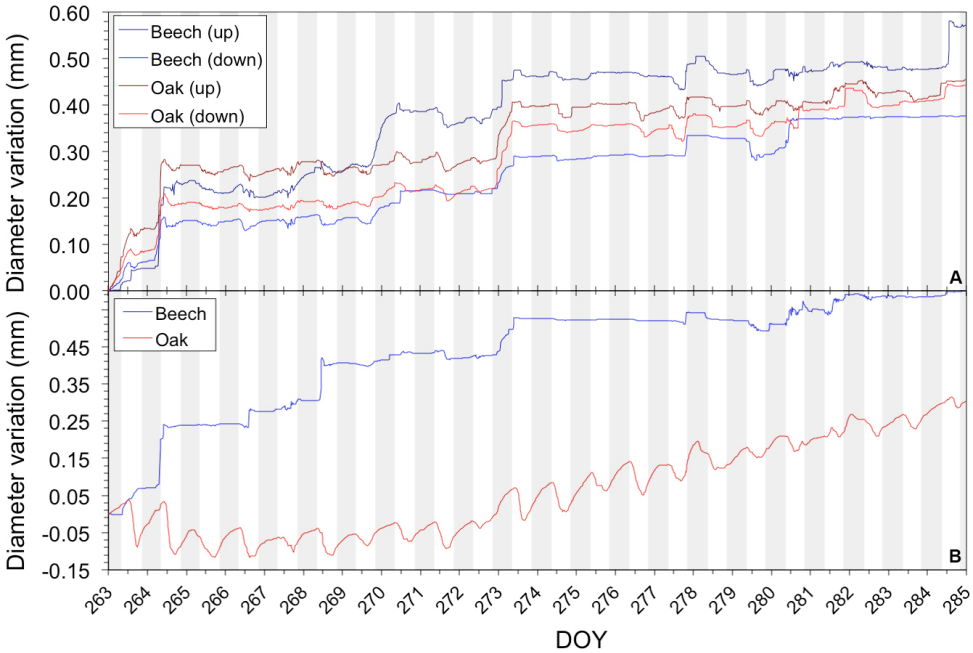

FIGURE 3.11: Diameter variations on bark (ΔD) measured at approximately DBH ('down') and right above the first larger branches ('up') (A) and diameter variations on xylem (ΔD_X) measured at DBH at the small scale set-up. Shaded areas represent nighttime.

Correlation between variables of the microclimate and ΔD of both trees is given in Table 3.3. There is no strong correlation present with the variables of the microclimate. A noticeable strong correlation is present between the diameter variation of both trees and $\Psi_{\text{soil,pot}}$. There is some correlation with $\Psi_{\text{soil,soil}}$, but less apparent.

TABLE 3.3: Correlation (r) between diameter variation on bark (ΔD) of beech (B)/oak (O) and T, RH, Ψ_{soil} in the small scale set-up. Three dendrometers on each tree: D = at DBH; U = right above first large branches; X = installed on the xylem.

	$\Delta D_{\text{B,U}}$	$\Delta D_{\text{B,D}}$	$\Delta D_{\text{B,X}}$	$\Delta D_{\text{O,U}}$	$\Delta D_{\text{O,D}}$	$\Delta D_{\text{O,X}}$
RH beech	0.03	0.02	-0.01			
T beech	-0.10	-0.20	-0.10			
RH oak				0.01	0.04	0.22
T oak				-0.22	-0.20	-0.33
$\Psi_{\text{soil,soil}}$ beech	-0.39	-0.18	-0.40			
$\Psi_{\text{soil,pot}}$ beech	-0.73	-0.69	-0.73			
$\Psi_{\text{soil,soil}}$ oak				-0.22	-0.14	0.16
$\Psi_{\text{soil,pot}}$ oak				-0.84	-0.87	-0.74

3.3.2 Sap flow rate

3.3.2.1 Experimental forest Aelmoeseneie

Sap flux density (F_{sapflux}) ($\text{cm}^3.\text{cm}^{-2}.\text{h}^{-1}$) is measured using the HRM method and converted to sap flow (F_{sapflow}) (L.h^{-1}) using the surface of the sapwood (Table 3.4). Beech 2, beech 5 and oak 2 are excluded from the results due to too much erroneous sections in the data and regions with high fluctuations.

TABLE 3.4: Example regarding the calculation of sap flow (L.h^{-1}) from sap flux ($\text{cm}^3.\text{cm}^{-2}.\text{h}^{-1}$) for beech (B) and oak (O) in the experimental forest Aelmoeseneie.

	B1	B3	B4	O1	O3	O4
$F_{\text{sapflux,max}}$ ($\text{cm}^3.\text{cm}^{-2}.\text{h}^{-1}$)	32.87	40.79	24.77	23.19	19.86	30.28
Radius trunk (cm)	33.39	28.55	19.93	25.46	17.75	21.17
Thickness bark (cm)	0.93	0.64	0.45	0.80	0.50	0.55
Radius xylem (cm)	32.46	27.91	19.48	24.66	17.25	20.62
Surface xylem (cm^2)	3310	2448	1192	1911	934.8	1336
Surface sapwood (cm^2)	893.7	660.8	321.9	382.1	187.0	267.2
$F_{\text{sapflow,max}}$ (L.h^{-1})	29.38	26.96	7.97	8.86	3.71	8.09

A typical yearly pattern is shown in Figure 3.12 for beech 1 and oak 1 using the maximum daily F_{sapflux}. Beech and oak followed more or less the same pattern. An obvious increase can be seen in spring reaching a plateau in summer. During the summer F_{sapflux} declined

steadily whereafter it almost completely ceased in fall. Around DOY 220 a sudden decrease is observed for both beech and oak (149.7 mm precipitation during DOY 220-238). An increase can already be noticed in the spring of 2015 indicating the beginning of the growing season and start of leaf development.

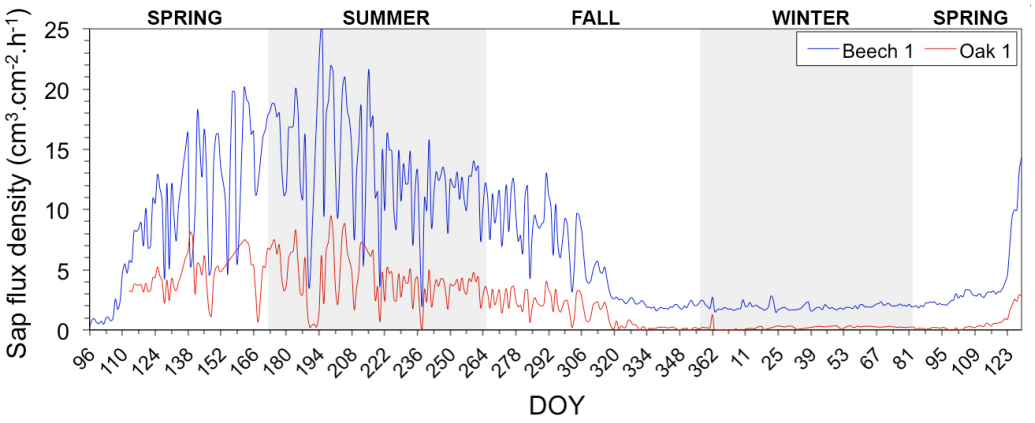

FIGURE 3.12: Maximum daily F_{sapflux} over a timespan of more than one year (5 April 2015 till 2 May 2015) for beech 1 and oak 1 in the experimental forest Aelmoeseneie.

Similar to ΔD, also F_{sapflux} (Figure 3.13A) and consequently F_{sapflow} (Figure 3.13B) described a clear diurnal pattern. The same five clear consecutive days as in Figure 3.9 are presented. The sap does not start to flow immediately after sunrise. A steep and stable increase is present until a maximum is reached around midday. After peaking at midday F starts to decline sharply and continues to do so after sunset during the night.

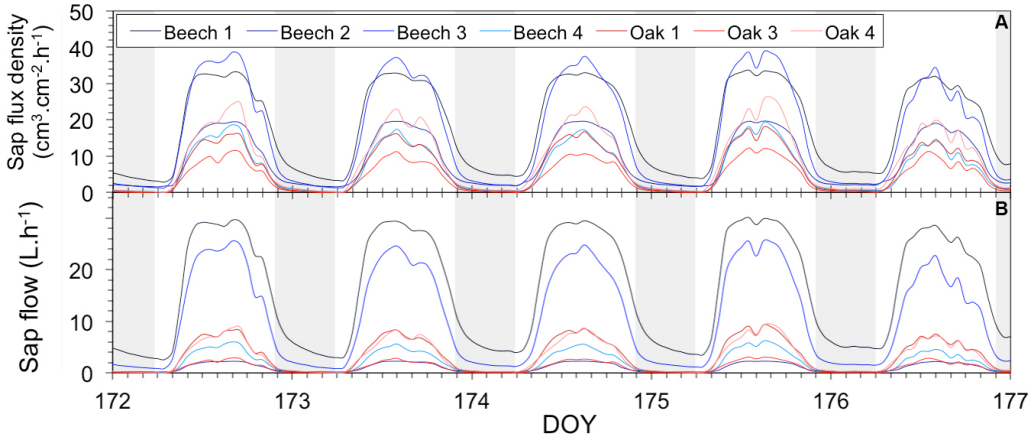

FIGURE 3.13: F_{sapflux} (A) and F_{sapflow} (B) for five consecutive (semi-)clear days (21-25 July 2014) using hourly averages in the experimental forest Aelmoeseneie. Shaded areas represent nighttime.

Beech 1 and 3 clearly have the largest sap flow when compared with the other five trees. For beech 3, this corresponds with the ΔD results as it has grown twice as much when compared to the other beech trees. This is not the case for beech 1, but it is the second largest tree (i.e. 894 cm^2 sapwood), after beech 5 (i.e. 1104 cm^2 sapwood).

Table 3.5 shows the correlation between several microclimatic parameters and F_{sapflux}. There is a strong correlation with T and PAR and moderately strong correlation with VPD. Only a weak correlation is present with RH. The correlation between F_{sapflux} and ΔD is moderate to strong (Table 3.6).

TABLE 3.5: Correlation (r) of F_{sapflux} (B = beech, O = oak) with PAR, RH_{ground}, RH_{P4}, T_{ground}, T_{P4}, VPD, precipitation ('Prec.'), wind speed ('Wind') and Ψ_{soil} in the experimental forest Aelmoeseneie.

	F_{B1}	F_{B2}	F_{B3}	F_{B4}	F_{B5}	F_{O1}	F_{O2}	F_{O3}	F_{O4}
RH_{ground}	-0.10	-0.12	-0.18	-0.25	-0.06	-0.22	-0.25	-0.16	-0.16
RH_{P4}	-0.26	-0.29	-0.33	-0.42	-0.28	-0.38	-0.31	-0.31	-0.31
T_{ground}	0.79	0.79	0.75	0.63	0.73	0.75	0.74	0.77	0.74
T_{P4}	0.80	0.80	0.77	0.63	0.75	0.77	0.77	0.79	0.76
VPD	0.47	0.47	0.55	0.59	0.48	0.59	0.52	0.54	0.53
PAR	0.68	0.69	0.73	0.71	0.74	0.77	0.72	0.71	0.71
Prec.	-0.14	-0.13	-0.15	-0.15	-0.16	-0.15	-0.14	-0.17	-0.10
Wind	-0.34	-0.33	-0.34	-0.35	-0.35	-0.35	-0.35	-0.38	-0.35
Ψ_{soil}	-0.31	-0.31	-0.22	-0.22	-0.24	-0.29	-0.11	-0.33	-0.34

TABLE 3.6: Correlation (r) of F_{sapflux} (B = beech, O = oak) with ΔD. '*' represents the respective tree number. '*X' = correlation with ΔD of the xylem of the respective tree in the experimental forest Aelmoeseneie.

	ΔD_{B1}	ΔD_{B2}	ΔD_{B3}	ΔD_{B4}	ΔD_{B5}	ΔD_{O1}	ΔD_{O2}	ΔD_{O3}	ΔD_{O4}
F_{*}	-0.50	-0.63	-0.54	-0.70	-0.55	-0.45	-0.59	-0.37	0.85
$F_{*\text{X}}$	-0.29	-0.68	0.48						

3.3.2.2 Small scale set-up

F_{sapflux} data is available using the HRM method. Erroneous measuring points are filtered from the data and correction for zero-flow was applied using nightly measurements. Parameters of the two trees in the small scale set-up are presented in Table 3.7.

TABLE 3.7: Information regarding the calculation of sap flow ($L.h^{-1}$) from sap flux ($cm^3.cm^{-2}.h^{-1}$) for the beech and oak trees in the small scale set-up.

	Beech	Oak
Radius trunk (cm)	8.258	7.094
Thickness bark (cm)	0.146	0.408
Radius xylem (cm^2)	8.112	6.686
Surface xylem (cm^2)	206.7	140.4
Surface sapwood (cm^2)	55.81	37.92

Figure 3.14 shows the data during the timespan of the experiment while Figure 3.15 shows a closer look at four particular days (DOY 271-275). During the night there was practically no sap flow. After sunrise the sap starts to flow, and while it is less apparent than the data of the experimental forest Aelmoeseneie, a time lag can still be noticed on some days, e.g. DOY 273. After peaking shortly after midday there is a sharp decrease. At sunset the sap flow has almost completely returned to zero-flow. While the surface of the sapwood of the oak tree is lower than that of the beech tree, F_{sapflux} is several times lower.

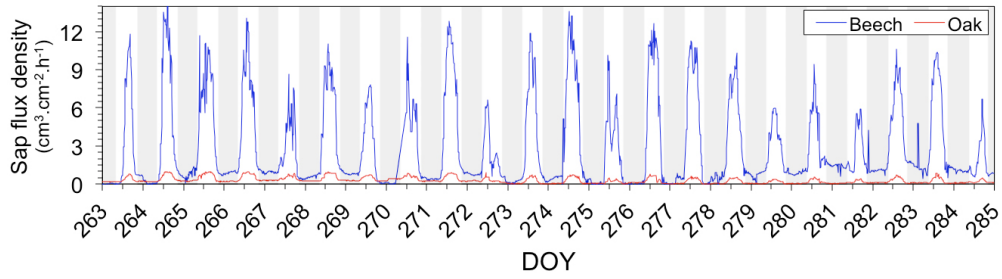

FIGURE 3.14: F_{sapflux} data for the beech tree and oak tree in the small scale set-up during the complete timespan. Shaded areas represent nighttime.

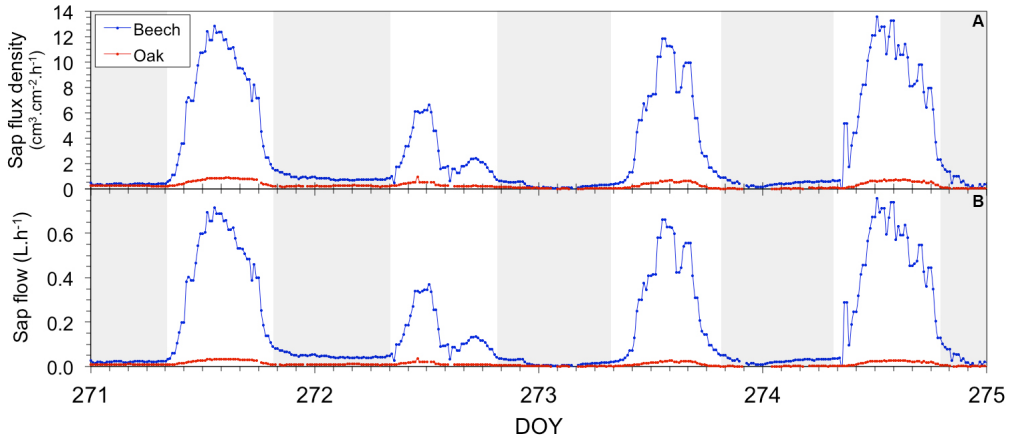

FIGURE 3.15: Detailed look at the F_{sapflux} (A) and F_{sapflow} (B) data for four days in the small scale set-up. Shaded areas represent nighttime.

F_{sapflux} correlates strongly with the meteorological variables and to a lesser extent with Ψ_{soil} (Table 3.8). For the beech tree F_{sapflux} is stronger correlated with $\Psi_{\text{soil,soil}}$ than $\Psi_{\text{soil,pot}}$. The opposite is true for the oak tree.

TABLE 3.8: Correlation (r) of F_{sapflux} from beech and oak in the small scale set-up with the variables T, RH $\Psi_{\text{soil,soil}}$ and $\Psi_{\text{soil,pot}}$.

	F_{beech}	F_{oak}		F_{beech}	F_{oak}
RH beech	-0.77		$\Psi_{\text{soil,soil}}$ beech	0.29	
T beech	0.65		$\Psi_{\text{soil,pot}}$ beech	0.05	
RH oak		-0.68	$\Psi_{\text{soil,soil}}$ oak		0.15
T oak		0.58	$\Psi_{\text{soil,pot}}$ oak		0.45

3.3.3 Stem and leaf water potential

3.3.3.1 Experimental forest Aelmoeseneie

Data of plant water potential in the experimental forest Aelmoeseneie is available through measurements with the pressure chamber. What follows are the results from the two measuring days as outlined in section 2.2.2, starting with the first one on 5 August 2014. On this day both Ψ_{leaf} and Ψ_{stem} were measured simultaneously Figure 3.16. The measurements were more or less stable throughout the timespan of the experiment as sunrise and sunset already occurred at 06:15 and 21:22, respectively. While there are some small fluctuations, the ratio remains practically constant with an average of 0.52 throughout the day.

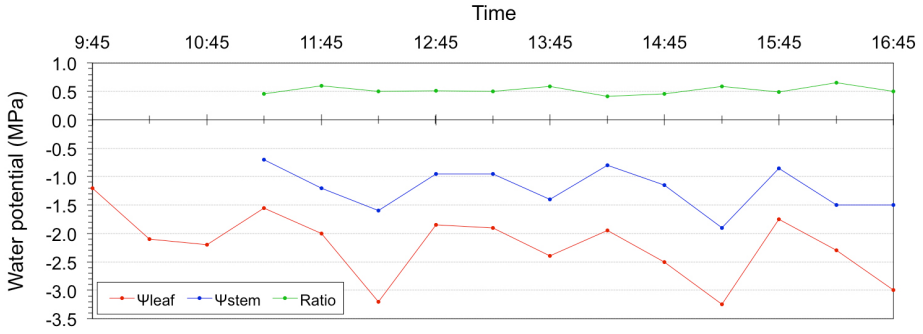

FIGURE 3.16: Ψ_{leaf} (red) and Ψ_{stem} (blue) of beech 1 on 5 August 2014 in the experimental forest Aelmoeseneie. The ratio Ψ_{leaf}/Ψ_{stem} is also visualized.

The second measuring experiment took place on 4 September 2014 from 6:00 (i.e. one hour before sunrise) till 20:00 (Figure 3.17). Averages of the Ψ_{leaf} measurements of the collected leaves from beech 1 on all three platforms (14.6 m, 21.6 m and 28.8 m) are shown. Because measurements are available one hour before sunrise, determination of the 'predawn' water potential is possible, which is representative for the soil water potential [Zhang et al., 1999]. In this case the predawn water potential was -0.23 MPa. A clear diurnal pattern can be noticed and Ψ_{leaf} decreases higher up the tree.

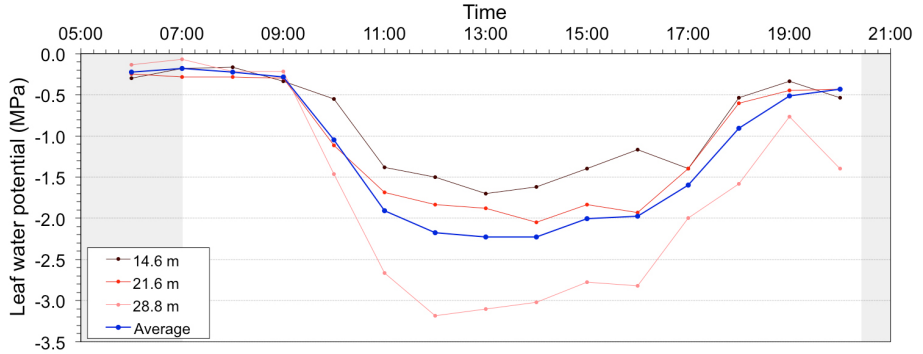

FIGURE 3.17: Ψ_{leaf} of beech 1 in the experimental forest Aelmoeseneie on 4 September 2014 on three different levels (platforms 2, 3 and 4 with a respective height of 14.6 m, 21.6 m and 28.8 m). Shaded areas represent nighttime

Correlation of Ψ_{leaf} with a whole list of other variables is listed in Table 3.9. There is obviously a strong correlation with the listed variables, except with Ψ_{soil}. In particular F_{sapflux} (r = -0.96), PAR (r = -0.89) and VPD (r = -0.87).

TABLE 3.9: Correlation (r) of Ψ_{leaf} with diameter variation on bark (ΔD), diameter variation on xylem (ΔD_X), F_{sapflux}, Ψ_{soil}, VPD, PAR, RH_{GR}, RH_{P4} and T_{GR} and T_{P4}. Data from 4 September 2014 in the experimental forest Aelmoeseneie.

	Ψ_{leaf}		Ψ_{leaf}
ΔD	0.58	PAR	-0.89
ΔD_X	0.84	RH_{ground}	0.81
F_{sapflux}	-0.96	RH_{P4}	-0.73
Ψ_{soil}	0.16	T_{ground}	0.86
VPD	-0.87	T_{P4}	-0.81

3.3.3.2 Small scale set-up

During the timespan of the small scale experiment measurements of Ψ_{stem} for both the beech and oak tree were collected using an ICT stem psychrometer (Figure 3.18). These sensors required an extensive calibration and meticulous installation as the thermocouples are very sensitive and susceptible to damage. This was unfortunately the case for the psychrometer installed on the oak tree. On 2 October 2014 the psychrometer started showing inconsistent results. After evaluation it was decided to remove the psychrometer from the tree whereby it was confirmed that the sample thermocouple was damaged.

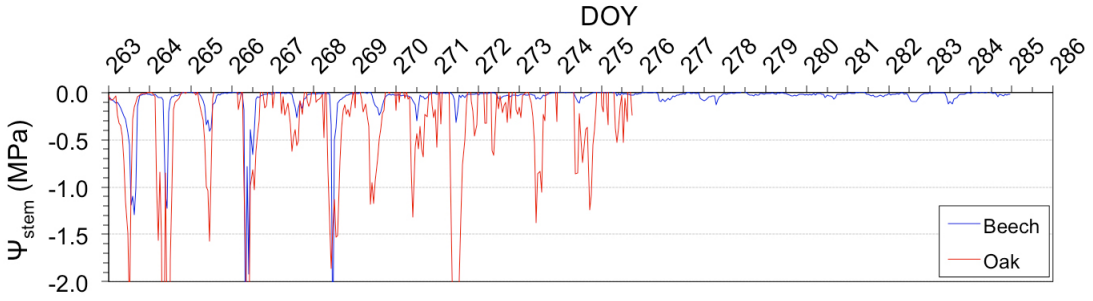

FIGURE 3.18: Ψ_{stem} data for beech and oak during the complete timespan of the small scale experiment, 20 September 2014 - 11 October 2014.

On 23 September 2014 Ψ_{leaf} was measured using the pressure chamber in order to verify the calibrated Ψ_{stem} measurements collected with the ICT stem psychrometer (dots in Figure 3.19). Correlation between both measurements is only moderate (beech r = 0.24, oak r = 0.17) although a similar trend is more or less visible. Correlation of Ψ_{stem} with F_{sapflow} is -0.17 and -0.25 for beech and oak, respectively.

Although the results from the ICT stem psychrometer are fluctuating, a diurnal pattern is noticeable as is a small time lag between Ψ_{stem} and F_{sapflow} on a few days (Figure 3.19).

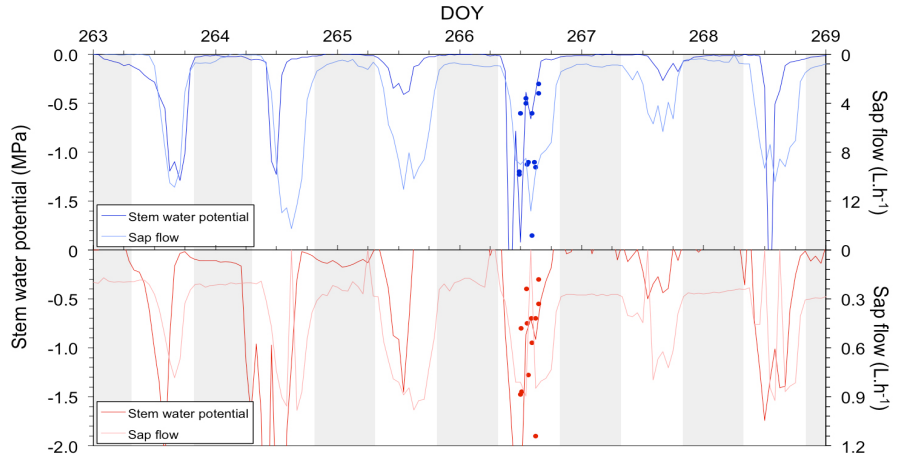

FIGURE 3.19: Diurnal pattern of Ψ_{stem} compared with that of F_{sapflow} for both beech (A) and oak (B) during the period 20 September 2014 - 25 September 2014 in the small scale set-up. Dots show pressure chamber measurements on 23 September 2014. Shaded areas represent nighttime.

3.3.4 Stem water content

The water content of the sapwood, measured as volumetric water content, VWC (m^3 water per m^3 wood), is measured at two positions on the tree in the small scale set-up: at DBH and at the location right above the first larger branches (Figure 3.20). A diurnal pattern in the VWC of the stem can be observed. This is obvious for the 'up' sapwood moisture sensors, but less for the 'down' sensors, especially the first few days (DOY 263-273). The VWC is lower at DBH than at the height of the first larger branches. While the distance between the two sapwood moisture sensors on each tree is approximately the same, the difference between the VWC measurements at the two locations on the beech tree is higher towards the end than between the measurements on the oak tree. Overall there is an increasing trend in the four VWC measurements during the timespan of the experiment.

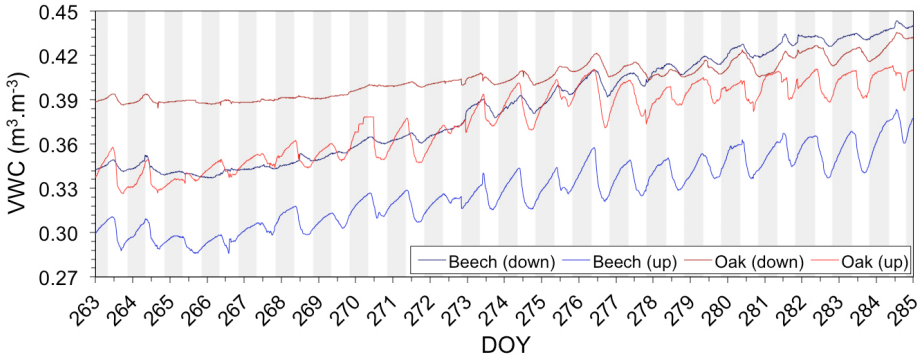

FIGURE 3.20: VWC measured at DBH (down) and right above the first larger branches (up) for beech and oak from 20 September 2014 till 11 October 2014 in the small scale set-up. Shaded areas represent nighttime.

From the correlation table (Table 3.10) it is clear that ΔD and $\Psi_{\text{soil,pot}}$ have a strong correlation with VWC. This is not the case with F_{sapflux}, at least for the beech tree. Correlation of F_{sapflux} with the VWC of the oak tree is stronger.

TABLE 3.10: Correlation (r) of VWC with F_{sapflux}, diameter variation on bark and Ψ_{soil} of beech and oak in the small scale set-up. U = up, D = down and X = xylem (*vide supra*).

beech	VWC_{D}	VWC_{U}	oak	VWC_{D}	VWC_{U}
F_{sapflux}	-0.03	-0.20	F_{sapflux}	-0.36	-0.53
ΔD_{U}	0.86	0.82	ΔD_{U}	0.83	0.87
ΔD_{D}	0.95	0.89	ΔD_{D}	0.89	0.92
ΔD_{X}	0.85	0.81	ΔD_{X}	0.91	0.89
$\Psi_{\text{soil,soil}}$	-0.07	-0.14	$\Psi_{\text{soil,soil}}$	-0.02	-0.20
$\Psi_{\text{soil,pot}}$	-0.71	-0.69	$\Psi_{\text{soil,pot}}$	-0.80	-0.88

3.3.5 Phenology

To analyse the phenology of the forest, two spectral indices are integrated in PhytoSense and calculated from the collected RGB-signals from PhenoCam 1 and 2: excess green index (ExG) and green chromatic coordinate (g_{cc}) [Sonnentag et al., 2012]. In this study two additional indices are added for testing purposes: the visible vegetation index (VVI) [UPRA, 2015] and green-red vegetation index (GRVI), based on the normalized difference vegetation index (NDVI) [Motohka et al., 2010]. The indices are calculated as follows:

$$\text{ExG} = 2 \times G - (R + B) \tag{3.4}$$

$$g_{cc} = \frac{G}{R + G + B} \tag{3.5}$$

$$\text{VVI} = \left[\left(1 - \left|\frac{R - R_0}{R + R_0}\right|\right) \times \left(1 - \left|\frac{G - G_0}{G + G_0}\right|\right) \times \left(1 - \left|\frac{B - B_0}{B + B_0}\right|\right)\right]^{1/w} \tag{3.6}$$

$$\text{GRVI} = \frac{G - R}{G + R} \tag{3.7}$$

with G, green color channel (—); R, red color channel (—), B, blue color channel (—); w, weight exponent to adjust the sensitivity of the scale and RGB_0, vector of the reference green color. UPRA [2015] found after various tests with color calibrated satellite images that $w = 1$ and RGB_0 = [30,50,0] works well. Furthermore they suggest adding a value of 10 to the channel values to avoid division by zero. Figure 3.21 gives a visual overview of the four discussed indices using average values from both PhenoCam 1 and 2.

The four indices were correlated with an extensive set of variables which can be found in Appendix C. It includes correlation with the already discussed microclimatic and tree variables, but also with 'Vitality check'. On four occasions, i.e. 22 September, 6 October, 2 November and 25 November 2014, leaf discoloration and defoliation was estimated of all nine trees in the experimental forest Aelmoeseneie using five classes or scores (0-4) as proposed in the technical report from ICP Forests 2014 [Lorenz et al., 2012]. The sum of both scores was calculated for each individual tree and finally the average of all trees for each of the four vitality check days was calculated.

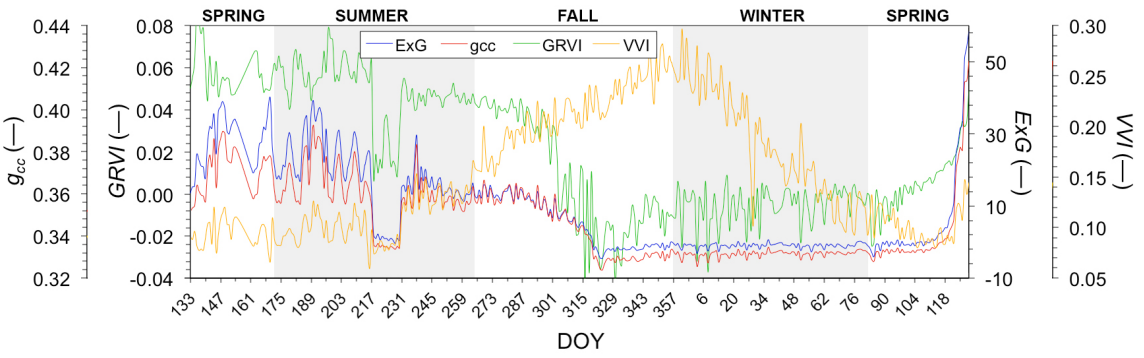

FIGURE 3.21: Calculated indices ExG, g_{cc}, GRVI and VVI using RGB signals from 13 May 2014 till 24 April 2015 in the experimental forest Aelmoeseneie.

GRVI has a strong correlation with F_{sapflux} and ΔD of the trees, except for ΔD_{B1X} which has the strongest correlation with VVI and for ΔD_{B4} and ΔD_{B5} where the correlation with ExG is 0.05 higher. GRVI also has the strongest correlation with 'Vitality check', T, PAR, precipitation and wind speed. The remaining microclimatic variables, i.e. RH and VPD, correlate strongest with VVI.

3.3.6 Specific leaf area

All the leaves that were used to measure Ψ_{leaf} of beech 1 in the experimental Aelmoeseneie on 4 September 2014, were carefully collected and labeled to calculate the specific leaf area, SLA ($\text{cm}^2.\text{mg}^{-1}$) (Figure 3.22). In order to calculate SLA the surface (cm^2) and the dry weight (mg) of each leaf was measured (section 2.2.2).

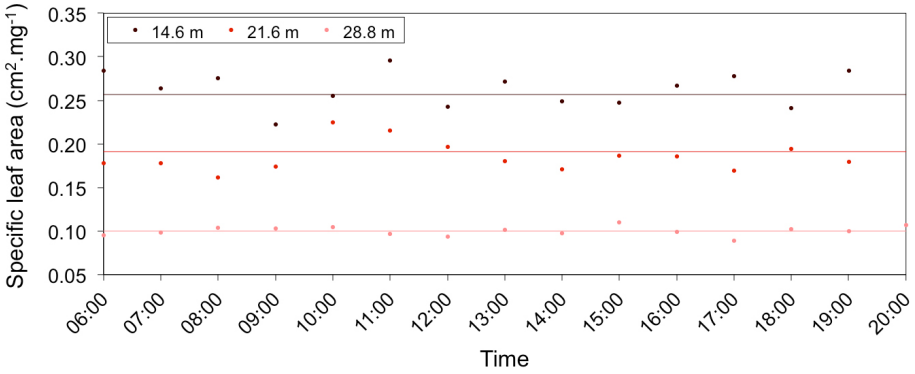

FIGURE 3.22: SLA of the collected leaves on 4 September 2014, from three different platforms in the experimental forest Aelmoeseneie.

The horizontal lines represents the average value of all the measurements on that respective height (14.6 m = P2, 21.6 m = P3, 28.8 = P4). Measurements are more or less stable with no obvious outliers. The horizontal lines give a good visual representation of how SLA varies with the height of the tree. The highest leaves have a lower SLA (0.100 $\text{cm}^2.\text{mg}^{-1}$) than the lowest leaves (0.256 $\text{cm}^2.\text{mg}^{-1}$). Between P2 and P3 SLA lowers with approximately 0.9 $\text{cm.mg}^{-1}.\text{m}^{-1}$ and between P3 and P4 with approximately 1.1 $\text{cm.mg}^{-1}.\text{m}^{-1}$.

Chapter 4

Discussion

From the data collected and analyzed in this study it is clear that there is an obvious interconnection between either meteorological, pedological and physiological variables. And while these relations have been confirmed several times in the literature [Zweifel et al., 2001, Meinzer et al., 2004, Zweifel et al., 2010, De Swaef and Steppe, 2010, Steppe et al., 2006, 2015a], the focus in this study is trying to explain the measured responses for beech and oak, and to some extend quantify these relations.

4.1 Drought followed by extreme rain events fatal for oak?

Almost the complete growing season of 2014, i.e. 10 May 2014 - 6 September 2014, is presented in Figure 4.1 using half hourly averages. This allows a detailed analysis of the diameter variations for both beech and oak.

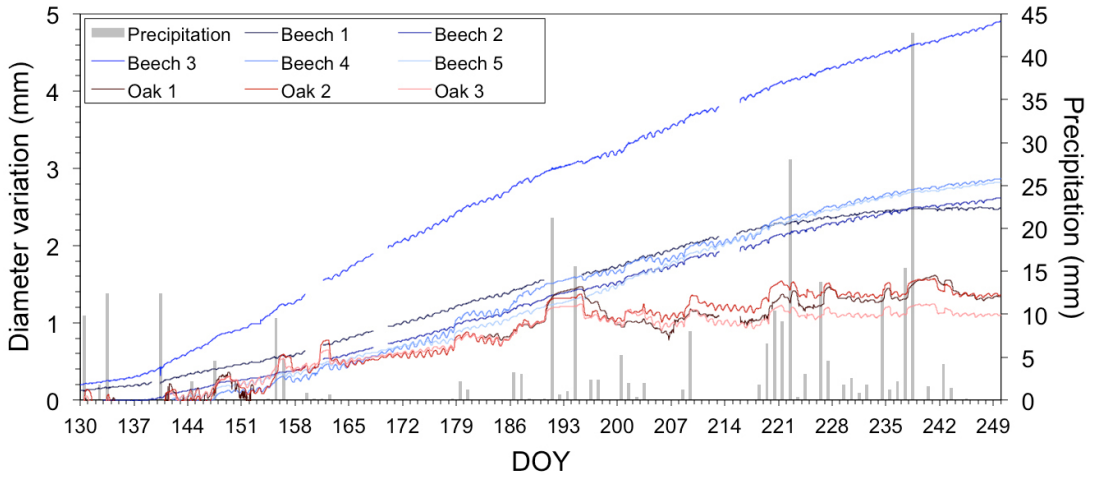

FIGURE 4.1: Diameter variation in the experimental forest Aelmoeseneie during the growing season of 2014 including 24 hour cumulated precipitation.

The diurnal shrinking and swelling of the trunk is clearly visible. At the start of the growing season it is obvious that oak has a very fluctuating growth pattern when compared with the beech tree. This is probably linked with precipitation as a high amount of swelling occurs consistently with a rainfall event. The correlation between precipitation and diameter variation is also stronger for oak ($r = 0.32$) than for beech ($r = 0.14$). At first it could be argued that oak is stressed by the amount of precipitation. It was however established during the study that the bark of oak swells considerably more than the bark of beech when water is poured directly onto the bark (Box 3.1). This should be taken into consideration upon analyzing these results. But even when taken this into consideration, it still looks like oak is more susceptible to stress caused by high amounts of precipitation. For example, DOY 191 (10 July 2014) was a day with 21.2 mm of rainfall and while the growth rate for beech and oak was more or less the same before this date, it is no longer the case after 10 July. Oak seems not to be able to recover after DOY 191.

The growth pattern of oak can be explained by combining knowledge from a wood anatomical point of view and from a meteorological one. Although both beech and oak are angiosperms, beech has diffuse-porous wood and oak ring-porous wood (Figure 4.2). Several studies (e.g. Cochard and Tyree [1990]) have already described the hydraulic differences and vulnerability between these two types. Diffuse-porous species have smaller vessels which all have more or less the same diameter, while ring-porous species differentiate between larger latewood-vessels and smaller earlywood-vessels. It is confirmed that certain weather circumstances, e.g. frost, are much more dramatic for ring-porous species than diffuse-porous species [Cochard and Tyree, 1990]. Because oak is unable to refill its cavitated vessels (Box 4.1) after the winter, it has to deal with this cavitation and in response it builds large vessels in the beginning of the growing season to be able to absorb enough water for its metabolism. The moment that the balance is restored, it builds smaller vessels. This is not the case for beech which can simply use most of the vessels it has built in the previous growing season and is thus more efficient.

Box 4.1 Cavitation and embolism

Cavitation is the generation of gas filled cavities in the xylem vessels. This occurs when a large xylem tension induced by a very negative Ψ_{leaf} is present in the tree, which in turn is caused by a dried soil. Water can no longer be transported by the roots and vessels will slowly fill with air. Cavitation also occurs when insoluble gasses form tiny air bubbles during a frost period. Upon thawing of the vessels and reinitiating the transpiration, the tiny bubbles will expand and cause cavitation. When a xylem vessel is completely filled with air, the water column is 'broken' and the xylem embolised, which will result in a whole-plant decrease of hydraulic conductivity.

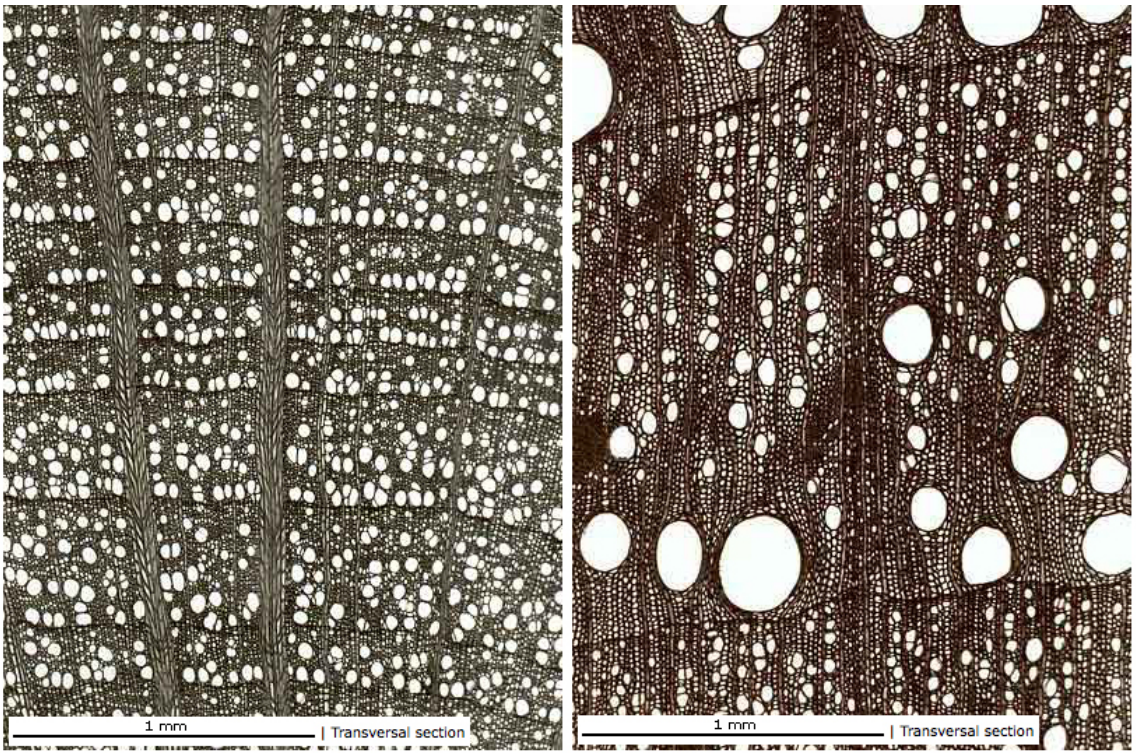

FIGURE 4.2: Microscopic images of a transversal section for beech (left) and oak (right) [`http://www.woodanatomy.ch/`, WSL].

Not particularly the winter of 2013-2014, but 2012-2013 was a very cold one with 16 ice days (i.e. maximum temperature below zero) and 65 frost days (i.e. temperature decreasing once below zero), compared to the average (1981-2010) which is 7 ice days and 46 frost days. As a matter of fact, every winter since 2009-2010 was above average regarding ice and frost days [RMI, 2015]. These winters probably caused a lot of vessels in oak to get cavitated, especially since stress events have a cumulative effect on whole-tree architecture [Meinzer et al., 2013]. Oak builds at the start of the growing season of 2014 large vessels in order to restore its balance. Beech is probably able to use the same vessels as the previous season or has less difficulty in refilling its cavitated vessels. This is the situation at the beginning of the growing season of 2014.

When furthermore (ii) precipitation measurements are compared with the averages from the Royal Meteorological Institute of Belgium (Table 4.1) (1981-2010), it can be observed that during the five months growing season in 2014 there is in total 22.6 mm less rainfall. This could well indicate some moderate drought stress, especially in the month June where there was as good as no rain (only 1.8 mm) for three consecutive weeks (i.e. 6 June - 27 June). This period can even be expanded from 6 June till 9 July where only 12.0 mm precipitation was collected. So proceeding further on through the growing season, keeping in mind that oak has built large vessels due to the cold winters, it is plausible that the moderate drought in June caused more cavitation (Box 4.1) in the large earlywood-vessels, compared with the smaller vessels of beech. Whereas the growth rate is more or less the

same at the beginning of the drought period, a sudden stagnation in the growing of the oaks can be noticed around DOY 169 (18 June 2014). This is more or less in the middle of the drought period and it is probably the moment where xylem embolism has started.

TABLE 4.1: Precipitation measurements in the experimental forest Aelmoeseneie compared with averages from the Royal Meteorological Institute of Belgium (1981-2010) [RMI, 2015].

	May	June	July	August	September
Measurements 2014 (mm)	63.6	20.0	68.6	165.6	18.6
RMI 1981-2010 average (mm)	66.5	71.8	73.5	79.3	68.9
Deficit (mm)	-1.9	-51.8	-4.9	86.3	-50.3

Right before DOY 191 (10 July 2014) the situation is most likely as follows: oak has only a few large intact earlywood-vessels (i) left due to cavitation during the drought period (ii). This is not the case for beech because of its smaller vessels. Oak grows until DOY 191 where 21.2 mm precipitation was measured, which is approximately one third of the total average amount of rainfall in July. (iii) This amount of rainfall is possibly causing a lot of stress for oak as the tree is trying to uptake as much water as possible but is not successful in doing this due to its air-filled vessels. Furthermore it is feasible that the roots cannot cope with the high amount of rainfall. Because the tree is not taking up the water fast enough the soil around the roots becomes completely saturated with water in a matter of a few hours, resulting in anaerobic conditions. Under moderate oxygen deficit root growth is reduced, but as the deficiency increases trees lose the ability to absorb nutrients and water [Hake et al., 1990]. Beech is not influenced by these events as the growth rate remains more or less similar as before.

When progressing further through the growing season (iv) the extreme amount of precipitation in August, 86.3 mm above average, can also not be ignored. In only two days, i.e. 25 and 26 August, 58.2 mm precipitation was measured. Actually the two month period after 10 July is characterized by several singular days with a high amount of rainfall: 13 July (15.6 mm), 8 August (10.4 mm), 9 August (9.2 mm), 10 August (28.0 mm), 14 August (13.8 mm), 22 August (12.0 mm), 25 August (15.4 mm), 26 August (42.8 mm).

The discussed succession of events: (i) successive cold winters, (ii) drought period and (iii) very high amounts of rainfall during a short period, were fatal for oak causing a premature end of its growing season around 10 July 2014. Every 'growth' or swelling after 10 July can be directly attributed to rainfall. The winter of 2014-2015 had 55 frost days (9 above average) and 2 ice days (5 below average), so more or less an 'average' winter. It is expected that the very few vessels oak was able to create and keep intact during the growing season of 2014 are mostly left intact and not cavitated. If there is no drought period and extreme rainfall events, it might be possible for oak to start recovering from the past few very cold winters. From the most recent results, it looks like oak is able to do so, except oak 3.

4.2 Bark hygroscopicity can not be ignored

The diameter of oak fluctuated more frequently and stronger than beech. It was also noticed that the diameter of oak swole considerably more during rain events when compared with beech. While it was thought this might be some kind of 'water' stress, where swelling of the tree is caused by internal absorption of water, it should be taken into consideration that the bark of both species differ quite a lot (Figure 4.3). (i) While beech has a smooth and thin (1-2 mm) bark with no cracks at all (Figure 4.3A), older individuals of oak have a very irregular, fissured and thick (4-5 mm) bark (Figure 4.3B). The cracks in the bark are sometimes up to 2 cm wide and several mms deep.

(A) (B)

FIGURE 4.3: Close-up image of the bark of a beech (A) and an oak (B) tree in the experimental forest Aelmoeseneie when it is dry (left half) and after wetting (right half).

The anatomy of the bark might already cause it to swell more when compared with beech due to the stronger adsorption power. (ii) It is however also well known that the bark of oak contains a high amount of tannins [Hathway, 1958]. Oak bark has been a traditional tanning material of Britain and northern Germany since medieval times. The tannic acid found in oak is called quercitannic acid and it is said that oak bark contains 12-16% tannin on average [Hathway, 1958]. No such references are found for the bark of beech. Tannins in beech are mostly located in the leaves [Bussotti et al., 1998] and the beechnuts (also called beechmast), but are generally very limited. The tannins in oak are hydrolysable tannins or pyrogallol-type tannins and are as said mainly found in the bark. Addition of weak acids or weak bases (e.g. water) results in the breaking of the chemical bonds and production of carbohydrate (most likely D-glucose) and phenolic acids.

Figure 3.10 shows the results of the executed experiment to enable quantification of the swelling of the bark of both trees (detailed in Box 3.1). The experiment always took place on clear days before spring 2015 and development of the leaves (confirmed with sap flow measurements). Hence, every swelling measured during this experiment can be directly attributed to the water being poured right onto the bark.

It is clear that the bark of oak swole considerably more than the bark of beech. After 10 minutes the ratio between the two remained more or less constant, 5.2. The two discussed hypothesis, (i) difference in anatomy and (ii) presence of tannins, are mostly the causes of this swelling. When evaluating diameter variation measurements for species with an irregular bark and/or bark containing tannins during rainfall, the hygroscopicity of the bark should be taken into account and results should be interpreted with caution.

Lövdahl and Odin [1992] discussed the influence of relative humidity and air temperature to diurnal changes in stem diameter of Norway spruce (*Picea abies* (L.) H.Karst.). They concluded that nearly all of the diurnal variation was caused by changes in relative humidity at the stem surface. While correction for swelling of the bark is necessary during moist situations (e.g. rain events), it is unlikely that all of the diurnal variation is caused by changes in relative humidity.

4.3 Usage of SF/PET to determine hydraulic problems?

Potential evapotranspiration or PET defines the amount of water a particular tree could potentially transpire if the tree had an ideal unlimited water supply. This can be calculated using two different approaches, as lined out in detail by the FAO [Allen et al., 1998]. The most used approach is the 'crop coefficient approach', particularly in agriculture, where crop evapotranspiration (ET_c) (mm.d^{-1}) is calculated by multiplying the reference crop evapotranspiration (ET_0) (mm.d^{-1}), using a calibrated reference crop under the same conditions, by a crop coefficient (K_c) (—). In agriculture, K_c varies with specific crop characteristics and to a limited extent with climate.

PET can also be calculated directly from meteorological and 'crop' data by using the Penman-Monteith equation. Detailed formulation of the Penman-Monteith equation can be found in Allen et al. [1998]. As meteorological data is readily available and measured continuously during the timespan of this study it is possible to calculate PET (L.h^{-1}.m^{-2}). To determine the surface area of the crown, i.e. transpiration surface, the tree diameter is used as a proxy [Bechtold, 2003, Hemery et al., 2005] and was multiplied with a factor of 28 for beech and 20 for oak. This allows obtaining a value for the tree crown diameter which can then be used to determine the surface area of the crown. This finally results in PET in L.h^{-1} which represents ET_0. In section 1.4.2 it was already mentioned that sap flow measurements (L.h^{-1}) can be used as a proxy for transpiration and are thus considered to be equal to the amount of water transpired by a tree [Reyes-Acosta and Lubczynski, 2013, Uddin et al., 2014]. Therefore SF measurements are used as ET_c data. Using these two data sets it is possible to determine a 'crop coefficient' for beech and oak, both not listed in FAO Crop Coefficient tables.

During this discussion the ratio SF/PET will be referred to as K_t or 'tree coefficient'. In theory a value of 1 indicates that the amount of water transpired by the tree (SF) is equal to the amount of water 'required' by the air (PET). Values lower than 1 indicate that the tree is unable to supply the amount of water that is demanded, i.e. how closer K_t is to 1, how better the hydraulic functioning of a particular tree.

K_t is calculated daily for all beeches and oaks in the experimental forest Aelmoeseneie during the growing season 2014. Average K_t values for beech and oak are shown in Figure 4.4. K_t fluctuates throughout the growing season, but not randomly. The drought period (DOY 157-190) is represented by the light grey area and precipitation with dark grey bars. Table 4.2 shows the average values of K_t before, during and after the drought period.

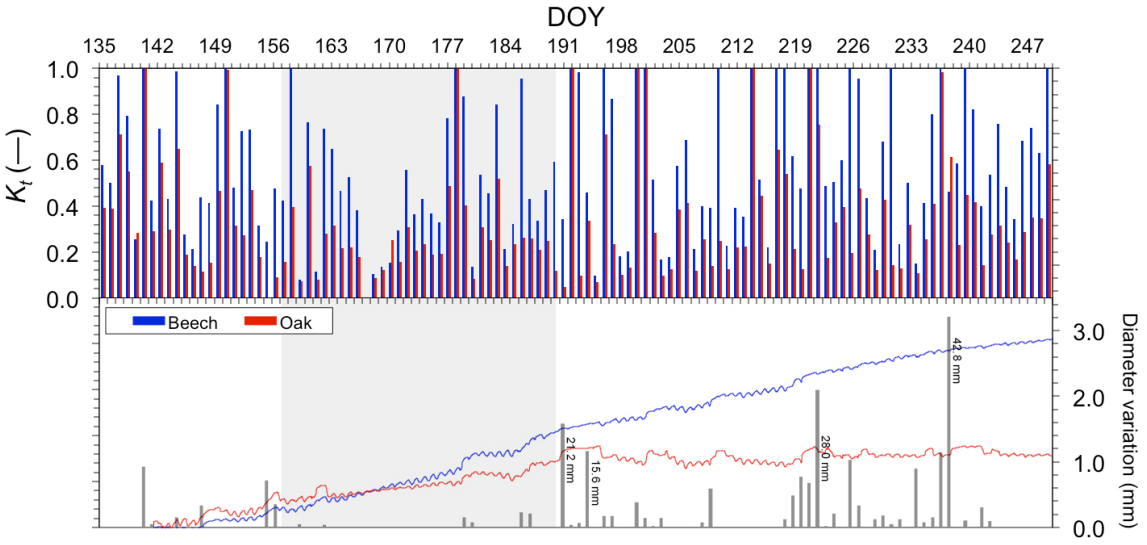

FIGURE 4.4: Mean tree coefficient K_t ($= SF/PET$) during the growing season for all beeches and oaks (top) and precipitation and diameter variation measurements for beech 4 and oak 3 (bottom) in the experimental forest Aelmoeseneie. The extended drought period, 6 June 2014 till 9 July 2014, is represented with a grey area.

TABLE 4.2: Average SF/PET before, during and after the 'drought' period for beech and oak in the experimental forest Aelmoesneie. Standardized values with the first value are between brackets. p-values from two sampled t-tests (5% significance level and H_0: difference in means is equal to 0).

	Before	During	After
Beech	0.656 (100)	0.516 (79)	0.770 (117)
Oak	0.505 (100)	0.238 (47)	0.312 (62)
p-value	0.276	0.005	0.013

K_t was lower for oak than for beech during the complete season indicating that oak was having more trouble with its hydraulic functioning. K_t was already quite low for oak in the beginning of the growing season which can probably be explained by the fact that oak was struggling to bring its water balance in order by building large vessels (section 4.1). During the drought period, K_t for oak decreased by more than half (-53%). This is not the case for beech although K_t also decreased (-21%). After the drought period the trees

were confronted with a very high amount of rainfall (Table 4.1). Beech seemingly restored and even improved its hydraulic functioning (+17%). Oak restored only a little bit, but K_t is still lower than at the start of the growing season (-38%). There is no significant ($p = 0.276$) difference in K_t for beech and oak before the drought period, but there is during ($p = 0.005$) and after ($p = 0.013$) the drought period. As discussed previously, there is a good possibility that the growing season for oak ended prematurely around DOY 191 and hence had no longer a very active metabolism (section 4.1).

The diameter variation for beech 4 and oak 3 were also plotted in Figure 4.4 to illustrate this hypothesis. Whereas they both have more or less the same growing trend before the drought period, the trend for oak decreased steadily during the drought period and almost no growth was measured after it. This was obviously not the case for beech although it can be noticed that during high amounts of rainfall there was some stagnation, but not very substantial be to defined as 'stressed'.

4.4 Distinguishing phenology and stress through imagery

The phenology results (section 3.3.5, Appendix C) clearly show promise in using imagery to distinguish phenological events such as budburst and leaf development, but also stress, which results in leaf discoloration and defoliation, can possibly be determined. Figure 4.5 gives a separate representation of the four indices along with sap flux density, diameter variation and precipitation measurements from 13 May 2014 till 24 April 2015.

It is clear that ExG, g_{cc} and GRVI are able to define the end and the beginning of the growing season. VVI, which correlates only moderately with sap flux and diameter variation, is less able to define these boundaries. Whereas ExG and g_{cc} show a very steep rise at the beginning of the growing season of 2015, GRVI increases more gradually. This may indicate that the first two are only able to detect leaf development at an already advanced stage while a value of GRVI higher than zero may indicate for example budburst. Even more so, a steeper increase in the GRVI can be noticed around DOY 123. This is the same day where ExG and g_{cc} start increasing steeply and thus may indicate full leaf development. The same can be said at the end of the growing season of 2014 where the decrease of GRVI is more subtle than ExG and g_{cc}.

Around DOY 218-231 a period of strongly decreased indices can be noticed. This is a period with a high amount of precipitation (83.0 mm in total) and is followed with a period of about the same amount of precipitation in a shorter timespan (75.4 mm from DOY 231-238). Simultaneously a more or less sudden decrease in sap flux density can be noticed. It is (currently) unclear why the indices decreased so much during DOY 218-231, it might be temporary noise because of the high amount of rain, or due to stress of the trees.

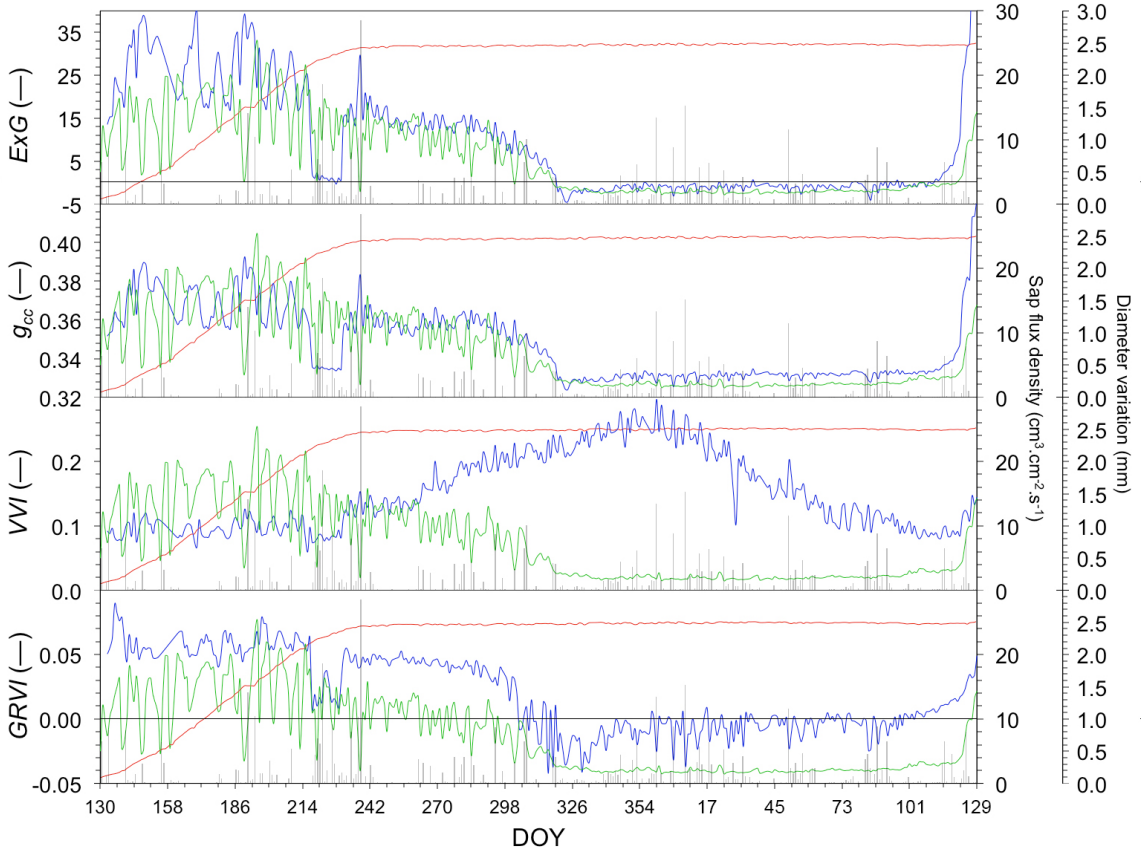

FIGURE 4.5: Spectral indices ExG, g_{cc}, VVI, GRVI (blue) plotted together with $F_{sapflux}$ (green), ΔD (red) and precipitation (grey bars) during the timespan 13 May 2014 - 24 April 2015.

While all four spectral indices correlate more or less with sap flux density and diameter variation, GRVI has the strongest correlation with these variables. This can also be observed visually. Where ExG and g_{cc} sometimes show an opposite trend with sap flux density, GRVI follows the same trend as sap flux density. Hence this index shows the most promise to determine stress as sap flux density is directly influenced by stress events (e.g. drought and predation). Furthermore the authors, Motohka et al. [2010], describe that GRVI can show a distinct response to subtle disturbance. Verification and calibration with field data is required to enable the full potential of this index.

4.5 Everything is interconnected

During the timespan of this study, monitoring the nine trees in the experimental forest Aelmoeseneie and the two trees in the small scale set-up, it has become more clear everyday that everything is interconnected (Figure 1.4). This is also illustrated by the multiple correlation tables found in the results. Meteorological variables such as PAR have a great impact. For example when PAR increases, T will increase and RH decrease which results in an increased VPD. Caused by an increased VPD, Ψ_{leaf} will decrease. Due to a decreasing

Ψ_{leaf} the sap will start to flow, first using water stored in the trunk. A few moments later, if available, water will be transported from the soil. Internal water is causing the lag between sap flow and Ψ_{leaf}. Usage of internal water will cause the trunk to shrink during the day. This will be refilled during the night where it will swell. By using water and light energy the tree grows causing a gradual rise in the diurnal pattern of shrinking and swelling.

4.6 Hysteresis everywhere

Another known phenomena observable in larger trees is 'hysteresis'. This trend is pictured for the xylem diameter variation in relation with the volumetric water content (Figure 4.6A) and the sap flow (Figure 4.6B) for oak in the small scale set-up using average data of 15 minute averages from 20 September - 11 October 2014. But also beech in the experimental forest Aelmoeseneie follows this pattern. Figure 4.6C visualizes Ψ_{leaf} in combination with the sap flow on 4 September 2014. Figure 4.6D shows the xylem diameter variation in relation with sap flow using average data of half hourly averages from 5 June - 6 July 2014.

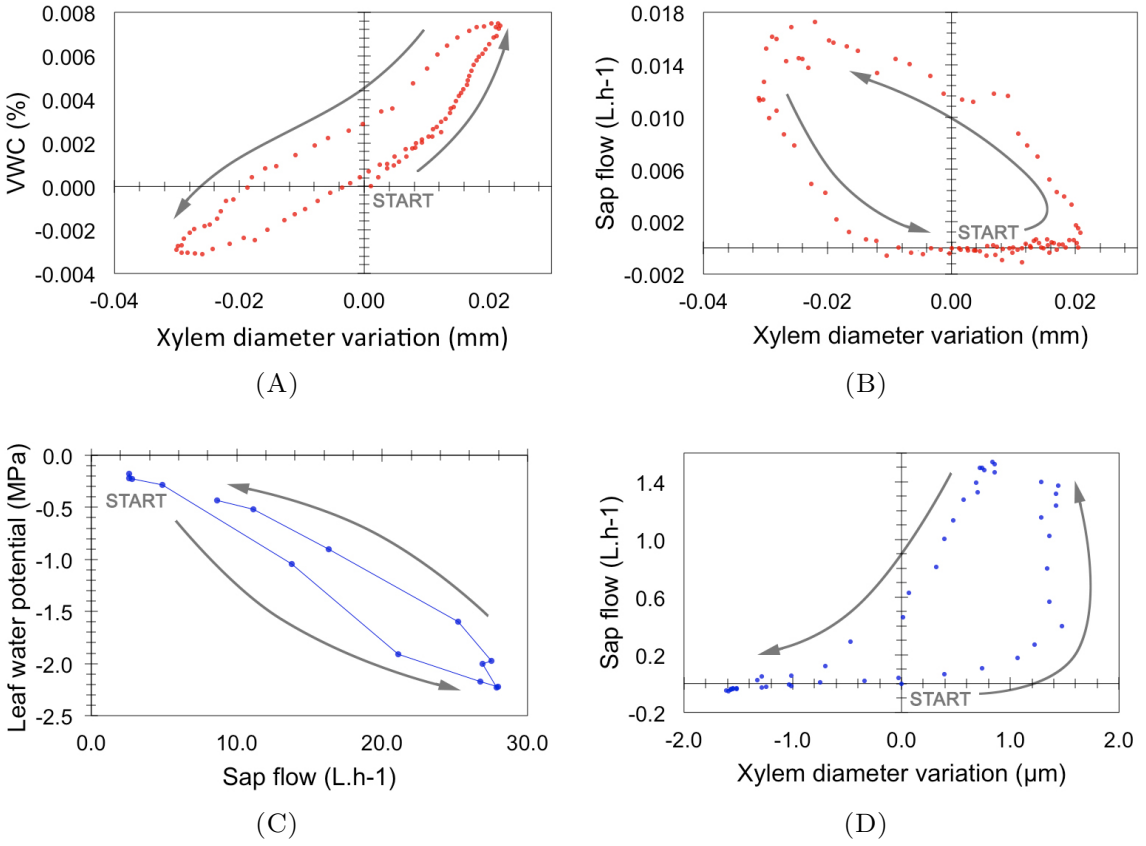

FIGURE 4.6: Examples of hysteresis in oak from the small scale set-up where diameter variation on xylem (ΔD_X) is plotted relative to VWC (A) and $F_{sapflow}$ (B). Examples of hysteresis in beech from the experimental forest Aelmoeseneie where $F_{sapflow}$ is plotted relative to the Ψ_{leaf} (C) and ΔD_X is plotted relative to $F_{sapflow}$ (D).

Hysteresis develops in trees because of the previously discussed time lag. Arrows represent the progress of the day. At sunrise water will transpire from the leaves, but the roots are not taking up water from the soil just yet so water from the internal storage of the tree is being used. During the day the balance will be restored and when transpiration stops in the evening the internal water reservoir will be refilled, i.e. going back to 'START'.

4.7 How many individual trees should be monitored?

In the forest Aelmoeseneie, with a total surface area of 28 ha, are currently five beech trees and four oak trees being monitored. A forest inventory is available, so in theory it is possible to upscale the data from these nine trees to the total forest stand. There are however at least two different forest stand types present (oak-beech and ash-maple). So it would be incorrect to use the measurements of beech and oak to make a conclusion on the status of the other stand types. It is hence necessary to make an evaluation of the forest to determine what the main forest stand types are. In an oak-beech stand it would be correct to only measure oak and beech. In an ash-maple stand it is required to monitor ash and maple. This information is readily available in a forest inventory.

During this study the response within both species was very similar from which it could be concluded that only one monitored tree per species in a forest stand is sufficient. Keeping in mind that large diameter trees (DBH $>$ 100 cm) have the largest contribution to ecophysiological processes in a forest and have the largest ecological importance, one could argue that monitoring these trees have the highest priority. This might differ significantly with the objective of the forest, e.g. production versus selection forest.

So as an absolute minimum one could monitor one tree of each dominant species in a forest stand, preferably large diameter individuals. In the oak-beech stand in the experimental forest Aelmoeseneie could for example beech 5 and oak 4 be selected. Monitoring these two trees is most likely sufficient to make a well-founded judgement on the status of the complete oak-beech stand. According to the forest inventory, beech and oak account for 36% of the total basal area making them the two most important species, besides poplar (*Populus* spp.) (25%). Other species include ash (*Fraxinus excelsior*) (11%) and alder (*Alnus glutinosa*) (10%). The forest inventory was carried out in 2007. It is possible that due to ash dieback (*Hymenoscyphus fraxineus*) there are a lot less ash trees present in the current forest Aelmoeseneie.

Besides tree species distribution it is also important to factor in the site conditions. In the Aelmoeseneie forest the soil is moderately wet (southeast) to very wet (northwest). The soil texture is mainly sandy loam with a few clay fragments and the profile is *c* in the southeast and *p* in the northwest. Generally the experimental forest is a more or less even forest with only a few very wet regions on the clay soils with *p* soil profile in the northwest.

One sap flow sensor and one dendrometer cost approximately €2200. Using the Aelmoeseneie forest with a surface area of 28 ha as example, required monitored tree species would be poplar, oak, beech, ash and alder which results in a total cost for the sensors of €11000. This excludes logging infrastructure, i.e. five (wireless) loggers, a remote server and software (PhytoSense). Even when the cost of the infrastructure is estimated €8900, resulting in a total of €20000, this is still less than half of the cost of an eddy covariance tower which integrates an area of approximately 20 ha. On top of that is this set-up, dendrometers and sap flow sensors, more easily established than a tower reaching above the canopy equipped with numerous high-end sensors. If a forest stand exceeds several dozens of hectares (> 50 ha), it might be beneficiary to monitor an additional tree of each present main species, especially if a logging infrastructure is already present.

4.8 Quantification of relations

4.8.1 Ratio between stem and leaf water potential

As it is not always possible to measure Ψ_{leaf} and Ψ_{stem} simultaneously it was attempted to find a ratio between both. In order to achieve this both variables were measured simultaneously, using the pressure chamber, for the beech tree next to the measuring tower in the experimental forest Aelmoeseneie.

Although there were some fluctuations between both measurements throughout the day, the ratio remained constant, 0.52 (Figure 3.17). It should be noted that this ratio is applicable for in this case beech. Pivovaroff et al. [2014] measured midday Ψ_{leaf} and Ψ_{stem} for 17 different woody species. While for some species (e.g. *Quercus agrifolia* and *Oleo europaea*) the ratio is the same, approximately 50%, this is not the case for other species, which were were mainly shrubs.

4.8.2 Contribution of xylem shrinkage to total shrinkage

The diameter of the stem shrinks and swells every day. It shrinks during the day because water from the internal water reservoirs is used and it swells during the night due to refilling of this internal storage. Part of this diurnal pattern is caused by the phloem (measured by dendrometer on bark) and another part by the xylem (measured by dendrometer on xylem after removing bark and cambium layers). Because there are quite some periods with heavy fluctuations in the xylem diameter variation measurements, it was not possible to do a random sampling. And while there is xylem diameter variation data available for beech 3, it was not possible to find enough data points where both measurements of diameter variation (i.e. phloem and xylem) were not heavily fluctuating. Therefore nine days were

selected systematically for beech 1 and 2, trying to sample one day each month. Results are shown in Table 4.3. While there is some fluctuation in the results, the averages are more or less on the same order: 29% for beech 1 and 20.1% for beech 2, averaging at 24.6%.

TABLE 4.3: % xylem shrinkage of total shrinkage for beech 1 and 2 on nine different occasions.

Date	$\Delta D_{B1X}/\Delta D_{B1}$ (%)	Date	$\Delta D_{B2X}/\Delta D_{B2}$ (%)
23/04/14	20.2	19/05/14	35.8
23/05/14	32.5	12/06/14	40.1
23/06/14	31.4	19/07/14	9.7
24/07/14	13.6	19/08/14	6.9
21/08/14	20.1	17/09/14	14.0
23/09/14	35.3	17/10/14	6.9
25/10/14	39.8	13/11/14	9.7
13/11/14	30.6	20/12/14	35.9
27/01/15	37.6	27/01/15	21.9
Average	29.0	**Average**	20.1

4.8.3 SLA trend along the tree crown

The results of the specific leaf area (SLA) clearly show a decreasing trend towards the top of the tree crown with the lowest leaves having an SLA of 0.256 $cm^2.mg^{-1}$ and the highest 0.100 $cm^2.mg^{-1}$ (Figure 3.22). On average SLA decreases with a rate of 1 $cm.mg^{-1}.m^{-1}$ from 14.6 m to 28.8 m tree height.

This is a confirmation of what is already know in literature, e.g. Nobel [1976] offers a very detailed quantification of the differences between sun and shade leaves and Givnish [1988] discusses the forms of adaption to sun and shade in detail. With an increasing photon flux density ($\mu mol.m^{-2}.s^{-1}$) the CO_2 gas exchange ($\mu mol.m^{-2}.s^{-1}$) will increase more rapidly for shade leaves than for sun leaves, but the maximum value is considerably higher for sun leaves. Sun leaves are thicker (increased mesophyll thickness) and have a lower surface area. Shade leaves contain large chloroplasts, have a higher thylakoid to grana ratio and are thinner with a larger surface area. All these characteristics allow shade leaves to harvest solar energy more efficiently at low light levels and results in a higher SLA.

Chapter 5

General conclusions

By using data collected for over a year from an extensive set of sensors, i.e. meteorological, pedological and physiological sensors, it was possible to distinguish several stress events for both beech and oak. The response of both trees to the changing microclimate was however not always equal. It was concluded that although the growing conditions are the same for both trees, oak severely suffered from the moderate drought period during June 2014 followed by a high amount of precipitation. This was not the case for beech which had a steady growth pattern and sap flow rate during the complete growing season. Upon evaluation of the hydraulic tree coefficient, K_t, it was noticed that beech did suffer slightly from the high amounts of rainfall during the months July and August.

As well as evaluating the responses of both tree species, it was attempted to explain these responses using an anatomical and physiological approach. Due to differences in wood anatomy, beech having diffuse-porous and oak having ring-porous wood, it is very likely that oak suffered from the harsh winters 2009-2010, 2010-2011 and 2012-2013 whereby its vessels were heavily cavitated diminishing its hydraulic functioning. Although a few big vessels in oak contribute much more to total conductivity than the many small vessels in beech [Steppe and Lemeur, 2007], they are excluded from water transport when cavitated.

While it was initially thought that oak suffered from 'water' stress because of the high amount of swelling during rain events when compared with beech, it was established during a field experiment that most of the swelling could be attributed to swelling of the bark. The bark's hygroscopicity differs both anatomically and in terms of chemical composition for beech and oak explaining the difference in swelling.

With the knowledge retrieved from this study, it was possible to make a well-founded and prompt judgement on the status of beech and oak in the experimental forest Aelmoeseneie. The power of individual tree monitoring has been demonstrated in this study as is the potential to only use a dendrometer to measure the diameter variation of the tree and a sap flow sensor to determine sap flux densities and flows. Furthermore using the forest as a potential climate predictor could serve as a true ecosystem service.

Chapter 6

Future research

This study is a stepping stone in the right direction towards developing a way to determine the status of our forests using individually monitored trees and show hydraulic function and growth of trees in real-time. Additionally there is the potential to use the determined status of the forests to derive the surrounding climate and with that develop a real-time climate map, fully predicted by individually monitored trees.

'Bringing together' and 'finetuning' are keywords in the next steps towards this ambitious goal. Bringing together refers to different fields such as ecophysiological research, forestry, software development by Phyto-IT (PhytoSense and PhytoSim), hardware development, web development and social knowledge. Combining these will allow development of a unique pioneering tool, currently online in an early stage at `http://TreeWatch.net/`. This project will show hydraulic functioning and growth of trees in real-time which will allow future studies to profit from information gained at the individual tree scale.

In order to achieve this high level of compatibility it is necessary to finetune the current monitoring procedure. Especially as one of the main objectives is to only use a dendrometer and a sap flow sensor. While it is already clear that information from these two sensors allows a very good insight in the hydraulic functioning of a particular tree, it is crucial to look further for objective variables derivable from these two sensors. Spectral indices to determine phenological events and ultrasonic acoustic emissions are only a few variables which offer great information about the hydraulic functioning of the plant and show potential to be linked with diameter variation and sap flow measurements. Subsequently the two sensors should also be fine-tuned whereby LVDT sensors should be used instead of LPS dendrometers and SapFlow+ mode instead of HRM mode. Finally, it should be precisely determined how many individual trees should actually be monitored in a forest stand and a fine-tuned upscaling method, as simple as possible, should be developed.

By combining all of the above it should be achievable to realize something unique which offers a list of possibilities not only for scientific research and current monitoring networks, but also for education and raising awareness on climate change to the general public.

Bibliography

Allen, R. G., Pereira, L. S., Raes, D., Smith, M., et al. 1998. Crop evapotranspiration - guidelines for computing crop water requirements - fao irrigation and drainage paper 56. *FAO, Rome*, 300(9).

Angelsen, A. et al. 2008. *Moving ahead with REDD: issues, options and implications*. Cifor.

Aris, R. 1978. *Mathematical modelling techniques*. Courier Corporation.

Atwell, B. J., Kriedemann, P. E., and Turnbull, C. G. 1999. *Plants in action: adaptation in nature, performance in cultivation*. Macmillan Education AU.

Aubinet, M., Vesala, T., and Papale, D. 2012. *Eddy covariance: a practical guide to measurement and data analysis*. Springer Science & Business Media.

Baldocchi, D. D. 2003. Assessing the eddy covariance technique for evaluating carbon dioxide exchange rates of ecosystems: past, present and future. *Global Change Biology*, 9(4):479–492.

Baldocchi, D. D. 2009. ESPM 228, Advanced topics in biometeorology and micrometeorology. Lecture.

Barford, C. C., Wofsy, S. C., Goulden, M. L., Munger, J. W., Pyle, E. H., Urbanski, S. P., Hutyra, L., Saleska, S. R., Fitzjarrald, D., and Moore, K. 2001. Factors controlling long-and short-term sequestration of atmospheric CO_2 in a mid-latitude forest. *Science*, 294(5547):1688–1691.

Baycheva, T., Inhaizer, H., Lier, M., Prins, K., and Wolfslehner, B. 2014. Implementing criteria and indicators for sustainable forest management in Europe. Report.

Bechtold, W. A. 2003. Crown-diameter prediction models for 87 species of stand-grown trees in the eastern united states. *Southern Journal of Applied Forestry*, 27(4):269–278.

Beer, C., Reichstein, M., Tomelleri, E., Ciais, P., Jung, M., Carvalhais, N., Rödenbeck, C., Arain, M. A., Baldocchi, D. D., Bonan, G. B., et al. 2010. Terrestrial gross carbon dioxide uptake: global distribution and covariation with climate. *Science*, 329(5993):834–838.

Berninger, F., Hari, P., Nikinmaa, E., Lindholm, M., and Meriläinen, J. 2004. Use of modeled photosynthesis and decomposition to describe tree growth at the northern tree line. *Tree Physiology*, 24(2):193–204.

Berry, C. 2000. A reconsideration of *Wattieza* Stockmans (here attributed to Cladoxylopsida) based on a new species from the Devonian of Venezuela. *Review of Palaeobotany and Palynology*, 112(1):125–146.

Bitterlich, W. et al. 1984. *The relascope idea. Relative measurements in forestry*. Commonwealth Agricultural Bureaux.

Boisvenue, C. and Running, S. W. 2006. Impacts of climate change on natural forest productivity – evidence since the middle of the 20th century. *Global Change Biology*, 12(5):862–882.

Bollmann, M. et al. 2010. World ocean review 1: living with the oceans. chapter 1: Earth's climate system – a complex framework. Digital image from `http://worldoceanreview.com/en/wor-1/climate-system/earth-climate-system/`.

Bower, D. R. and Blocker, W. W. 1966. Notes and observations: Accuracy of bands and tape for measuring diameter increments. *Journal of Forestry*, 64(1):21–22.

Boyer, J. S. 1995. Thermocouple psychometry. In *Measuring the water status of plants and soils*, chapter 3. Academic Press, Inc.

Brandon, K. 2014. Ecosystem services from tropical forests: Review of current science. Technical report, CGD Working Paper 380, Center for Global Development, Washington DC.

Buchmann, N. and Schulze, E.-D. 1999. Net CO_2 and H_2O fluxes of terrestrial ecosystems. *Global Biogeochemical Cycles*, 13(3):751–760.

Burba, G. and Anderson, D. 2007. *Introduction to the Eddy Covariance method: general guidelines, and conventional workflow*. LI-COR Biosciences.

Burgess, S. S., Adams, M. A., Turner, N. C., Beverly, C. R., Ong, C. K., Khan, A. A., and Bleby, T. M. 2001. An improved heat pulse method to measure low and reverse rates of sap flow in woody plants. *Tree Physiology*, 21(9):589–598.

Burgess, S. S. and Dawson, T. E. 2008. Using branch and basal trunk sap flow measurements to estimate whole-plant water capacitance: a caution. *Plant and Soil*, 305(1-2):5–13.

Bussotti, F., Gravano, E., Grossoni, P., and Tani, C. 1998. Occurrence of tannins in leaves of beech trees (fagus sylvatica) along an ecological gradient, detected by histochemical and ultrastructural analyses. *New Phytologist*, 138(3):469–479.

Canadell, J. G. and Raupach, M. R. 2008. Managing forests for climate change mitigation. *Science*, 320(5882):1456–1457.

Carter, J., Schmid, K., Waters, K., Betzhold, L., Hadley, B., Mataosky, R., and Halleran, J. 2012. Lidar 101: An introduction to lidar technology, data, and applications. *National Oceanic and Atmospheric Administration (NOAA) Coastal Services Center*.

Carter, R. 2011. Tree topics: The barlett tree experts blog. drought stress crown dieback. Digital image from `http://blog.bartlett.com/?attachment_id=761`.

Čermák, J. and Kučera, J. 1990. Scaling up transpiration data between trees, stands and watersheds. *Silva Carelica (Finland)*.

Čermák, J., Kučera, J., and Nadezhdina, N. 2004. Sap flow measurements with some thermodynamic methods, flow integration within trees and scaling up from sample trees to entire forest stands. *Trees*, 18(5):529–546.

Ceulemans, R. J. 1999. *Forest ecosystem modelling, upscaling and remote sensing*. Kugler Publications.

Chapin III, F. S., Eugster, W., and McFadden, J. P. 2002. Arctic tundra flux study in the Kuparuk river basin (Alaska), 1994-1996. Available on-line [http://www.daac.ornl.gov] from Oak Ridge National Laboratory Distributed Active Archive Center, Oak Ridge, Tennessee, U.S.A.

Chapin III, F. S., Matson, P. A., and Vitousek, P. 2011. *Principles of terrestrial ecosystem ecology*. Springer Science & Business Media.

Clark, N. A., Wynne, R. H., and Schmoldt, D. L. 2000. A review of past research on dendrometers. *Forest Science*, 46(4):570–576.

Cochard, H. and Tyree, M. T. 1990. Xylem dysfunction in *Quercus*: vessel sizes, tyloses, cavitation and seasonal changes in embolism. *Tree Physiology*, 6(4):393–407.

Cohen, Y., Fuchs, M., and Green, G. C. 1981. Improvement of the heat pulse method for determining sap flow in trees. *Plant, Cell & Environment*, 4(5):391–397.

Daudet, F.-A., Améglio, T., Cochard, H., Archilla, O., and Lacointe, A. 2005. Experimental analysis of the role of water and carbon in tree stem diameter variations. *Journal of Experimental Botany*, 56(409):135–144.

David, T. S., Pinto, C. A., Nadezhdina, N., Kurz-Besson, C., Henriques, M. O., Quilhó, T., Čermák, J., Chaves, M. M., Pereira, J. S., and David, J. S. 2013. Root functioning, tree water use and hydraulic redistribution in *Quercus suber* trees: A modeling approach based on root sap flow. *Forest Ecology and Management*, 307:136–146.

De Schepper, V. and Steppe, K. 2010. Development and verification of a water and sugar transport model using measured stem diameter variations. *Journal of Experimental Botany*, 61(8):2083–2099.

De Swaef, T., Hanssens, J., Cornelis, A., and Steppe, K. 2013. Non-destructive estimation of root

pressure using sap flow, stem diameter measurements and mechanistic modelling. *Annals of botany*, 111(2):271–282.

De Swaef, T. and Steppe, K. 2010. Linking stem diameter variations to sap flow, turgor and water potential in tomato. *Functional Plant Biology*, 37(5):429–438.

Decagon Devices 2015. *Soil moisture sensors. GS3 Greenhouse Sensor. Volumetric water content, electrical conductivity, and temparture.* 2365 NE Hopkins Ct / Pullman, WA 99163 USA.

Dixon, M. and Downey, A. 2013. *PSY1 Stem Psychrometer Manual.* ICT International, 4.4 edition.

Drew, D. M. and Downes, G. M. 2009. The use of precision dendrometers in research on daily stem size and wood property variation: a review. *Dendrochronologia*, 27(2):159–172.

Drew, D. M., Downes, G. M., and Battaglia, M. 2010. Cambium, a process-based model of daily xylem development in eucalyptus. *Journal of Theoretical Biology*, 264(2):395–406.

Eichhorn, J., Roskams, P., Ferretti, M., Mues, V., Szepesi, A., and Durrant, D. 2010. Visual assessment of crown condition and damaging agents. *Manual on methods and criteria for harmonized sampling, assessment, monitoring and analysis of the effects of air pollution on forests. Manual Part IV. UNECE ICP Forests Programme Co-ordinating Centre.*

EXELIS 2012. ITT Exelis delivers imaging system for next-generation, high-resolution GeoEye-2 satellite. Press release.

Fagan, M. and DeFries, R. 2009. Measurement and monitoring of the world's forests. a review and summary of remote sensing technical capability 2009-2015. RFF REPORT.

FAO 2010. *Global forest resources assessment (FRA) 2010: Main report.* Food and Agriculture Organization of the United Nations.

Fisher, J. B., Tu, K. P., and Baldocchi, D. D. 2008. Global estimates of the land–atmosphere water flux based on monthly avhrr and islscp-ii data, validated at 16 fluxnet sites. *Remote Sensing of Environment*, 112(3):901–919.

Foley, J. A., Asner, G. P., Costa, M. H., Coe, M. T., DeFries, R., Gibbs, H. K., Howard, E. A., Olson, S., Patz, J., Ramankutty, N., et al. 2007. Amazonia revealed: forest degradation and loss of ecosystem goods and services in the Amazon Basin. *Frontiers in Ecology and the Environment*, 5(1):25–32.

ForNaLab 2007. Uitgebreid bosbeheerplan aelmoeseneiebos 26 november 2007, eindversie. *UGent Laboratorium voor Bosbouw.*

Frank, D., Poulter, B., Saurer, M., Esper, J., Huntingford, C., Helle, G., Treydte, K., Zimmermann, N., Schleser, G., Ahlström, A., et al. 2015. Water-use efficiency and transpiration across european forests during the anthropocene. *Nature Climate Change.*

Gamfeldt, L., Snäll, T., Bagchi, R., Jonsson, M., Gustafsson, L., Kjellander, P., Ruiz-Jaen, M. C., Fröberg, M., Stendahl, J., Philipson, C. D., et al. 2013. Higher levels of multiple ecosystem services are found in forests with more tree species. *Nature communications*, 4:1340.

Gea-Izquierdo, G., Bergeron, Y., Huang, J., Lapointe-Garant, M., Grace, J., and Berninger, F. 2014. The relationship between productivity and tree-ring growth in boreal coniferous forests. *Boreal Environment Research*, 19.

Gibbs, H. K., Brown, S., Niles, J. O., and Foley, J. A. 2007. Monitoring and estimating tropical forest carbon stocks: making REDD a reality. *Environmental Research Letters*, 2(4).

Givnish, T. J. 1988. Adaptation to sun and shade: a whole-plant perspective. *Functional Plant Biology*, 15(2):63–92.

Goldstein, G., Andrade, J. L., Meinzer, F. C., Holbrook, N. M., Cavelier, J., Jacksosn, P., and Celis, A. 1998. Stem water storage and diurnal patterns of water use in tropical forest canopy trees. *Plant, Cell & Environment*, 21(4):397–406.

Granier, A. 1985. Une nouvelle méthode pour la mesure du flux de sève brute dans le tronc des arbres. *Annales des Sciences Forestieres*, 42:193–200.

Green, S., Clothier, B., and Perie, E. 2008. A re-analysis of heat pulse theory across a wide range of sap flows. In *VII International Workshop on Sap Flow 846*, pages 95–104.

Hake, K., Cassman, K., Whisler, F., and Upchurch, D. 1990. Root physiology and management. Newsletter of the Cotton Physiology Education Program — NATIONAL COTTON COUNCIL, Physiology Today.

Hao, G.-Y., Wheeler, J. K., Holbrook, N. M., and Goldstein, G. 2013. Investigating xylem embolism formation, refilling and water storage in tree trunks using frequency domain reflectometry. *Journal of experimental botany*, 64(8):2321–2332.

Hathway, D. 1958. Oak-bark tannins. *Biochemical Journal*, 70(1):34.

Hemery, G., Savill, P., and Pryor, S. 2005. Applications of the crown diameter–stem diameter relationship for different species of broadleaved trees. *Forest Ecology and Management*, 215(1):285–294.

Holmgren, P. 2008. Role of satellite remote sensing in REDD. *UN-REDD PROGRAMME*, page 11.

Holmgren, P. and Thuresson, T. 1998. Satellite remote sensing for forestry planning - a review. *Scandinavian Journal of Forest Research*, 13(1-4):90–110.

Huber, B. and Schmidt, E. 1937. Eine kompensationsmethode zur thermoelektrischen messung langsamer saftströme.

ICT International 2015. Hrm heat ratio method. Digital image from `http://www.ictinternational.com/products/heat-ratio-method/hrm-heat-ratio-method/`.

Imboden, D. M. and Pfenninger, S. 2012. *Introduction to systems analysis: mathematically modeling natural systems*. Springer Science & Business Media.

IPCC 2013. Summary for policymakers. In Stocker, T., Qin, D., Plattner, G.-K., Tignor, M., Allen, S., Boschung, J., Nauels, A., Xia, Y., Bex, V., and Midgley, P., Eds., *Climate Change 2013: The Physical Science Basis. Contribution of Working Group I to the Fifth Assessment Report of the Intergovernmental Panel on Climate Change*, page 1535. Cambridge University Press, Cambridge, United Kingdom and New York, NY, USA.

Jansen, J. J., Sevenster, J. G., and Faber, P. 1996. *Opbrengst tabellen voor belangrijke boomsoorten in Nederland*. Landbouwuniversiteit Wageningen, IBN-DLO.

Jones, C. G., Lawton, J. H., and Shachak, M. 1996. Organisms as ecosystem engineers. In *Ecosystem Management*, pages 130–147. Springer.

Keeland, B. D. and Sharitz, R. R. 1993. Accuracy of tree growth measurements using dendrometer bands. *Canadian Journal of Forest Research*, 23(11):2454–2457.

Keeland, B. D. and Young, P. J. 2014. Installation of traditional dendrometer bands. *US Geological Survey*, 23.

King, S. L., Allen, J. A., and McCoy, J. W. 1998. Long-term effects of a lock and dam and greentree reservoir management on a bottomland hardwood forest. *Forest Ecology and Management*, 112(3):213–226.

Lee, X., Massman, W. J., and Law, B. E. 2006. *Handbook of micrometeorology: a guide for surface flux measurement and analysis*, volume 29. Springer, Science & Business Media.

Lindner, M., Fitzgerald, J. B., Zimmermann, N. E., Reyer, C., Delzon, S., van der Maaten, E., Schelhaas, M., Lasch, P., Eggers, J., van der Maaten-Theunissen, M., et al. 2014. Climate change and European forests: What do we know, what are the uncertainties, and what are the implications for forest management? *Journal of environmental management*, 146:69–83.

Liu, D., Cai, W., Xia, J., Dong, W., Zhou, G., Chen, Y., Zhang, H., and Yuan, W. 2014. Global validation of a process-based model on vegetation gross primary production using eddy covariance observations. *PloS one*, 9(11).

Lorenz, M., Becher, G., Mues, V., Fischer, R., Becker, R., Calatayud, V., Dise, N., Krause, G. H. M., Sanz, M., and Ulrich, E. 2012. *Forest condition in Europe*. Thünen-Institut, Bundesforschungsinstitut für Ländliche Räume, Wald und Fischerei.

Lövdahl, L. and Odin, H. 1992. Diurnal changes in the stem diameter of norway spruce in relation to relative humidity and air temperature. *Trees*, 6(4):245–251.

Lowman, M. D. 2009. Canopy research in the twenty-first century: a review of arboreal ecology. *Tropical Ecology*, 50(1):125.

Lubczynski, M. W. 2009. The hydrogeological role of trees in water-limited environments. *Hydrogeology Journal*, 17(1):247–259.

Lutz, J. A., Larson, A. J., Freund, J. A., Swanson, M. E., and Bible, K. J. 2013. The importance of large-diameter trees to forest structural heterogeneity. *PloS one*, 8(12).

Lutz, J. A., Larson, A. J., Swanson, M. E., and Freund, J. A. 2012. Ecological importance of large-diameter trees in a temperate mixed-conifer forest. *PLoS One*, 7(5).

Matyssek, R., Paoletti, E., Bytnerowicz, A., Kozovits, A. R., Wieser, G., and Feng, Z. 2015. Supersites for superior forest science. IUFRO Spotlight 29.

McLaughlin, S. B., Wullschleger, S. D., and Nosal, M. 2003. Diurnal and seasonal changes in stem increment and water use by yellow poplar trees in response to environmental stress. *Tree Physiology*, 23(16):1125–1136.

Meinzer, F. C., Brooks, J. R., Domec, J.-C., Gartner, B. L., Warren, J. M., Woodruff, D. R., Bible, K., and Shaw, D. C. 2006. Dynamics of water transport and storage in conifers studied with deuterium and heat tracing techniques. *Plant, Cell & Environment*, 29(1):105–114.

Meinzer, F. C., Clearwater, M. J., and Goldstein, G. 2001. Water transport in trees: current perspectives, new insights and some controversies. *Environmental and Experimental Botany*, 45(3):239–262.

Meinzer, F. C., James, S. A., and Goldstein, G. 2004. Dynamics of transpiration, sap flow and use of stored water in tropical forest canopy trees. *Tree Physiology*, 24(8):901–909.

Meinzer, F. C., Woodruff, D. R., Eissenstat, D. M., Lin, H. S., Adams, T. S., and McCulloh, K. A. 2013. Above-and belowground controls on water use by trees of different wood types in an eastern us deciduous forest. *Tree physiology*, 33(4):345–356.

Meiresonne, L., Sampson, D. A., Kowalski, A. S., Janssens, I. A., Nadezhdina, N., Cermak, J., Van Slycken, J., and Ceulemans, R. 2003. Water flux estimates from a belgian scots pine stand: a comparison of different approaches. *Journal of Hydrology*, 270(3):230–252.

Mencuccini, M., Hölttä, T., Sevanto, S., and Nikinmaa, E. 2013. Concurrent measurements of change in the bark and xylem diameters of trees reveal a phloem-generated turgor signal. *New Phytologist*, 198(4):1143–1154.

Meroni, M., Rossini, M., Guanter, L., Alonso, L., Rascher, U., Colombo, R., and Moreno, J. 2009. Remote sensing of solar-induced chlorophyll fluorescence: Review of methods and applications. *Remote Sensing of Environment*, 113(10):2037–2051.

Michalak, R. 2014. Forest monitoring in europe and its importance to clean air policies and sustainable forest management. In *Forests under pressure - Local responses to global issues*, chapter 26, page 411. IUFRO Special Project World Forests, Society and Environment (IUFRO WFSE).

Michel, A., Seidling, W., and editors 2014. Forest Condition in Europe: 2014 Technical Report of ICP Forests. Report under the UNECE Convention on Long-Range Transboundary Air Pollution (CLRTAP). Vienna: BFW Austrian Research Centre for Forests. *BFW-Dokumentation*, 18.

Miller, G. R., Chen, X., Rubin, Y., and Baldocchi, D. D. 2007. A new technique for upscaling sap flow transpiration measurements to stand or landscape scale fluxes. American Geophysical Union, Fall Meeting Poster.

Misson, L. 2004. Maiden: a model for analyzing ecosystem processes in dendroecology. *Canadian Journal of Forest Research*, 34(4):874–887.

Mooney, H., Cropper, A., and Reid, W. 1996. Ecosystems and human well-being: a framework for assessment.

Mooney, H., Larigauderie, A., Cesario, M., Elmquist, T., Hoegh-Guldberg, O., Lavorel, S., Mace, G. M., Palmer, M., Scholes, R., and Yahara, T. 2009. Biodiversity, climate change, and ecosystem services. *Current Opinion in Environmental Sustainability*, 1(1):46–54.

Morales, P., Hickler, T., Rowell, D. P., Smith, B., and Sykes, M. T. 2007. Changes in European ecosystem productivity and carbon balance driven by regional climate model output. *Global Change Biology*, 13(1):108–122.

Morison, J. I. L. and Lawlor, D. W. 1999. Interactions between increasing CO_2 concentration and temperature on plant growth. *Plant, Cell & Environment*, 22(6):659–682.

Motohka, T., Nasahara, K. N., Oguma, H., and Tsuchida, S. 2010. Applicability of green-red vegetation index for remote sensing of vegetation phenology. *Remote Sensing*, 2(10):2369–2387.

Nadezhdina, N., Vandegehuchte, M. W., and Steppe, K. 2012. Sap flux density measurements based on the heat field deformation method. *Trees*, 26(5):1439–1448.

Nadrowski, K., Wirth, C., and Scherer-Lorenzen, M. 2010. Is forest diversity driving ecosystem function and service? *Current Opinion in Environmental Sustainability*, 2(1):75–79.

Nobel, P. S. 1976. Photosynthetic rates of sun versus shade leaves of hyptis emoryi torr. *Plant Physiology*, 58(2):218–223.

Pan, Y., Birdsey, R. A., Fang, J., Houghton, R., Kauppi, P. E., Kurz, W. A., Phillips, O. L., Shvidenko, A., Lewis, S. L., Canadell, J. G., et al. 2011. A large and persistent carbon sink in the world's forests. *Science*, 333(6045):988–993.

Pan, Y., Birdsey, R. A., Phillips, O. L., and Jackson, R. B. 2013. The structure, distribution, and biomass of the world's forests. *Annual Review of Ecology, Evolution, and Systematics*, 44:593–622.

Pautasso, M., Dehnen-Schmutz, K., Holdenrieder, O., Pietravalle, S., Salama, N., Jeger, M. J., Lange, E., and Hehl-Lange, S. 2010. Plant health and global change–some implications for landscape management. *Biological Reviews*, 85(4):729–755.

Peel, M. C., Finlayson, B. L., and McMahon, T. A. 2007. Updated world map of the Köppen-Geiger climate classification. *Hydrology and earth system sciences discussions*, 4(2):439–473.

Pivovaroff, A. L., Sack, L., and Santiago, L. S. 2014. Coordination of stem and leaf hydraulic conductance in southern california shrubs: a test of the hydraulic segmentation hypothesis. *New Phytologist*, 203(3):842–850.

Prentice, I. C., Farquhar, G. D., Fasham, M. J. R., Goulden, M. L., Heimann, M., Jaramillo, V. J., Kheshgi, H. S., LeQuéré, C., Scholes, R. J., and Wallace, D. W. R. 2001. The carbon cycle and atmospheric carbon dioxide. In *Climate Change 2001: The Scientific Basis. Contribution of Working Group I to the Third Assessment Report of the Intergovernmental Panel on Climate Change*, chapter 3, pages 184–238. Cambridge University Press.

Rainforest Foundation US 2015. Commonly asked questions and facts. http://www.rainforestfoundation.org/commonly-asked-questions-and-facts.

Ramoelo, A., Dzikiti, S., van Deventer, H., Maherry, A., Cho, M. A., and Gush, M. 2015. Potential to monitor plant stress using remote sensing tools. *Journal of Arid Environments*, 113:134–144.

Reddy, A. R., Rasineni, G. K., and Raghavendra, A. S. 2010. The impact of global elevated CO_2 concentration on photosynthesis and plant productivity. *Current Science*, 99(1):46–57.

Reyes-Acosta, J. L. and Lubczynski, M. W. 2013. Mapping dry-season tree transpiration of an oak woodland at the catchment scale, using object-attributes derived from satellite imagery and sap flow measurements. *Agricultural and forest meteorology*, 174:184–201.

RMI 2015. Average climate values in ukkel, belgium (1981-2010) from the royal meteorological institute of belgium. http://meteo.be/.

Rocha, A. V., Goulden, M. L., Dunn, A. L., and Wofsy, S. C. 2006. On linking interannual tree ring variability with observations of whole-forest CO_2 flux. *Global Change Biology*, 12(8):1378–1389.

Samson, R., Nachtergale, L., Schauvliege, M., Lemeur, R., and Lust, N. 1997. Experimental set-up for biogeochemical research in the mixed deciduous forest Aelmoeseneie (East Flanders). *Silva Gandavensis*, 61:1–14.

Sano, Y., Okamura, Y., and Utsumi, Y. 2005. Visualizing water-conduction pathways of living trees: selection of dyes and tissue preparation methods. *Tree Physiology*, 25(3):269–275.

Santos, R. and Bond, S. 2014. New York Asian Longhorned Beetle Eradication Program announces its efforts for 2014. *United States Department of Agriculture (USDA) Animal and Plant Health Inspection Service*.

Satō, T. and Madgwick, H. A. I. 1982. *Forest biomass*. Springer Science & Business Media.

Schaphoff, S., Lucht, W., Gerten, D., Sitch, S., Cramer, W., and Prentice, I. C. 2006. Terrestrial biosphere carbon storage under alternative climate projections. *Climatic Change*, 74(1-3):97–122.

Schelhaas, M.-J., Eggers, J., Lindner, M., Nabuurs, G., Pussinen, A., Päivinen, R., Schuck, A., Verkerk, P., Van der Werf, D., and Zudin, S. 2007. *Model documentation for the European forest information scenario model (EFISCEN 3.1. 3)*. Alterra Wageningen, The Netherlands.

Schott, J. 2007. *Remote sensing*. Oxford University Press.

Schowengerdt, R. 2007. *Remote sensing: models and methods for image processing*. Academic press.

Schulze, E.-D., Čermák, J., Matyssek, M., Penka, M., Zimmermann, R., Vasicek, F., Gries, W., and Kučera, J. 1985. Canopy transpiration and water fluxes in the xylem of the trunk of *Larix* and *Picea* trees – a comparison of xylem flow, porometer and cuvette measurements. *Oecologia*, 66(4):475–483.

Seidl, R., Schelhaas, M., and Lexer, M. J. 2011. Unraveling the drivers of intensifying forest disturbance regimes in Europe. *Global Change Biology*, 17(9):2842–2852.

Sioen, G. and Roskams, P. 2014. Bosvitaliteitsinventaris 2013. resultaten uit het bosvitaliteitsmeetnet (Level 1). *Rapporten van het Instituut voor Natuur- en Bosonderzoek 2014. Instituut voor Natuur- en Bosonderzoek, Brussel*.

Slik, J. W., Paoli, G., McGuire, K., Amaral, I., Barroso, J., Bastian, M., Blanc, L., Bongers, F., Boundja, P., Clark, C., et al. 2013. Large trees drive forest aboveground biomass variation in moist lowland forests across the tropics. *Global Ecology and Biogeography*, 22(12):1261–1271.

Sonnentag, O., Hufkens, K., Teshera-Sterne, C., Young, A. M., Friedl, M., Braswell, B. H., Milliman, T., O'Keefe, J., and Richardson, A. D. 2012. Digital repeat photography for phenological research in forest ecosystems. *Agricultural and Forest Meteorology*, 152:159–177.

Steppe, K., De Pauw, D. J., and Lemeur, R. 2008. Validation of a dynamic stem diameter variation model and the resulting seasonal changes in calibrated parameter values. *Ecological Modelling*, 218(3):247–259.

Steppe, K., De Pauw, D. J. W., Doody, T. M., and Teskey, R. O. 2010. A comparison of sap flux density using thermal dissipation, heat pulse velocity and heat field deformation methods. *Agricultural and Forest Meteorology*, 150(7):1046–1056.

Steppe, K., De Pauw, D. J. W., Lemeur, R., and Vanrolleghem, P. A. 2006. A mathematical model linking tree sap flow dynamics to daily stem diameter fluctuations and radial stem growth. *Tree physiology*, 26(3):257–273.

Steppe, K. and Lemeur, R. 2004. An experimental system for analysis of the dynamic sap-flow characteristics in young trees: results of a beech tree. *Functional Plant Biology*, 31(1):83–92.

Steppe, K. and Lemeur, R. 2007. Effects of ring-porous and diffuse-porous stem wood anatomy on the hydraulic parameters used in a water flow and storage model. *Tree physiology*, 27(1):43–52.

Steppe, K., Sterck, F., and Deslauriers, A. 2015a. Diel growth dynamics in tree stems: linking anatomy and ecophysiology. *Trends in Plant Science*.

Steppe, K., Vandegehuchte, M. W., Tognetti, R., and Mencuccini, M. 2015b. Sap flow as a key trait in the understanding of plant hydraulic functioning. *Tree Physiology*, 35(4):341–345.

Stockmans, F. 1968. *Végétaux mésodévoniens récoltés aux confins du massif du Brabant (Belgique)*.

Institut royal des sciences naturelles de Belgique.

Stoy, P. C., Richardson, A. D., Baldocchi, D. D., Katul, G. G., Stanovick, J., Mahecha, M. D., Reichstein, M., Detto, M., Law, B. E., Wohlfahrt, G., et al. 2009. Biosphere-atmosphere exchange of CO_2 in relation to climate: a cross-biome analysis across multiple time scales. *Biogeosciences*, 6(10):2297–2312.

Taiz, L. and Zeiger, E. 2010. *Plant Physiology*. Sinauer Associates Inc., 5th revised edition.

Thenkabail, P. S., Lyon, J. G., and Huete, A. 2011. *Hyperspectral remote sensing of vegetation*. CRC Press.

Tobin, B. and Nieuwenhuis, M. 2012. Forest carbon research in ireland: The importance of long-term monitoring of forest growth and climate. *Earthzine*.

Tol, C., Berry, J., Campbell, P., and Rascher, U. 2014. Models of fluorescence and photosynthesis for interpreting measurements of solar-induced chlorophyll fluorescence. *Journal of Geophysical Research: Biogeosciences*.

Tyree, M. T. and Ewers, F. W. 1991. The hydraulic architecture of trees and other woody plants. *New Phytologist*, 119(3):345–360.

Uddin, J., Smith, R., Hancock, N., and Foley, J. 2014. Evaluation of sap flow sensors to measure the transpiration rate of plants during canopy wetting and drying. *Journal of Agricultural Studies*, 2(2):105–119.

UNESCO 2014. People and nature — better together. Promotion video `https://www.youtube.com/watch?v=5EhLKoAU5Vc`.

UPRA 2015. Visible vegetation index (vvi) planetary habitability laboratory project. http://phl.upr.edu/projects/visible-vegetation-index-vvi by University of Puerto Rico at Arecibo.

van den Honert, T. H. 1948. Water transport in plants as a catenary process. *Discuss. Faraday Soc.*, 3:146–153.

Vandegehuchte, M. W. and Steppe, K. 2012a. Improving sap flux density measurements by correctly determining thermal diffusivity, differentiating between bound and unbound water. *Tree physiology*, 32(7):930–942.

Vandegehuchte, M. W. and Steppe, K. 2012b. Interpreting the heat field deformation method: Erroneous use of thermal diffusivity and improved correlation between temperature ratio and sap flux density. *Agricultural and Forest Meteorology*, 162:91–97.

Vandegehuchte, M. W. and Steppe, K. 2012c. Sapflow+: a four-needle heat-pulse sap flow sensor enabling nonempirical sap flux density and water content measurements. *New Phytologist*, 196(1):306–317.

Vandegehuchte, M. W. and Steppe, K. 2013. Sap-flux density measurement methods: working principles and applicability. *Functional Plant Biology*, 40(3):213–223.

Vergeynst, L., Dierick, M., Bogaerts, J., Cnudde, V., and Steppe, K. 2015. Cavitation: a blessing in disguise? new method to establish vulnerability curves and assess hydraulic capacitance of woody tissues. *Tree Physiology*, 35:400–409.

Vicharnakorn, P., Shrestha, R. P., Nagai, M., Salam, A. P., and Kiratiprayoon, S. 2014. Carbon stock assessment using remote sensing and forest inventory data in Savannakhet, Lao PDR. *Remote Sensing*, 6(6):5452–5479.

Watson, R. T., Noble, I. R., Bolin, B., Ravindranath, N. H., Verardo, D. J., Dokken, D. J., et al. 2000. *Land use, land-use change and forestry: a special report of the Intergovernmental Panel on Climate Change*. Cambridge University Press.

Wouters, J., Quataert, P., Onkelinx, T., Bauwens, D., et al. 2008. Ontwerp en handleiding voor de tweede regionale bosinventarisatie van het vlaamse gewest. Report INBO.

Yang, J., Gong, P., Fu, R., Zhang, M., Chen, J., Liang, S., Xu, B., Shi, J., and Dickinson, R. 2013. The role of satellite remote sensing in climate change studies. *Nature climate change*, 3(10):875–883.

Zhang, H., Morison, J. I., and Simmonds, L. P. 1999. Transpiration and water relations of poplar trees growing close to the water table. *Tree physiology*, 19(9):563–573.

Zimmermann, M. H. 1983. *Xylem structure and the ascent of sap*. Springer-Verlag, Berlin.

Zweifel, R. 2012. Natkon point dendrometer ZN11-T-WP. Datasheet.

Zweifel, R., Eugster, W., Etzold, S., Dobbertin, M., Buchmann, N., and Häsler, R. 2010. Link between continuous stem radius changes and net ecosystem productivity of a subalpine norway spruce forest in the swiss alps. *New Phytologist*, 187(3):819–830.

Zweifel, R., Item, H., and Häsler, R. 2000. Stem radius changes and their relation to stored water in stems of young Norway spruce trees. *Trees*, 15(1):50–57.

Zweifel, R., Item, H., and Häsler, R. 2001. Link between diurnal stem radius changes and tree water relations. *Tree Physiology*, 21(12-13):869–877.

Appendix A. Overview of meteorological sensors

What follows is a listing of the different meteorological sensors used in the experimental forest Aelmoeseneie and in the small scale set-up. This includes the sensor type, the producer and the most relevant technical information. For more information about a particular device, please refer to the manual or datasheet for that device.

- *Temperature* (°C): Thermistor TH-10-44006-1/8-4-40 by `Omega Engineering`. Accuracy of ±0.1°C. Usage in temperature ranges from -80 to 150°C.
- *Relative humidity* (%): SHT25 humidity and temperature sensor IC with CMOSens® chip by `SENSIRION`. Mounted in ventilated radiation screen. Accuracy of 1.8%.
- *PAR* ($\mu mol.m^{-2}.s^{-1}$): Quantum Sensor QS2-UM-1.0 by `Delta-t Devices`. Using a high quality Silicon Photodiode. Accuracy of ±5% of reading at 20°C.
- *Net radiation* ($W.m^{-2}$): Q-7.1 net radiometer Q*7.1 by `Campbell Scientific, Inc.` measuring the algebraic sum of incoming and outgoing all-wave radiation.
- *Albedo* (%): Dome solarimeter/albedometer GS1 & GS2 by `Delta-t Devices`. Spectral sensitivity (350-1500 nm) of ± 5%.
- *Wind speed* ($km.h^{-1}$): Anemometer AN1 by `Delta-t Devices`. Accuracy of 1% of reading for wind speeds of 10-55 $m.s^{-1}$) and 2% of reading for wind speeds higher than 55 $m.s^{-1}$.
- *Wind direction* (°): Windvane WD1 by `Delta-t Devices`. Maximum speed of 75 $m.s^{-1}$ and a resolution of 0.2 degrees.
- *Precipitation* (mm): Pluviometer RG1 by `Delta-t Devices` using the tipping bucket raingauge principle. Nominal sensitivity of 0.2 mm per tip.

- *Air pressure* (hPa): Barometer BS4 by `Delta-t Devices`. Error contributions at 20°C: pressure transmitter ± 0.5 hPa, output attenuator ± 0 hPa at 600 hPa to ± 0.6 hPa at 1060 hPa and logger measurement ± 0 hPa at 600 hPa to ± 0.3 hPa at 1060 hPa.

- *Surface wetness*: Surface wetness sensor type SWS by `Delta-t Devices`. Measures surface moisture. Outputting 0 V when dry and > 1 V when wet.

Appendix B. Conversion of μmol.m^{-2}.s^{-1} to W.m^{-2}

Using the typical solar energy distribution, it can be calculated that in the visible region (400-700 nm), i.e. PAR, the 400-500 nm band represents 31%, the 500-600 nm band 36% and the 600-700 band 33%. The mean wavelengths, i.e. 450 nm, 550 nm and 650 nm respectively, are used to calculate the amount of energy they hold using [Taiz and Zeiger, 2010] (Equation 1).

$$E = \frac{h \times c}{\lambda} \tag{1}$$

with E, energy (J.quanta^{-1}); h, Planck's constant; c, speed of light and λ, wavelength of light (m). Thus, visible light (400-700 nm) contains 3.680 $\times$ 10^{-19} J per quanta. Subsequently calculation of the conversion factor for μmol.m^{-2}.s^{-1} to W.m^{-2} is possible:

$$\begin{aligned}
\frac{1\ \mu\text{mol}}{\text{m}^2.\text{s}} &= \frac{10^{-6}\ \text{mol}}{\text{m}^2.\text{s}} \\
&= \frac{10^{-6}\ \text{mol}}{\text{m}^2.\text{s}} \times \frac{6.022 \times 10^{23}\ \text{quanta}}{\text{mol}} \\
&= \frac{6.022 \times 10^{17}\ \text{quanta}}{\text{m}^2.\text{s}} \times \frac{3.68 \times 10^{-19}\ \text{J}}{\text{quanta}} \\
&= 0.223\ \frac{\text{W}}{\text{m}^2}
\end{aligned}$$

Hence multiplying x μmol.m^{-2}.s^{-1} with 0.223 will result in y W.m^{-2}.

Appendix C. Correlation table for spectral indices

TABLE 1: Correlation (r) of the four calculated phenological indices with the variables: RH_{ground}, RH_{P4}, T_{ground}, T_{P4}, VPD, PAR, precipitation ('Prec'), wind speed ('Wind'), Ψ_{soil}, F_{sapflux}, ΔD and 'vitality check'. Data from experimental forest Aelmoeseneie.

	ExG	g_{cc}	VVI	GRVI
RH_{ground}	0.01	0.06	0.47	-0.11
RH_{P4}	-0.22	-0.17	0.68	-0.32
T_{ground}	0.70	0.71	-0.56	0.79
T_{P4}	0.68	0.69	-0.57	0.79
VPD	0.34	0.28	-0.66	0.47
PAR	0.46	0.40	-0.79	0.68
Prec.	0.00	0.01	0.09(6)	-0.10(0)
Wind	-0.33	-0.32	0.32	-0.43
Ψ_{soil}	-0.18	-0.20	-0.43	-0.18
SF_{B1}	0.71	0.69	-0.52	0.86
SF_{B2}	0.65	0.64	-0.48	0.82
SF_{B3}	0.61	0.57	-0.54	0.81
SF_{B4}	0.56	0.50	-0.53	0.78
SF_{B5}	0.54	0.52	-0.45	0.77
SF_{O1}	0.60	0.56	-0.51	0.81
SF_{O2}	0.57	0.53	-0.56	0.81
SF_{O3}	0.53	0.50	-0.47	0.78
SF_{O4}	0.65	0.60	-0.49	0.79
ΔD_{B1}	-0.64	-0.55	0.47	-0.62
ΔD_{B1X}	-0.15	-0.15	-0.31	-0.21
ΔD_{B2}	-0.68	-0.59	0.53	-0.68
ΔD_{B2X}	-0.66	-0.61	0.58	-0.72
ΔD_{B3}	-0.67	-0.58	0.52	-0.68
ΔD_{B3X}	0.48	0.45	-0.46	0.47
ΔD_{B4}	-0.69	-0.60	0.52	-0.64
ΔD_{B5}	-0.69	-0.60	0.51	-0.64
ΔD_{O1}	-0.31	-0.24	0.33	-0.43
ΔD_{O2}	-0.49	-0.41	0.42	-0.53
ΔD_{O3}	-0.47	-0.40	0.44	-0.48
ΔD_{O4}	0.62	0.52	-0.50	0.66
Vitality check	0.96(7)	0.94	-0.93	0.97(4)